



# **Preeclampsia is Related to Uric Acid: an Anthropometric Model with the Fetus**

Mador Emmanuel Stephen  
Ishaya Chuwang Pam  
Christian Ogoegbunem Isichei



# **Preeclampsia is Related to Uric Acid:**

## *An Anthropometric Model*

### *with the Fetus*

---

Dr. Mador Emmanuel Stephen

Dr. Ishaya Chuwang Pam

Dr. Christian Ogoegbunem Isichei



**SciencePG**

Science Publishing Group

Science Publishing Group

548 Fashion Avenue  
New York, NY 10018

[www.sciencepublishinggroup.com](http://www.sciencepublishinggroup.com)

Published by Science Publishing Group 2015

Copyright © Mador Emmanuel Stephen 2015

Copyright © Ishaya Chuwang Pam 2015

Copyright © Christian Ogoegbunem Isichei 2015

All rights reserved.

First Edition

**ISBN: 978-1-940366-39-5**

This work is licensed under the Creative Commons Attribution-NonCommercial 3.0 Unported License. To view a copy of this license, visit

<http://creativecommons.org/licenses/by-nc/3.0/>



or send a letter to:  
Creative Commons  
171 Second Street, Suite 300  
San Francisco, California 94105  
USA

To order additional copies of this book, please contact:  
Science Publishing Group  
[book@sciencepublishinggroup.com](mailto:book@sciencepublishinggroup.com)  
[www.sciencepublishinggroup.com](http://www.sciencepublishinggroup.com)

Printed and bound in India

## **Acknowledgement**

We are much indebted to Dr Kilani of Comprehensive Health Centre Dadin-kowa Jos Nigeria for allowing us to take blood samples for uric acid analysis from pregnant women receiving antenatal care in this government facility. Our appreciation also goes to the Institutional Health Research Ethical Committee of Jos University Teaching Hospital Jos, Nigeria for giving us ethical clearance/approval to carry out this study.



## **Preface**

This book on the aetiology of preeclampsia-eclampsia has been written keeping in mind the findings of scientists who have researched on the aetiology of this disease which is exclusive to human pregnancy. Research efforts on identifying the cause of preeclampsia have traditionally been focused on subjects that have manifested the disease. Our experience has shown that the culprit that triggers the disease returns to hiding as soon as the disease begins to manifest.

In this book care has been taken to ensure that the text provides all the information necessary for an intelligent understanding of uric acid as the cause of preeclampsia-eclampsia. At the same time, innovation has been used to make the subject easy to understand.

In an endeavor of this sort it is to be expected that some errors of omission or commission are likely to creep in. To avert as many of these as possible a number of renowned scientists were requested to read through the text. Their suggestions have greatly added to the accuracy and usefulness of this book. Nevertheless, there is still room for further improvement and the authors would welcome suggestions to this end both from researchers and clinicians.

*Mador Emmanuel Stephen*

*Ishaya Chuwang Pam*

*Christian Ogoegbunem Isichei*





# Contents

<b>Chapter 1</b>	<b>Introduction</b>	<b>1</b>
<b>Chapter 2</b>	<b>Evolution</b>	<b>11</b>
<b>Chapter 3</b>	<b>The Quest</b>	<b>17</b>
<b>Chapter 4</b>	<b>Genetic Code</b>	<b>25</b>
<b>Chapter 5</b>	<b>Uric Acid &amp; Preeclampsia</b>	<b>31</b>
<b>Chapter 6</b>	<b>Fetal Biometrics</b>	<b>39</b>
<b>Chapter 7</b>	<b>The Hypothesis</b>	<b>173</b>



# 1

## Introduction

(Dr Mador)



Every minute a woman dies from pregnancy-related causes and almost 99% of these maternal mortalities occur in developing nations (Nawal, 2008). Despite this shocking death rate, there is little or no research efforts from developing nations geared towards solving this health challenge. In 1987, the international safe motherhood conference convened in Kenya. The conference raised a global awareness of the overwhelming maternal mortality rates in developing nations and formally established the safe motherhood initiative. The goal of the initiative was to reduce maternal mortality by 50% by the year 2000, and announce to the global community the predicament of the pregnant women. Initially, United Nations (UN) agencies and governments focused on 2 strategies to reduce maternal mortality which were increasing antenatal care and training for traditional birth attendants. From all indications, there was no place for research in the strategies employed. By the year 2000, the goal was far from realized. The global community reaffirmed its commitment in 2000, and the United Nations issued 8 Millennium Development Goals (MDGs); the fifth goal (MDG-5) stipulated a reduction of the maternal mortality rate by 75% by 2015. With 2015 around the corner, it is like the outcome will be the same as it was with the safe motherhood initiative in the year 2000.

According to World Health Organization (2005) report, the main causes of maternal deaths are postpartum haemorrhage (24%); indirect causes such as anemia, malaria, and heart disease (20%); infection (15%); unsafe abortion (13%); preeclampsia-eclampsia (12%); obstructed labour (8%); and ectopic pregnancy, embolism, and anesthesia complications (8%). Preeclampsia-eclampsia is a hypertensive, multi-system disease exclusive to human pregnancy whose cause remains unknown (Pennington *et al.*, 2012). This disease is characterized by placental hypoxia and/or ischemia, excessive oxidative stress, in association with endothelial dysfunction. It is the most common medical complication of pregnancy

whose incidence has continued to increase worldwide. Risk factors for preeclampsia include nulliparity, multifetal gestations, previous history of preeclampsia, obesity, diabetes mellitus, vascular and connective tissue disorders like systemic lupus erythematosus and antiphospholipid antibodies, age >35 years at first pregnancy, smoking, and African American race (Elosha *et al.*, 2012). Among primiparous women, there is a disparity among ethnic groups as the risk in African American women is twice that of Caucasian women, and the risk is also very high in women of Indian and Pakistani origin (Rao *et al.*, 2006). Although management of this medical condition is evidence-based, preventive measures/screening tools are lacking and delivery remains the only cure. But why is this disease exclusive to human pregnancy?

Just like any other living organism, man is made from chemical elements which are combined to form molecules such as including fats, carbohydrates, proteins and nucleic acids. These molecules put together make up cells, the basic units of the human body, capable of carrying out life processes which are nutrition, respiration, excretion, growth, movement, irritability and reproduction. An organism either takes in food or if it is a green plant, makes its food from raw materials. The process of taking in or making food and preparing it for use in such activities as respiration and growth is called nutrition. Secondly, an organism is constantly using up energy as it carries out the processes which keep it alive. It obtains the energy it needs by breaking down complex materials into simpler ones. This process is called respiration. Again, an organism increases in size and mass at least while it is young. It also replaces and repairs worn-out or damaged parts of its body throughout life. Once more, an organism is sensitive to changes in the surrounding and responds to them, often by some form of movement. The ability to perceive and respond to stimuli is called irritability. Apart from this, most animals can walk, swim or fly from one place to another. Plants also show movements but most move only parts of themselves while the plant itself remains

fixed to one spot. Movement of the whole organism from one place to another is called locomotion. It is general in animals but rare in plants. Once more, organisms can produce new members of their species through a process called reproduction. Finally, many chemical activities go on in an organism and produce waste products which are substances the organism does not need and which may poison it if they are allowed to build up in the body. Every organism has some means of getting rid of its waste products. The process is called excretion. The common excretory products formed in the bodies of animals are water, carbon dioxide, mineral salts and nitrogenous compounds such as urea, uric acid and ammonia compounds. These products may come either from every cell in the body or from certain parts of the body only. Most of them are products of the body's metabolism, and can be referred to as metabolites. For the purpose of removing waste products from the body, almost all animals are equipped with special excretory organs. The excretory organs in mammals are the kidneys, the lungs, the liver and the skin.

Unlike the majority of mammals, uric acid is the end product of purine metabolism in man, due to the loss of uricase activity during the evolution of hominids. This loss, together with uric acid balance in the kidney and the lifestyle and eating habits of developed countries, has led to a high prevalence of hyperuricaemia and its consequences. Majority of mammals have very low serum urate levels because uric acid is transformed by uricase to allantoin, a very soluble excretion product, which is freely eliminated by the urine (Hayashi *et al.*, 2000). The lack of uricase makes uric acid the end product of purine metabolism in humans and other higher primates (Richette *et al.*, 2010; Riches *et al.*, 2009) and is the main reason why serum uric acid levels in adult males are ~6.0 mg/dl, compared with the majority of mammals who have uric acid levels <0.5–1 mg/dl (Ames *et al.*, 1981; Watanabe *et al.*, 2002; Johnson *et al.*, 2003). This makes human beings particularly susceptible to changes induced by diet (Feig and Johnson,

2009), and hence this is the main reason for humans to be the only mammals who develop gout spontaneously (Doherty, 2009). The origin of uricase is very old, being present in a great variety of organisms, from bacteria to mammals and it has different metabolic activities depending on the host organism. There is a cross-reaction between the uricases of different species, having the same tissue specificity and cell location, as well as similar molecular weight. Hence, it suggests that the uricases of diverse species have a common evolutionary origin (Oda *et al.*, 2009). Humans, some higher primates and certain New World monkeys do not show any detectable level of uricase activity. This is due to the appearance of several mutations of its gene during the evolutionary process, which made it non-functional (Wu *et al.*, 1992). In other monkeys in the Old and New Worlds, uricase activity is moderate, between two and four times lower than that in mice and rabbits (Oda *et al.*, 2009), and also less stable (Wu *et al.*, 1992). Wu *et al.* (1992) identified three mutations in the uricase gene in humans, chimpanzees and gorillas, including two nonsense mutations, one of codon 33 and another of codon 187, and a mutation in the splice acceptor signal of exon 3. The codon 33 mutation is also present in the orangutan. Based on the phylogeny of human evolution, Wu *et al.* (1992) established that the codon 33 mutation happened 24 million years ago; the mutation of codon 187 took place 16 million years ago, when the orangutan had already followed another line; and the exon 3 mutation occurred 13 million years ago, affecting the human/gorilla/chimpanzee line ((Wu *et al.*, 1992). Later on, Oda *et al.*, (2009) did not find any uricase activity in humans, chimpanzees, gorillas, orangutans or gibbons, but they find functional uricase in other monkeys, such as baboons and rhesus monkey. They have found up to eight independent nonsense mutations in hominids without uricase activity. They mainly attribute the loss of uricase activity to the nonsense mutation of codon 33 of exon 2, dating it to 15 million years ago. The promoter region of the gene had probably already been degraded in the evolutionary process by previous mutations, being more likely a gradual loss of uricase activity rather than a single step loss (Oda *et al.*, 2009;



Jhonson *et al.*, 2005). This is reasonable because the inactivation of the uricase gene in the mouse causes a pronounced hyperuricaemia nephropathy due to urate, resulting in more than half the mutant mice dying before 4 weeks of age (Wu *et al.*, 1994). A gradual loss of activity would allow adaptation measures to the new situation to be developed (Jhonson *et al.*, 2005). Several independent mutations in the uricase gene occurred during the evolution of hominids as well as in monkeys of the Old and the New Worlds. These mutations have been interpreted as clear evidence of an important evolutionary advantage for the early primates that had increased uric acid (Wu *et al.*, 1992; Christen *et al.*, 1970). In the same way, as purine degradation is much less complete in higher animals than in others that we consider lower, it is obvious that certain enzymes had been lost during animal evolution and it is assumed that it provided some evolutionary advantage (Hayashi *et al.*, 2000). On the other hand, if uric acid was a harmful waste product, it would be difficult to explain how the kidneys recover 90% of filtered uric acid (Kutzing and Firestein, 2008), instead of eliminating it. The evolution of hominids and the physiology of renal urate balance have associated uric acid as something beneficial that we must keep instead of something harmful that has to be removed. These facts have led various authors to propose some hypotheses on the evolutionary advantages of the loss of uricase and the subsequent increase in uric acid.

With this background information one might be led into wondering whether uric acid is not the sole cause of preeclampsia-eclampsia. According to Austin Hill, the causal link between a specific factor (e.g., cigarette smoking) and a disease (such as emphysema or lung cancer) must fulfill certain minimal conditions (Hill, 1965) needed to establish a causal relationship between two items referred to as Hill's criteria of causation. These criteria for causation are:

1. Temporal Relationship: Exposure always precedes the outcome. If factor "A" is believed to cause a disease, then it is clear that factor "A" must

necessarily always precede the occurrence of the disease. This is the only absolutely essential criterion.

2. **Strength:** This is defined by the size of the association as measured by appropriate statistical tests. The stronger the association, the more likely it is that the relation of “A” to “B” is causal. For example, the more highly correlated hypertension is with a high sodium diet, the stronger is the relation between sodium and hypertension.
3. **Dose-Response Relationship:** An increasing amount of exposure increases the risk. If a dose-response relationship is present, it is strong evidence for a causal relationship. However, as with *specificity*, the absence of a dose-response relationship does not rule out a causal relationship. A threshold may exist above which a relationship may develop. At the same time, if a specific factor is the cause of a disease, the incidence of the disease should decline when exposure to the factor is reduced or eliminated.
4. **Consistency:** The association is consistent when results are replicated in studies in different settings using different methods. That is, if a relationship is causal, we would expect to find it consistently in different studies and among different populations. This is why numerous experiments have to be done before meaningful statements can be made about the causal relationship between two or more factors. For example, it required thousands of highly technical studies of the relationship between cigarette smoking and cancer before a definitive conclusion could be made that cigarette smoking increases the risk of (but does not cause) cancer. Similarly, it would require numerous studies of the difference between male and female performance of specific behaviors by a number of different researchers and under a variety of different circumstances before a conclusion could be made regarding whether a gender difference exists in the performance of such behaviors.

5. **Plausibility:** The association agrees with currently accepted understanding of pathological processes. In other words, there needs to be some theoretical basis for positing an association between a vector and disease, or one social phenomenon and another.
6. **Consideration of Alternate Explanations:** In judging whether a reported association is causal, it is necessary to determine the extent to which researchers have taken other possible explanations into account and have effectively ruled out such alternate explanations. In other words, it is always necessary to consider multiple hypotheses before making conclusions about the causal relationship between any two items under investigation.
7. **Experiment:** The condition can be altered (prevented or ameliorated) by an appropriate experimental regimen.
8. **Specificity:** This is established when a single putative cause produces a specific effect. This is considered by some to be the weakest of all the criteria. The diseases attributed to cigarette smoking, for example, do not meet these criteria. When specificity of an association is found, it provides additional support for a causal relationship. However, absence of specificity in no way negates a causal relationship. Because outcomes (be they the spread of a disease, the incidence of a specific human social behavior or changes in global temperature) are likely to have multiple factors influencing them, it is highly unlikely that we will find a one-to-one cause-effect relationship between two phenomena. Causality is most often multiple. Therefore, it is necessary to examine specific causal relationships within a larger systemic perspective.
9. **Coherence:** The association should be compatible with existing theory and knowledge. In other words, it is necessary to evaluate claims of causality

within the context of the current state of knowledge within a given field and in related fields. What do we have to sacrifice about what we currently know in order to accept a particular claim of causality?

The connection between these risk factors and preeclampsia is poorly understood hence the need of further research. The differences in risk among ethnic groups suggest a strong role for genetic factors in the pathogenesis of preeclampsia. Towards this end, whatever is causing this disease condition should fit into the Hill's causative criteria. Most theories on the aetiology of preeclampsia suggest that the disease is a cascade triggered by combination of abnormal maternal inflammatory response, endothelial cell activation/damage with deranged haemodynamic milieu, and deranged immunity. The precise trigger that unifies the deranged vascular, immune and inflammatory response remains to be explained. In this book, emerging concept in pathogenesis of preeclampsia is discussed and therapeutic options reviewed.

# 2

## Evolution

(Dr Pam)



The ability to produce new living individuals is a characteristic feature of all living organisms and is known as reproduction. Reproduction is the only means by which life is maintained. Every living thing whether it be a plant or animal, strives to exist forever but this is not possible as each living form has only a certain life span. Therefore, living organisms have resorted to reproduction of new individuals resembling themselves so that their species can go on existing.

Each plant and animal usually give rise to several new individuals each time it reproduces. If this went on indefinitely, the number of individuals of each kind would increase greatly and there would hardly be any space for Man himself to live. However, such a problem has never occurred. This is because the older organisms die and in so doing, make room for the younger ones. At the same time, not all the newly-produced young ones survive. When there are large number of a particular plant or animal in any one place, competition occurs among the individuals and only the stronger ones manage to survive. The weak ones die off sooner or later. Thus, of the total number of organisms produced, there will always be only a few that survive. These in turn will produce new ones to keep the species going. The formation of new types of plant and animals from old types is known as evolution. Several biologists have attempted to explain how evolutionary changes take place. For example, Lamarck, a Frenchman who lived in the nineteenth century postulated that new organs or characteristics arose in an animal when there was need for them. Organs which were not needed were discarded. He later postulated that these changed or acquired characteristics were passed on to the next generation. Lamarck and his colleagues sited evidence of evolution in certain anatomical features of vertebrates. According to these biologists, there is a progressive evolutionary change in the anatomy of the heart in the various classes of vertebrates. Fishes have a simple heart with one auricle and one ventricle, amphibians have two auricles and one ventricle, reptiles have

two auricles and a partially divided ventricle, and birds and mammals have two auricles and two ventricles. In the course of these changes, the circulation of blood also changes from a “single” to a perfected “double” circulation. Other evolutionary changes in anatomy can be traced in the progressive development of the brain, sense organs like ears, and the limbs. They explained that the limbs of various vertebrates have been modified for a number of functions. For example the pentadactyl fore limb is modified into

1. Wings for flying in birds and bats.
2. Flippers for swimming in whales.
3. Legs for walking and running in horses and
4. Arms for grasping and holding in human beings and other bipeds.

The fact that these various types of limbs have the same basic pentadactyl structure indicates that all these animals must have come from a common ancestor. They further posited that the presence of a vestigial organs is readily, explained by the theory of evolution. The muscles of the ear for example are usually mere vestiges in man unlike those which are found, say, in the horse. The reason for this is, should a noise come from one side, man is able to turn his mobile neck quickly, on the other hand, the horse cannot turn its neck so easily and instead, twists back its ears to catch the sound. In some men, however, the muscles that “twitch” the ears remain quite well-developed and they can move their ears in much the same way as the horse, though possibly not so extensively. Another interesting human rudiment is the body’s hair which is very poor when compared with the fur of cats, foxes and other animals. In spite of this, each hair is fitted with a complete muscular and nervous apparatus for “bristling”. Often, a newly-born baby has a more or less complete downy coat (lanugo) which does not, however, grow on the palms of the hands and the sole of the feet. The appendix, an organ which is so often the cause of serious illnesses, is also a



vestigial organ. In herbivorous animals there is a long blind tube called caecum which helps in the digestion of cellulose. It is probably the result of changing over to flesh-eating that this caecum in man has shrunk and become a worm-like blind tube about 10 cm long. A study of comparative embryology provides further evidence for evolution according to these biologists. A very young human embryo looks very similar to the young embryos of other mammals, birds and reptiles. At certain stages in their development all these embryos have fish-like characteristics with gill slits in their pharynx and a vascular system with a single circulation. From these and other characteristics it is possible to infer that land vertebrates probably had aquatic ancestors.

Charles Darwin, an Englishman, together with Wallace put forward the theory of natural selection where only the fittest individuals survive. He thought that there would always be only a certain number of particular plant or animal on earth and as years go by, accompanied by climatic changes, new types of plants and animals would be produced. The struggle for existence suggested by Darwin arises out of the high rate of increase and reproduction which is present among all animals, Man perhaps being the only one to show signs of being an exception. As a result of overcrowding, some members of a community get pushed out of a favourable environment into less ideal surroundings. Here, they will either disappear or, by virtue of unusual characteristics survive and even thrive. Again, in the course of time some variants will arise which are more adapted to the climate and environment than the original inhabitants. They will overpower and eventually eliminate the original species. On the other hand, other variants will possess features which make life almost impossible. These, which are called monsters, are soon eliminated from the competition of life. However, in a way the monster is very closely allied to the genius who is an equally strange variation from the normal and as such a matter of chance. Today, we know that mutation is one of the important mechanisms which confer certain advantageous

characteristics to certain species. Thus, a mutant may have a slight advantage in the struggle for existence and could become widespread in the population within a few generations.

The question often arises as to whether evolution and natural selection apply to man nowadays as to other animals. The answer is either yes or no. This is because man has so profoundly altered his environment that the meaning of the word “fittest” is changed. “Fittest for what?” is the question that must be asked/ until man arrived on the world-stage, animals that survived were those fittest to combat such difficulties as presented by the climate – heat, cold, winds and rain in whatever combination possible. Obtaining food and warmth were the main considerations, even of the first wandering tribes of man. But gradually these elemental difficulties have been solved, at least in part, by the progress of civilization, particularly by trade, commerce and science, until they form nowadays but a minor consideration in man’s life. Man’s intelligence is now free to be devoted to his job, to the learning of the arts and sciences, and to conscious study of his own conditions. No longer does each man fight his individual battle for life. He depends on other fellow men, each having a special part to play, while he himself takes a portion of what they produce and provides his own contribution in return. If you consider how an object like a loaf of bread reaches you, you will realize how many people you depend on for it. This is only one example of the idea of service and dependence within a community.

# 3

## The Quest

(Dr Mador)



Preeclampsia is the occurrence of hypertension and significant proteinuria in a previously healthy woman on or after the 20th week of gestation and is said to occur in about 2–8% of pregnancies. Literature search shows that the aetiology of this disease has been studied by a large number of investigators in different parts of the world and the search is still going on. According to McMillen (2003), Francois Mauriceau was the first person to scientifically describe eclampsia and to point out that primigravidas were at greater risk for convulsions compared to multigravidas. As for the causes of convulsions, Mauriceau ascribed convulsions to either abnormalities in lochial flow or intrauterine fetal death. After the introduction of the word “eclampsia,” Bossier de Sauvages (1739) differentiated eclampsia from epilepsy (Chesley, 1978; Friedlander, 2001). In 1797, Demanet noted a connection between edematous women and eclampsia (Chesley, 1978) while John Lever discovered albumin in the urine of eclamptic women in 1843 (Thomas, 1935). The connection between premonitory symptoms during the later months of pregnancy and the development of puerperal convulsions was also recognized in 1843 by Dr. Robert Johns. These premonitory symptoms included headache, temporary loss of vision, severe pain in the stomach, and edema of the hands, arms, neck, and face (Johns, 1843). With these developments, physicians were now aware that the presence of edema, proteinuria, and headaches should raise concern about the possibility of convulsions (Sinclair & Johnston, 1858). In 1897, Vaquez and Nobecourt were credited with the discovery of eclamptic hypertension (Chesley, 1978). As a result of these contributions, the concept of the preeclamptic state was recognized. Today, preeclampsia is known to be a pregnancy associated disease of primigravidas, occurring mainly after 20weeks gestation. When present in multiparous women, it is commonly associated with multiple pregnancies or in their first pregnancy with a new partner. The occurrence of preeclampsia in molar pregnancy hints that the presence of a fetus is not essential to the development of the disease.

Despite active research for centuries, the aetiology of this disorder exclusive to human pregnancy is a mystery, and that is why it is still a disease of theories. In the 18<sup>th</sup> century for example, Boissier de Sauvages distinguished eclampsia from epilepsy. Along with the distinction he made in disease classification, de Sauvages offered his views on the cause of convulsions. He believed that convulsions resulted from nature trying to free the organism of any morbid element (Temkin, 1971). Theories on disease causation continued to be proposed and thoroughly discussed in the writings of 19<sup>th</sup> century physicians. In his work entitled *Introduction to the Practice of Midwifery*, Dr. Thomas Denman (1821) focused much attention on the labours affected by convulsions. Although Denman credited convulsions to certain traditions and etiquettes associated with living in big cities and towns, he noted that the greatest risk of convulsions came from the uterus. According to Denman, as the uterus expanded with pregnancy, greater pressure was placed upon the descending blood vessels. Such an increase in pressure lead to the regurgitation of blood in the head and resulted in an overload of the cerebral vessels and subsequent convulsions (Denman, 1821).

In his 1849 work titled “Parturition and the Principles and Practice of Obstetrics”; Dr. William Tyler Smith challenged the theory of cerebral congestion, for he believed that pregnancy was a state of increased fullness in circulation. Given that contractions during the second stage of labour normally interfered with the circulation of blood, he believed that more cases of convulsions would be observed if such congestion caused convulsions. In contrast, Smith attributed puerperal convulsions to several other causes which include: any mechanical or emotional stimulus applied in excess to the spinal centre; bloodletting; variations in the wind, temperature, and other atmospheric changes; irritation of the uterus, uterine passages, intestinal canal, and the stomach; and “toxic” elements. As for Smith’s theory on “toxic” elements, he believed that preservation of health during pregnancy depended on the exponential increase in the elimination of wastes (e.g.,

secretions of the bowels) and debris from the maternal and fetal systems. Failure to do so resulted in a “toxemia” in which morbid elements accumulated in the blood causing irritation to the nervous center (Smith, 1849).

Although researchers in the 20<sup>th</sup> century failed to uncover the aetiology of preeclampsia, much progress was made in the understanding of pathophysiological changes associated with its development. In the 1960's, several groups described dramatic differences in placental physiology between placentas from pregnancies affected by preeclampsia versus placentas from pregnancies unaffected by preeclampsia. Through the examination of placental bed biopsies, it was discovered that placental trophoblast cells failed to adequately invade maternal spiral arteries and convert the arteries from small muscular vessels into large, low resistant vessels in preeclampsia. With the lack of spiral artery conversion, arterial lumen diameter and distensibility was limited, resulting in restricted blood flow to the placenta and growing fetus (Brosens *et al.*, 1967; Brosens *et al.*, 1972; Gerretson *et al.*, 1981; Kong *et al.*, 1986). Although these findings were instrumental in laying the groundwork for the current understanding of preeclampsia-eclampsia, not all theories or scientific discoveries have readily been accepted by the scientific community. Published in the American Journal of Obstetrics and Gynecology in 1983, the *Hydatoxi lualba* (parasitic worm) theory of preeclampsia was one such conjecture swiftly refuted by the scientific community. Under this theory, it was posited that the development of preeclampsia-eclampsia may be associated with the presence of a worm-like organism. Specimens collected from women with preeclampsia-eclampsia, including peripheral circulating blood, bloody fluid on the maternal surface of the placenta, and umbilical cord blood, were found to be positive for *Hydatoxi lualba* (Lueck *et al.*, 1983). However, several other research groups demonstrated that starch powder from gloves, cellulose debris from common laboratory paper products, and alterations in staining technique

produced the same characteristic worm-like organisms (Papoutsis *et al.*, 1983; Sibai & Spinnato, 1983), which lead to refutation of the theory.

Unlike the parasitic worm theory, the theory posited by Roberts and his colleagues in 1989 continues to guide research related to preeclampsia-eclampsia aetiology. Roberts and his colleagues posited that preeclampsia represented an endothelial disorder. Drawing on past work that associated preeclampsia with shallow trophoblast invasion and subsequent reduction in placental perfusion, they hypothesized that the ischemic placenta released a damaging factor(s) into the maternal circulation. Although factor identity was unknown, the circulating factor was hypothesized to have caused endothelial dysfunction and would lead to activation of the coagulation cascade, blood pressure abnormalities, and loss of fluid from the intravascular space (Roberts *et al.*, 1989). In the opinion of Mador *et al.*, (2013), this placental factor is unsatisfactory for two reasons. Firstly, they believe that the factor which causes endothelial dysfunction is a genetic material of embryonic origin and not a gene product released by the placenta. Without the genetic material, it is not clear why the disease condition will be seen in primigravidas or during first pregnancy in multiparous women who have changed partner. Secondly, the placental factor does not cause endothelial dysfunction in subsequent pregnancies if it did not cause damage in the first pregnancy except when there is multiple gestation or molar pregnancy.

The 1980 discovery of nitric oxide as an endothelial cell-derived relaxing factor resulted in an unprecedented biomedical research of nitric oxide and established it as one of the most important cardiovascular system molecule. A reduction in endothelial cell nitric oxide levels leading to “endothelial dysfunction” has been identified by several investigators as a key pathogenic event preceding the development of hypertension. The reduction in endothelial nitric oxide in cardiovascular disease has been attributed to the action of



antioxidants that either directly react with nitric oxide or uncouple its substrate enzyme. Gersch and his co-worker demonstrated in 2008 that uric acid reacts directly with nitric oxide in a rapid irreversible reaction resulting in the formation of 6-aminouracil and depletion of nitric oxide. As a follow-up to this research finding, a study was designed (Mador *et al.*, 2013) to assess the level of uric acid in maternal circulation during normal pregnancy and it was found out that uric acid level was significantly higher in pregnant women than nonpregnant women with levels in the 4<sup>th</sup>, 7<sup>th</sup> and 8<sup>th</sup> months being higher when compared to the other months of gestations. Based on this, it was proposed that the damaging factor released into the maternal circulation by the ischaemic placenta is uric acid produced from genetic material of cells of embryonic/fetal origin.



# 4

## Genetic Code

(Dr Isichei)



In 1869, Friedrich Miescher isolated a substance from the nucleus of a cell. He had no idea of its importance and did not pursue his discovery to its logical conclusion. It was only after half a century later that scientists began to suspect that Miescher's forgotten chemical, now called deoxyribonucleic acid (DNA) was the missing link between inanimate and animate matter. In 1903 a medical student by name Sutton proposed the chromosome theory of inheritance. He suggested that genes, the basic units of heredity capable of transmitting characteristics from one generation to the next, are carried on chromosome. In the 1940s Avery and his colleagues discovered that the chromosomes carry some acids and they quickly named them nucleic acids because they were associated with the nucleus. The basic unit of nucleic acids is the nucleotide. Nucleotides are found in the cell either as components of nucleic acids or as individual molecules, in which form they play several different functions. Each nucleotide is a complex molecule made up three distinct components: a sugar, a nitrogenous base, and phosphoric acid. The phosphate of one nucleotide is linked to the sugar of the nucleotide. The nucleic acids were later discovered that they were deoxyribonucleic acid (DNA) and ribonucleic acid (RNA) respectively based on their sugar components. DNA is the store of genetic information while RNA is used in the expression of genetic information. There are four different bases in each class of nucleic acid. Three are common to both and one is unique to each. It was postulated that the genes were carried by the DNA; but the question is that "how can a DNA carry gene?" Research has proven that the biological information carried by a gene is contained in the nucleotide sequence. This information is in essence a set of instructions for the synthesis of an enzyme or other protein molecule. In 1953, Francis Crick and James Watson of Cambridge University deduced that DNA resembled a twisted ladder capable of zipping apart. They developed the double helix model of the DNA which suggested that the DNA was made up of a nucleotide base which could be purine or pyrimidine and

that each base is attached to a pentose sugar that is phosphorylated. They explained further that the nucleotides are arranged in a ladder-like structure. Each rung of the ladder is formed by a pair of nitrogenous bases. The frame of the ladder is made of deoxyribose sugars and phosphates arranged alternately and in a linear manner. The two chains of DNA are not held straight but are coiled double and twisted to form a spiral helix or a double helix. The gene contains the message that is responsible for inherited traits or characters. This message is stored in the form of a code. It has been shown by scientists that the code is responsible for a message that allows protein synthesis in the body. This code is known as the genetic code. It resides in the DNA molecules and is recorded in such a way that it can be replicated and passed on from one generation to generation. Very detailed experimental studies have shown that the genetic code resides in the sequence on the nitrogenous bases of the nucleotides down on the length of the DNA chain. The nitrogenous bases in nucleic acids are adenine, guanine, cytosine, thymine and uracil. Adenine and guanine are purine bases while cytosine, thymine and uracil are pyrimidine bases.

Uric acid is generated in mammalian systems as an end product of purine metabolism. In most mammals, uric acid is further degraded to allantoin by the enzyme Uricase; however, this enzyme was mutated in hominoids five to fifteen million years ago (Wu *et al.*, 1992). This loss of Uricase activity does not only result in higher plasma uric acid levels, but also limits our ability to regulate uric acid, such that widely varied levels may be observed in man. Uric acid possesses free radical –scavenging properties (Kuzkaya *et al.*, 2005; Robinson *et al.*, 2004) and is the most abundant antioxidant in human plasma (Ames *et al.*, 1981; Kand'ar *et al.*, 2006; Hediger, 2002). It may also act as a prooxidant under conditions of oxidative stress (Aruoma and Halliwell, 1989; Bagnati *et al.*, 1999; Sanguinetti *et al.*, 2004; Kittridge and Willson, 1984). Markedly increased levels are known to cause gout and nephrolithiasis, but more importantly have been

associated with increased risk of the development of cardiovascular disease, particularly hypertension, obesity/metabolic syndrome, and kidney disease (Iseki *et al.*, 2001; Tomita *et al.*, 2000; Johnson *et al.*, 2005; Nakagawa *et al.*, 2006; Masuo *et al.*, 2003). Recent experimental and clinical studies have linked elevated uric acid with endothelial dysfunction and a reduction in nitric oxide levels (Khosla *et al.*, 2005). Experimental studies have reported that uric acid can reduce nitric oxide levels in endothelial cells in culture (Khosla *et al.*, 2005), block acetylcholine-induced vasodilatation of aortic rings (Khosla *et al.*, 2005) and reduce circulating nitrites in experimental animals (Khosla *et al.*, 2005). In human, a circadian rhythm has been identified in which uric acid and nitric oxide levels are inversely correlated (Kanabrocki *et al.*, 2000). Chronic hyperuricemia is also associated with endothelial dysfunction (Khosla *et al.*, 2005) and reducing uric acid levels with xanthine oxidase inhibitors have been found to markedly improve endothelial function. However, xanthine oxidase inhibitors also reduce oxidant generation, so the improvement in endothelial function could reflect a direct reduction of xanthine oxidase-associated oxidants as opposed to a reduction in uric acid per se.

While the importance of endothelial dysfunction in cardiovascular disease is well accepted, most evidence suggests that the primary mechanism by which this occurs is via oxidative stress in which superoxides either directly inactivates nitric oxide (by forming peroxynitrite), uncouples the endothelial nitric oxide synthase, or passively increase an inhibitory substrate (asymmetric dimethylarginine) by inhibiting the enzyme, dimethylarginine dimethylaminohydrolase (Forstermann, 2006). In this regard, uric acid has been shown to help preserve endothelial nitric oxide levels via its role as an antioxidant, either by blocking the uncoupling of endothelial nitric oxide synthase by reacting with peroxynitrite (Forstermann, 2006) or by preventing the oxidant-induced inactivation of extracellular superoxide dismutase (Goldstone *et al.*, 2006). A paradox then develops, how can uric acid,

Preeclampsia is Related to Uric Acid: An Anthropometric Model with the Fetus

which is the most abundant (about six times as ascorbate) antioxidant in plasma (Hediger, 2002) induce endothelial dysfunction in vivo?



# 5

## **Uric Acid & Preeclampsia**

**(Dr Mador)**



The association of hyperuricemia with Preeclampsia has been known since 1917 (Slemons and Bogert, 1917) while the relationship of the degree of hyperuricemia and the severity of disease has been known since 1934 (Stander and Cadden, 1934). What is not clear is the role that uric acid plays in the pathophysiology of preeclampsia – whether it is a marker of disease or whether it actively takes part in the pathogenesis of disease. Although hyperuricemia does not predict the development of preeclampsia, the severity of hyperuricemia has been observed to correlate with maternal and fetal morbidity and severity of renal lesion, and to be inversely proportional to birth weight. Most often, increase of the uric acid level precedes the onset of proteinuria and hypertension, suggesting a possible causal role of uric acid. In human blood plasma, the reference range of uric acid is between 139  $\mu\text{mol/l}$  – 393  $\mu\text{mol/l}$  in women. Serum uric acid can be elevated due to reduced excretion by the kidneys, fasting or rapid weight loss.

Each organism has a strictly defined genetic makeup. This is inherited from its predecessors and used by the organism itself to direct its cellular functions. It then passes on its own genetic information to its progeny. Each cell of a particular organism contains the same genetic information. This genetic information is stored in the chromosomes of the cell as nucleic acids. The nucleic acids are subdivided into two types: deoxyribonucleic acid (DNA) and ribonucleic acid (RNA). The two types are both polymers built from the same type of subunit called nucleotides. Each nucleic acid is a polymer usually many thousands of nucleotides long, but each polymer is composed of a variable sequence of only four different nucleotide structures. Each nucleotide consists of:

1. a base composed of a carbon and nitrogen ring structure,
2. a pentose (5 carbon) sugar which is either deoxyribose or ribose, and
3. one, two or three phosphates attached to the sugar.

There are four different bases in each class of nucleic acid. Three are common to both and one is unique to each. The bases are described as either a purine type or a pyrimidine type. The five bases are:

1. adenine (A) – purine type.
2. guanine (G) – purine type.
3. cytosine (C) – pyrimidine type.
4. thymine (T) – pyrimidine type.
5. uracil (U) – pyrimidine type.

There are subtle but important differences between the subunits used in the synthesis of DNA and those which are incorporated into RNA. In addition, there are differences in the structure of the two nucleic acids.

DNA	RNA
Contains A, G, C and T	Contains A, G, C and U
Contains deoxyribose	Contains ribose
Is double stranded	Is single stranded
Stores genetic information	Is used in the EXPRESSION of genetic information

Uric acid is generated in mammalian systems as an end product of purine metabolism. Metabolism is an inclusive term for the chemical reactions by which the cells of an organism transform energy, maintain their identity, and reproduce. All life forms are dependent on many hundreds of simultaneous and precisely regulated metabolic reactions to support them from conception through growth and maturity to the final stages of death. Each of these reactions is triggered, controlled, and terminated by specific cell enzymes or catalysts, and each reaction is coordinated with the numerous other reactions throughout the organism. Two metabolic processes are recognized. These are anabolism and catabolism. Anabolism, or constructive metabolism, is the process of synthesis required for the

growth of new cells and the maintenance of all tissues. Catabolism or destructive metabolism on the other hand, is a continuous process concerned with the production of the energy required for all external and internal physical activity. Catabolism also involves the maintenance of body temperature and the degradation of complex chemical units into simpler substances that can be removed as waste products from the body through the kidneys, intestines, lungs, and skin.

Anabolic and catabolic reactions follow what are called pathways that are linked to produce specific, life-essential end products. Scientists have been able to determine how some of these pathways weave together, but many of the finer intricacies are still only partly explored. Basically, anabolic pathways begin with relatively simple and diffuse chemical components, called intermediates. Taking their energy from enzyme-catalyzed reactions, the pathways then build toward specific end products, especially macromolecules in the forms of carbohydrates, proteins, fats and nucleic acids. Using different enzyme sequences and taking the opposite direction, catabolic pathways break down complex macromolecules into smaller chemical compounds for use as relatively simple building blocks. When anabolism exceeds catabolism, growth or weight gain occurs. When catabolism exceeds anabolism, such as during periods of starvation or disease, weight loss occurs. When the two metabolic processes are balanced, the organism is said to be in state of dynamic equilibrium.

The fact that cells and tissues retain their dynamic equilibrium throughout the life of an organism clearly shows that metabolic processes are under fine control. Cells and entire tissues are constantly dying, yet all the chemical ingredients that replenish and form new cells and their products are supplied by metabolism, striking a nearly perfect balance. Although much remains to be revealed about metabolic processes, scientists now agree that regulatory, or rate-limiting, enzymes figure largely in the reactions involved. Affecting metabolic pathways

at the earliest steps, each enzyme molecule has a specific, or active, site that matches, or “fits,” its particular substrate—the compound with which the enzyme forms a product. The precision with which rate-limiting enzymes and substrates join to set off a particular reaction inhibits reactions from occurring indiscriminately in cells, where so many diverse chemical compounds are in flux. Tiny amounts of a rate-limiting enzyme can cause profound changes in the metabolism of a cell. Another way in which metabolic pathways are controlled is through negative feedback. Thus, once a cell synthesizes the correct balance of a product, such as ATP, the accumulation of that product will inhibit the enzymes that trigger its production. Metabolism, especially in higher animals, is also regulated by the nervous system and by the pancreas, the pituitary and adrenal glands of the endocrine system. Hormones, secreted into the bloodstream, reach target tissues, often altering the permeability of cell membranes and thereby altering the amounts of substances that get into and out of cells. Liver is the major organ involved in degradation of purine nucleotides. Lysosomal enzymes convert nucleic acids to nucleotides. Majority of purine nucleotides so produced are AMP and GMP. AMP is converted to IMP by adenylate deaminase present in most of the tissues. Next, nucleotidases convert IMP, AMP and GMP to corresponding nucleosides namely inosine, adenosine and guanosine. By the action of adenosine deaminase adenosine is converted to inosine. Now purine nucleoside phosphorylase converts guanosine to guanine and inosine to hypoxanthine by transferring ribose. Deamination of guanine by guanase produces xanthine. Finally hypoxanthine and xanthine are converted to uric acid by xanthine oxidase. Uric acid produced in different tissues diffuses into circulation and carried to kidneys for elimination. Uric acid daily production is about 500-600mg. However, most of it is removed by kidney. Daily output is about 0.3-0.5 g/day on normal diet. The normal blood uric acid level is below 6 mg/100ml. So, one can expect that impaired renal function may lead to accumulation of uric acid in blood. Gout is common disease associated with excessive purine catabolism. It is

characterized by hyperuricemia and excessive excretion of uric acid in urine. It is more common in men (95%). Incidence rate is 3 in 1000. Since uric acid is less soluble in the body fluid aqueous environment excessive uric acid leads to formation and deposition of urate crystals in joints, cartilage of fingers, big toe and other soft tissues. Deposition of urate in joints leads to gouty arthritic attacks.

Humans and great apes have higher uric acid levels than most vertebrates because they lack the enzyme Uricase in the liver which breaks down uric acid into allantoin. In normal pregnancy, serum uric acid level slowly decreases until 16 weeks of gestation, secondary to plasma volume expansion, increased renal clearance, and the uricosuric effect of oestrogen. For most of the 2<sup>nd</sup> trimester, the uric acid level remains stable and then increases during the 3<sup>rd</sup> trimester because of increase catabolism/production. The placenta in normal pregnancy is an abundant source of purines because of its high cell turn over, resulting in higher production of uric acid. Serum uric acid is also higher in normal multifetal pregnancies compared with normal pregnancies, which could be explained by the fetus as an additional source of xanthine oxidase. Alternatively, increased serum uric acid levels in multifetal pregnancies could be secondary to the increased number of placentas. In a report of patient with xanthuria (Simmonds *et al.*, 1984), an autosomal recessive disorder that results in XO deficiency, serum uric acid levels were found to be increased at 32 weeks of gestation, but returned to baseline low levels by 6 weeks postpartum, suggesting a definitive role for fetal and/or placental uric acid production.

Fetuses exposed to hypoxia (e.g. because of decreased placental perfusion) have been shown to have increased serum levels of purine metabolites (Saugstad, 1975). Of note, since 1944, there have been 6 reported cases of gout attacks in women during or around the time of pregnancy, 4 of whom were felt to have primary or idiopathic gout (Lee and Loeffler, 1962; Irgens *et al.*, 2001). Two of

the 6 patients have a history of preeclampsia documented. The relationship of uric acid with nitric oxide has been explored in a number of studies. A circadian reciprocal pattern of nitric oxide and uric acid levels has been observed (Kanabrock *et al.*, 2000). Infusion of allopurinol into hyperuricemia patients with congestive heart failure has been shown to improve endothelium-dependent (i.e. acetylcholine co-infusion) but not endothelium-independent (e.g. nitroprusside, nitroglycerin) forearm vasodilatation (Doehner *et al.*, 2002; Farquharsan *et al.*, 2002). These patients also had improved peak blood flow distally after treatment with allopurinol (Doehner *et al.*, 2002).

To date, only one study has looked at allopurinol use in clinical preeclampsia (Gulmezoglu *et al.*, 1997). Women with severe preeclampsia between 24 and 32 weeks of gestation were given allopurinol 200mg, vitamin E 800i.u, and vitamin C 1000mg/dl for up to 14 days. The median uric acid level was 5.3, range 3.1 – 13.4mg/dl (0.32; range 0.19 – 0.81 mmol/l) in antioxidant group; and 7.1, range 4.6 – 9.1mg/dl (0.43; range 0.28 – 0.55mmol/l) in the control group. Although there was a trend towards prolonging pregnancy in the treatment group, this was not significant. Fetal outcome was not different in both groups, and there was no significant change in level of lipid peroxides between the two groups.



# 6

## **Fetal Biometrics**

**(Dr Mador)**



Biometrics is the mathematical study of variation between individuals of a certain species in a population. Information derived from the study of biometrics can give clues to variability, such as whether it is due to heredity or to the environment. Variation or deviation from the standard is a feature of living organisms. No two rabbits or maize grains for example are exactly alike when examined in detail, although in most respects, they may be similar. In fact, it is because of these similarities that we are able to classify living plants and animals into various phyla and genera. Variation is of interest to biologists who, on studying its causes and characteristics, can gain an insight into our past origin and possible future trends. Variation in an organism may be primarily due to heredity, or to environmental influences, or to a combination of the two. Seeds from a common parent plant when sown under different conditions or soil composition can give rise to plants of different health and appearance, although they possess the same genetic constitution. Identical twins with the same genotype, when brought up under different circumstances, may develop differences in height, weight, behaviour, intelligence and so on. Variation can be of two types; continuous variation or discontinuous variation. In the former, like the height or weight of man, a whole range of intermediate values exist, different only very slightly in magnitude. This continuous variation is not controlled by a single gene but is controlled by the interaction of multiple genes, in addition to influences imposed by the environment. A person may inherit the gene for tallness but if he is undernourished in his initial years of growth, he may not grow as tall as he is expected to. Hence, in man, there is a wide variation in height. In discontinuous variation, there is no gradation of a certain trait. For example, the inheritance of sex in animals is a discontinuous variation. With few exceptions, one is either a male or female and there is no intermediate. In blood grouping, we are members of one of the four groups, A, B, AB or O. Variation of a number of characters in living organisms conforms approximately to a bell-shaped curve or Gaussian

(after the mathematician, Gauss) mathematical curve which may be symmetrical or asymmetrical, i.e. skew.

From a random sampling of a large number of human fetuses, the frequency distribution for fetal biparietal diameter, fetal head circumference, fetal occipitofrontal diameter, fetal abdominal circumference, fetal femur length and fetal weight were obtained. The cross-sectional study involved pregnant women with fetuses from 12 – 42 weeks of gestation undergoing ultrasound examination. The study which was carried out in two stages was approved by the Ethics Committee of Jos University Teaching Hospital and before inclusion of the patients, informed consent was obtained. The first stage was mainly for the establishment of normal distribution of fetal parameters. In this stage only singleton pregnancies were included. Pregnant women with concomitant disease possibly affecting fetal growth (e.g. diabetes mellitus, asthma, hypertension, renal disease, thyroid disease) were not included as were those with complications of pregnancy known at the moment of the ultrasound scan (e.g. bleeding, pre-eclampsia). If a fetal malformation was detected during the examination the patient was excluded. Patients with a history of obstetric complications, intrauterine growth retardation or macrosomia were also excluded. The investigator did not take into account complications or diagnosis that occurred later in the pregnancy, after the ultrasound measurements were performed. Every fetus was measured and included only once so that a pure cross-sectional set of data was constructed. For each patient the gestational age was recorded, as were last menstrual period, maternal age and parity. Maternal age was calculated in completed years at the moment of the ultrasound. The subject to be scanned had to lie on the examination couch such that she is able to see the screen easily. Most scans were performed with the patient supine. However, in later pregnancy many patients feel dizzy in this position and it was necessary for such patients to be tilted to one side. This is easily achieved by

placing a pillow under one of the buttocks. The patient had to be uncovered just sufficiently to allow the examination to be performed. This will include the first inch of the area covered by the pubic hairs and will extend far enough upwards to allow the fundus of the uterus to be visualized. A full bladder was the only prerequisite for an ultrasound examination.

All the fetal biometric measurements were performed using Philips Real time ultrasound machine equipped with 3.5MHz transducer and an electronic caliper system set at a velocity of 1540m/s. Fetal head measurements were made in an axial plane at the level where the continuous midline echo is broken by the cavum septum pellucidum in the anterior third and that includes the thalamus. This transverse section should demonstrate an oval symmetrical shape. Measurement of BPD was from the outer edge of the closest temporomandibular bone to the outer edge of the opposite temporomandibular bone. Measurement of OFD was from the outer edge of the frontal bone to the outer edge of the occipital bone. The HC was measured around the calvarium from the same axial image as for the BPD. The abdominal circumference was measured through the transverse section of the fetal abdomen at the level of the stomach and bifurcation of the main portal vein into its right and left branches. The femur length was measured from the greater trochanter to the lateral condyle, with both ends clearly visible and at a horizontal angle  $<45^{\circ}$ . All measurements were expressed in millimeters. Estimated fetal weight was calculated in grams by the formulae described by Shepard and by Hadlock, as these are included in the software of most commercially available ultrasound scanners (Shepard *et al.*, 1982).

The second stage of the study involved blood sample collection from women who were not pregnant and those women with normal singleton/multiple pregnancies. Estimated age of pregnancy was determined using ultrasound machine and compared with age calculated from last menstrual period. The

Venous blood samples were collected from the non-pregnant women and pregnant women at various gestational ages into plain vacutainers and serum removed from cells by centrifugation as quickly as possible. This prevents possible dilution by intracellular contents. Grossly lipaemic and significantly haemolysed samples (concomitant glutathione release leads to low values) were not used. Samples were stored refrigerated for 3 – 5 days (Tietz, 1995) until analyzed for uric acid in batches and protein free filtrate used. Uricase method (Urate Oxidase, EC 1.7.3.3), the enzyme that catalyses the oxidation of Uric Acid to Allantoin which is more specific was used. The Uricase Method measures the differential absorption of Uric Acid and Allantoin at 293nm (Feichtmeier and Wrenn, 1995). The difference in absorbance before and after incubation with Uricase is proportional to the Uric Acid in a protein free filtrate, with subsequent reduction of phosphotungstic Acid to tungsten blue with sodium carbonate providing the alkaline necessary for colour development (Caraway, 1965). Each assay was validated using commercial quality control samples, standards as well as previously assayed human sera. Samples were also duplicated in-between batches. Data were then subjected to descriptive statistical analysis.

## **Biometrics of Fetal Head Circumference**

Fetal head circumference measurements were classified into thirty one groups (Tab. 6.1). The group with the highest number of observations was from 34 to 34 + 6 while 42 to 42+6 group had the lowest number of observations. Marked variability in the measurements was seen in groups 18 to 18+6, 29 to 29+6 and 40 to 42+6. In group 13 to 13+6, variation in the measurements was minimal. Standard error of mean of head circumference measurements from 12 – 42 weeks gestation was found to be less than 1 with the exception of groups 12, 18 and 29 where the standard error of mean is above 1.

The geometric mean values of head circumference measurements as seen in Tab. 6.2 were found to be less than their arithmetic means but greater than their harmonic means indicating that all the fetal head circumference measurements were not identical. The centile values of fetal head circumference measurements from 12 – 42 weeks gestation are as shown in Tab. 6.3. This table gives the 3<sup>rd</sup>, 5<sup>th</sup>, 10<sup>th</sup>, 50<sup>th</sup>, 90<sup>th</sup>, 95<sup>th</sup>, and 97<sup>th</sup> centile values for fetal head circumference measured at different gestational age ranging from 12 – 42 weeks. For example, it can be seen from the table that the 10<sup>th</sup> percentile of head circumference at 18 to 18 + 6 weeks gestation is 146 millimeters. This means that 10% of the fetuses in Jos at 18 to 18 + 6 had a mean head circumference less than 146 millimeters, while 90% had a mean head circumference greater than 146 millimeters. Similarly, the 97<sup>th</sup> percentile of head circumference at 39 to 39 + 6 is 378 millimeters. Hence 97% of fetuses at 39 to 39 + 6 had a mean head circumference less than 378 millimeters while 3% had a mean head circumference greater than 378 millimeters.

The standard score or z-score of head circumference measurements in 13,740 fetuses in Jos ranging from 12 – 42 weeks of gestation is as shown in Tab. 6.4. The z-score enables one to look at head measurements at each gestational age and see how they compare on the same standard; taking into account the mean and standard deviation of each gestational age. For example, head circumference measurements at 12 weeks are – 0.002 standard deviations from the mean while measurements at 14 weeks are 0.003 standard deviations from the mean. Again, from the above z-score table, it can be seen that the head circumference measurements at 20 and 38 weeks are 0.000 deviations from the mean.

While comparing the z-score at 12, 14, 20 and 38 weeks of gestation, it can be seen that z-score at 14 weeks gestation is higher followed by 20 weeks while at 12 weeks it is much lower because it is negative (-0.002).

**Tab. 6.1** *Frequency distribution table of fetal head circumference measurements showing arithmetic mean, standard deviation and standard error of mean from 12 – 42 weeks gestation.*

<b>GA (week, days)</b>	<b>Number of fetuses (n)</b>	<b>Mean HC (mm)</b>	<b>SD</b>	<b>SEM</b>
12 to 12+6	49	80.9	10.5	1.5
13 to 13+6	384	94.1	9.6	0.5
14 to 14+6	371	108.6	11.8	0.6
15 to 15+6	351	122.5	13.8	0.7
16 to 16+6	505	133.0	9.7	0.4
17 to 17+6	427	146.1	10.9	0.5
18 to 18+6	446	162.1	23.5	1.1
19 to 19+6	282	169.4	15.2	0.9
20 to 20+6	553	180.7	12.7	0.5
21 to 21+6	400	193.0	11.7	0.6
22 to 22+6	398	201.9	11.3	0.6
23 to 23+6	478	212.7	13.9	0.6
24 to 24+6	520	225.8	13.3	0.6
25 to 25+6	388	238.7	14.0	0.7
26 to 26+6	511	249.3	15.2	0.7
27 to 27+6	432	260.0	15.4	0.7
28 to 28+6	548	269.1	13.3	0.6
29 to 29+6	484	274.2	23.3	1.1
30 to 30+6	625	284.9	17.0	0.7
31 to 31+6	523	292.2	14.9	0.7
32 to 32+6	583	299.5	14.7	0.6
33 to 33+6	516	306.9	12.9	0.6
34 to 34+6	744	314.6	15.0	0.6
35 to 35+6	739	318.8	13.5	0.5
36 to 36+6	599	324.9	14.7	0.6
37 to 37+6	532	330.9	13.7	0.6
38 to 38+6	481	337.6	15.1	0.7
39 to 39+6	525	342.9	14.4	0.6
40 to 40+6	252	345.2	14.1	0.9
41 to 41+6	72	349.6	11.8	1.4
42 to 42+6	22	347.4	23.6	5.5
<b>Total</b>	<b>13740</b>			



**Tab. 6.2** Frequency Distribution Table of Fetal Head Circumference Measurements Showing Arithmetic mean, Geometric mean and Harmonic mean from 12 – 42 weeks Gestation.

GA (week, days)	Number of fetuses (n)	Arithmetic mean (mm)	Geometric mean (mm)	Harmonic mean (mm)
12 to 12+6	49	80.87755	80.19505	79.49107
13 to 13+6	384	94.08594	93.57099	93.02122
14 to 14+6	371	108.6388	108.0839	107.5773
15 to 15+6	351	122.4758	121.847	121.3091
16 to 16+6	505	132.9644	132.612	132.2597
17 to 17+6	427	146.1148	145.7095	145.3004
18 to 18+6	446	162.1435	160.8212	159.7357
19 to 19+6	282	169.3652	168.754	168.1866
20 to 20+6	553	180.6998	180.2787	179.8754
21 to 21+6	400	192.9975	192.6456	192.2944
22 to 22+6	398	201.8869	201.58	201.2776
23 to 23+6	478	212.7113	212.2518	211.7762
24 to 24+6	520	225.8308	225.4465	225.0655
25 to 25+6	388	238.6649	238.2416	237.7988
26 to 26+6	511	249.2681	248.8127	248.3601
27 to 27+6	432	260.0023	259.5373	259.0611
28 to 28+6	548	269.135	268.7951	268.4434
29 to 29+6	484	274.2252	272.6465	269.6992
30 to 30+6	625	284.8512	284.3175	283.7497
31 to 31+6	523	292.1931	291.7838	291.3389
32 to 32+6	583	299.5266	299.1455	298.7357
33 to 33+6	516	306.8663	306.5755	306.2606
34 to 34+6	744	314.5565	314.1824	313.7874
35 to 35+6	739	318.7767	318.4873	318.1912
36 to 36+6	599	324.9232	324.5829	324.2289
37 to 37+6	532	330.8741	330.5896	330.302
38 to 38+6	481	337.6008	337.2799	336.973
39 to 39+6	525	342.8629	342.5604	342.2585
40 to 40+6	252	345.2064	344.9261	344.6524
41 to 41+6	72	349.5555	349.3567	349.1544
42 to 42+6	22	347.3636	346.5916	345.81
Total	13740			

**Tab. 6.3** Centiles of fetal head circumference measurements.

Head circumference centiles (mm)							
Gestational age	3rd	5th	10th	50th	90th	95th	97th
12 to 12+6	56.0	61.5	69.0	79.0	96.0	98.5	101.0
13 to 13+6	75.0	78.0	82.0	94.0	106.0	108.0	109.0
14 to 14+6	92.2	94.0	96.0	108.0	118.8	122.0	126.0
15 to 15+6	104.6	110.0	111.0	120.0	134.0	141.0	155.4
16 to 16+6	116.0	119.0	121.0	133.0	145.0	149.0	151.0
17 to 17+6	122.7	130.0	135.0	146.0	159.0	163.0	170.0
18 to 18+6	131.0	134.0	146.0	159.0	172.2	196.2	203.0
19 to 19+6	140.0	150.0	156.3	168.0	183.0	191.9	200.5
20 to 20+6	160.0	164.0	169.0	180.0	195.0	201.0	210.0
21 to 21+6	171.0	175.0	181.0	193.0	206.9	214.0	222.0
22 to 22+6	181.0	186.0	190.0	201.0	215.0	220.1	223.0
23 to 23+6	183.0	191.0	199.0	212.0	227.0	233.0	239.6
24 to 24+6	200.0	205.0	214.0	225.0	239.9	247.0	250.0
25 to 25+6	206.4	216.5	225.9	238.0	253.0	261.7	265.0
26 to 26+6	220.0	226.0	232.2	249.0	265.0	272.0	279.0
27 to 27+6	230.0	232.7	240.3	260.0	278.0	287.0	292.0
28 to 28+6	243.0	247.0	255.0	270.0	284.0	289.0	292.0
29 to 29+6	229.2	246.3	260.0	277.0	290.0	294.0	302.0
30 to 30+6	250.0	262.3	269.0	286.0	300.0	309.0	315.4
31 to 31+6	253.0	267.0	276.0	293.0	309.0	311.0	314.3
32 to 32+6	274.1	279.2	284.4	300.0	316.0	320.0	322.0
33 to 33+6	280.0	286.0	293.0	308.0	321.0	324.0	328.0
34 to 34+6	286.0	290.5	300.0	315.0	330.5	335.0	340.0
35 to 35+6	291.2	297.0	301.0	320.0	333.0	338.0	340.8
36 to 36+6	301.0	303.0	306.0	326.0	339.0	346.0	351.0
37 to 37+6	300.0	302.7	312.3	333.0	344.7	351.0	358.0
38 to 38+6	310.9	315.0	320.0	337.0	352.0	359.0	364.0
39 to 39+6	318.0	320.3	326.2	342.0	359.0	372.0	378.0
40 to 40+6	323.0	324.3	330.0	344.0	360.0	373.5	382.5
41 to 41+6	316.0	329.0	335.0	348.5	366.0	366.0	367.6
42 to 42+6	306.0	306.0	306.0	353.0	387.0	387.0	387.0

**Tab. 6.4** Standard score (z-score) of head circumference measurements in 13,740 Nigerian fetuses in Jos ranging from 12 – 42 weeks gestation.

GA (weeks, days)	Fetuses (n)	Mean z-score
12 to 12+6	49	-2.14E-03
13 to 13+6	384	-1.46E-03
14 to 14+6	371	3.29E-03
15 to 15+6	351	-1.75E-03
16 to 16+6	505	-3.67E-03
17 to 17+6	427	1.35E-03
18 to 18+6	446	1.85E-03
19 to 19+6	282	-2.29E-03
20 to 20+6	553	-1.42E-05
21 to 21+6	400	-2.14E-04
22 to 22+6	398	-1.16E-03
23 to 23+6	478	8.13E-04
24 to 24+6	520	2.31E-03
25 to 25+6	388	-2.50E-03
26 to 26+6	511	-3.48E-03
27 to 27+6	432	1.50E-04
28 to 28+6	548	2.63E-03
29 to 29+6	484	1.08E-03
30 to 30+6	625	-2.87E-03
31 to 31+6	523	-4.62E-04
32 to 32+6	583	1.81E-03
33 to 33+6	516	-2.61E-03
34 to 34+6	744	-2.90E-03
35 to 35+6	739	-1.72E-03
36 to 36+6	599	1.58E-03
37 to 37+6	532	-1.89E-03
38 to 38+6	481	5.51E-05
39 to 39+6	525	-2.58E-03
40 to 40+6	252	4.50E-04
41 to 41+6	72	-3.77E-03
42 to 42+6	22	-1.56E-03
Total	13740	

When head circumference data of 13,740 Nigerian fetuses in Jos was subjected to skewness analysis at different gestational age ranging from 12 – 42 weeks (Fig. 6.1), it was found that the distribution of head circumference measurements has a longer “tail” to the right of the central maximum than to the left or is skewed to the right from 13 – 24 weeks. From 25 – 37 weeks, the distribution has a longer “tail” to the left of the central maximum than to the right or is skewed to the left. By the time pregnancy reaches term, the distribution becomes skewed to the right before skewing again to the left as from 41 weeks. When the head circumference data was subjected to kurtosis analysis (Fig. 6.2), the analysis was found to be leptokurtic at 14, 15, 18, 19, 29, 33 and 38 weeks of gestation while at 12, 13, 16, 17, 20, 21, 22, 23, 24, 25, 26, 27, 28, 30, 31, 32, 34, 35, 36, 39, 40, 41 and 42 weeks of gestation, the kurtosis was mesokurtic. The coefficient of dispersion of head circumference data of 13,740 fetuses in Jos at different gestational age shows a decrease in value as gestational age advances except at 18, 23, 25, 26, 29, 30 and 42 weeks where it peaks (Fig. 6.3). The head circumference scattergram in Fig. 6.4 shows that there are very few bad data points or outliers in the head circumference measurements of 13,740 fetuses in Jos. The outliers are more from 26 – 42 weeks of gestation. This shows the pattern of growth recognized for neural tissue which suggests growth of brain.

In Fig. 6.5, mean head circumference is plotted against gestational age with error bars showing standard deviation. Mathematical modeling of head circumference data plotted against gestational age demonstrated that the best-fitted regression model (Fig. 6.6) to describe the relationship between head circumference and gestational age was the third order polynomial regression equation  $y = -0.0029x^3 + 0.0518x^2 + 13.136x - 78.198$  with a correlation of determination of  $R^2 = 0.9996$  ( $P < 0.0001$ ) where  $y$  is the head circumference in millimeters and  $x$  is the gestational age in weeks. This means that head circumference could predict the gestational age of fetuses in Jos by 99.96 percent

( $R^2 = 0.9996$ ) in 13,740 fetuses in this study.

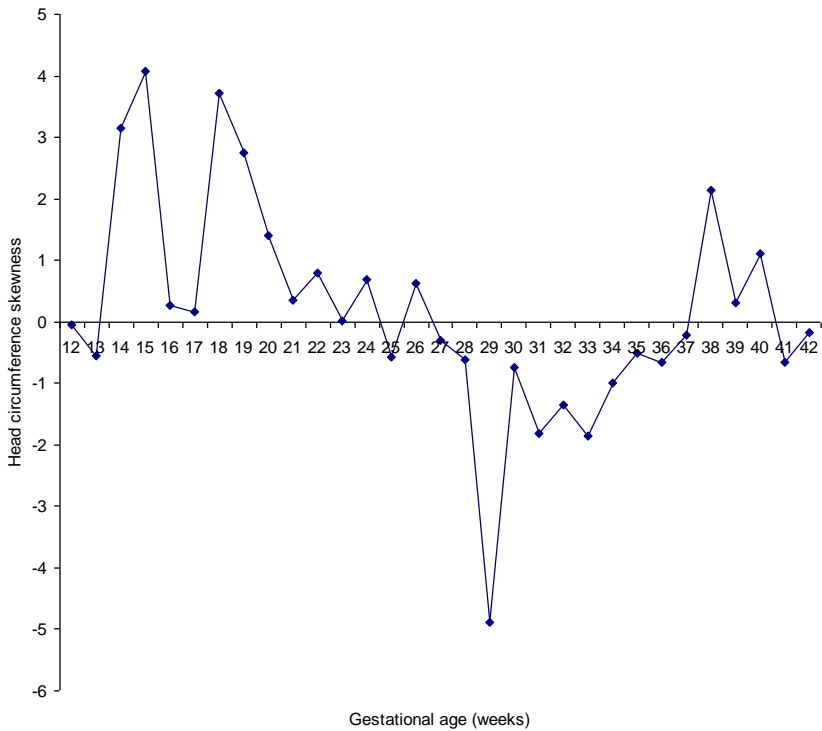


**Fig. 6.1** Head Circumference data of 13,740 Fetuses Subjected to Skewness Analysis at Different Gestational Age Ranging from 12 – 42 weeks.

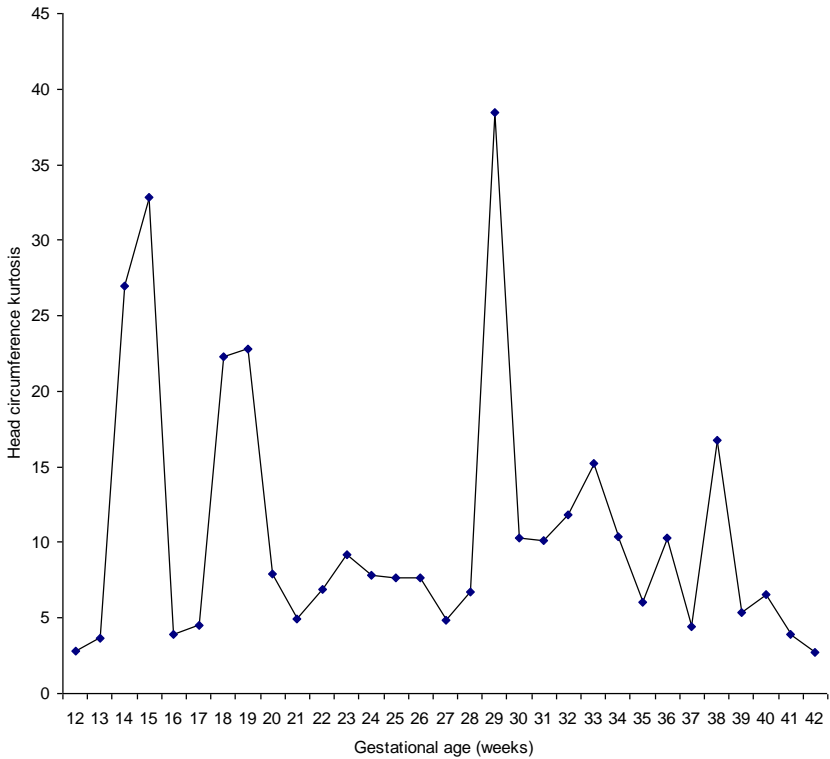


**Fig. 6.2** Head circumference data of 13,740 fetuses subjected to kurtosis analysis at different gestational age ranging from 12 – 42 weeks.

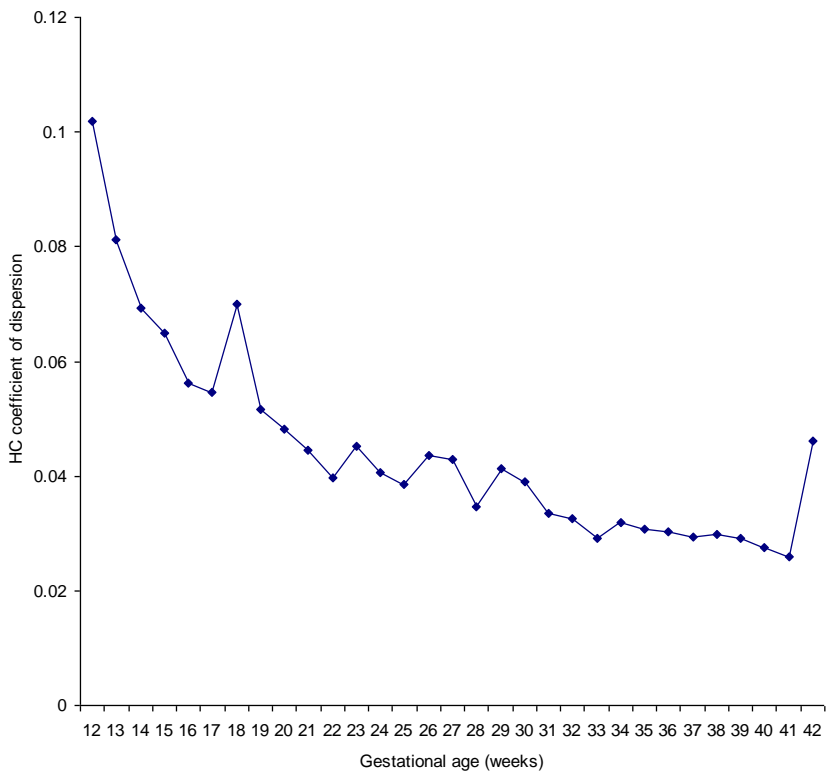


**Fig. 6.3** Head circumference coefficient of dispersion in 13,740 fetuses of gestational ages between 12 to 42 weeks.

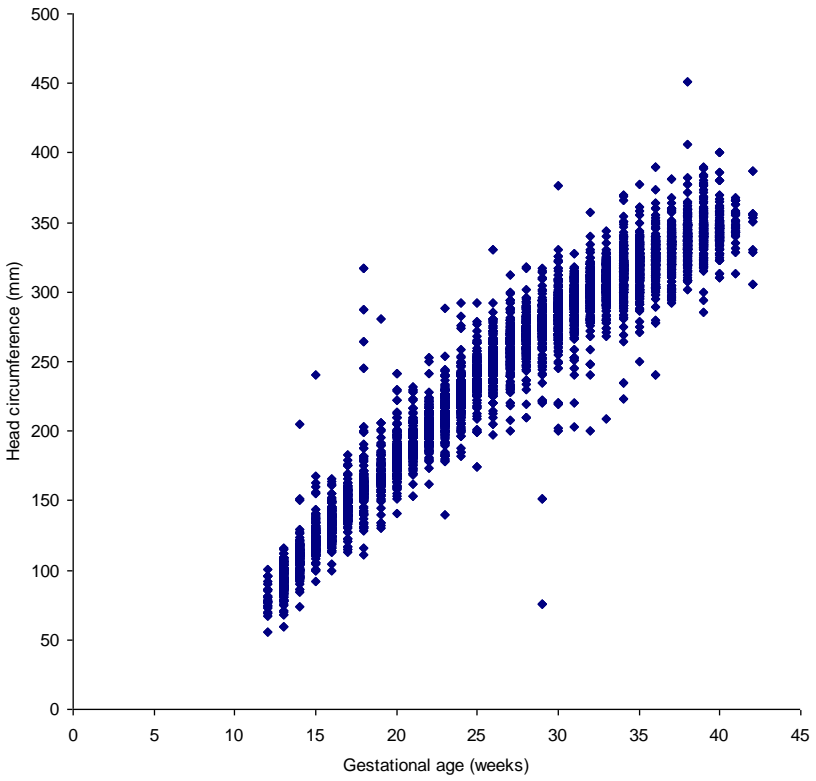


**Fig. 6.4** Scattergram of 13,740 fetal head circumference measurements from 12 – 42 weeks gestation.



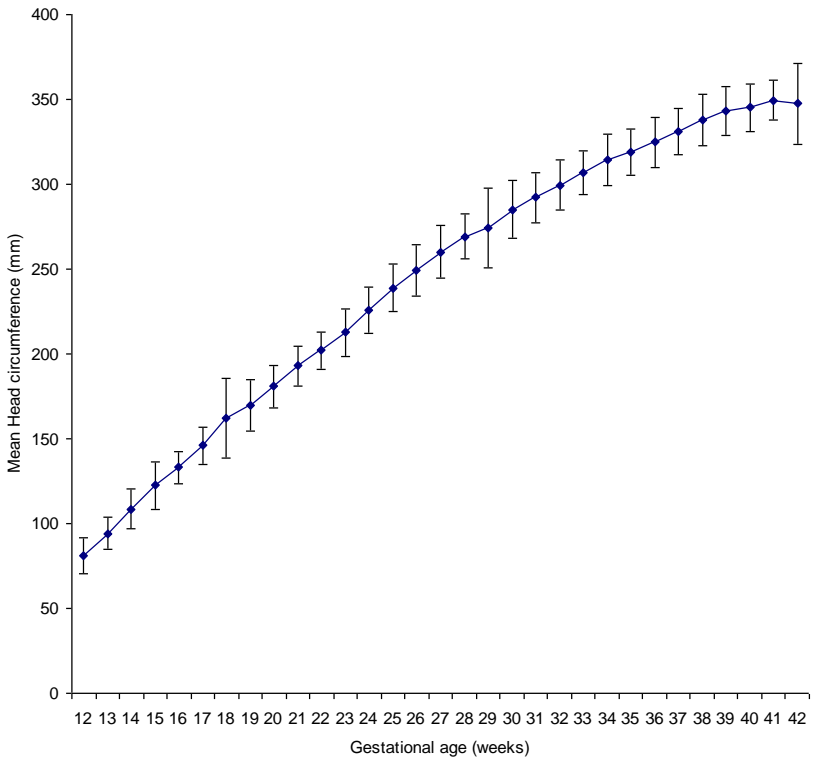


**Fig. 6.5** Mean fetal head circumference values in 13,740 fetuses of women at different gestational ages between 12 – 42 weeks. The vertical bars show the values of  $\pm SD$ .

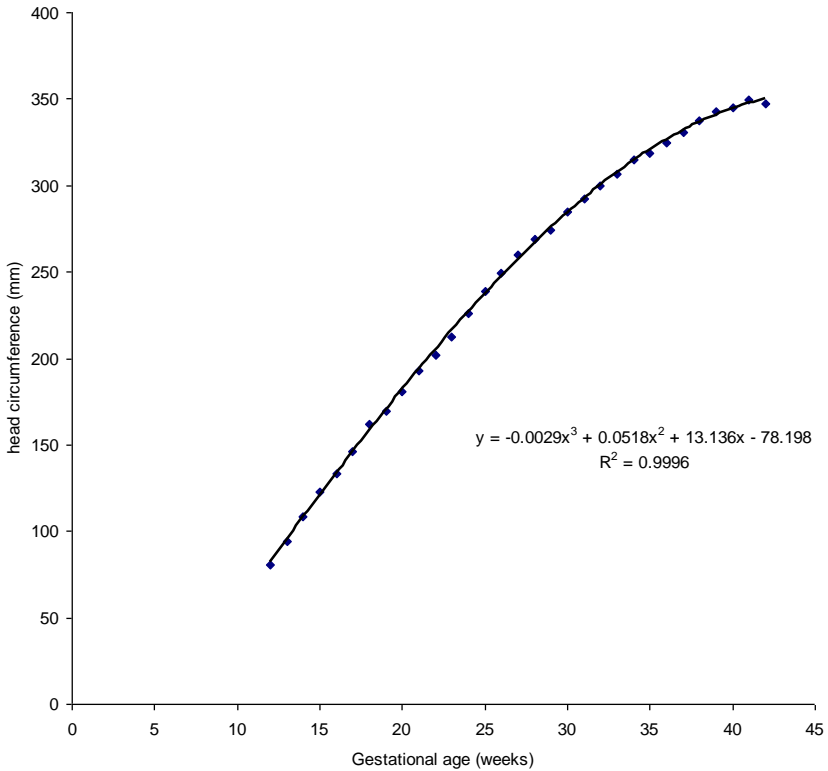


**Fig. 6.6** Correlation and regression equation of mean head circumference values in 13,740 Nigerian fetuses in Jos plotted against gestational age in weeks.

When other fetal anthropometric parameters like biparietal diameter, occipitofrontal diameter, abdominal circumference, femur length and weight are plotted against head circumference certain hidden relationships can be forced out. For example, Fig. 6.7 shows the relationship of head circumference with biparietal diameter. From the graph, it can be seen that there is a positive linear correlation between biparietal diameter and head circumference with a correlation of determination of  $R^2 = 0.9997$  ( $P < 0.0001$ ) in Nigerian fetuses in Jos. The relationship is best described by the linear regression equation  $y = 0.2792x - 0.8656$  where  $y$  is the biparietal diameter in millimeters and  $x$  is the head circumference in millimeters. Fig. 6.8 shows relationship of head

circumference with occipitofrontal diameter (OFD) which has regression equation of  $y = 0.347 + 0.0528x$ ;  $R^2 = 1$ ;  $P < 0.0001$ . Other relationships can be calculated outside the skull. Fig. 6.9 shows relationship of head circumference with abdominal circumference. From the graph, it can be seen that there is a positive linear correlation between abdominal circumference and head circumference with a correlation of determination of  $R^2 = 0.994$  ( $P < 0.0001$ ) in Nigerian fetuses in Jos. The relationship is best described by the linear regression equation  $y = 1.0644x - 29.032$  where  $y$  is the abdominal circumference in millimeters and  $x$  is the head circumference in millimeters.

Fig. 6.10 shows relationship between femur length and head circumference. There is a positive power correlation between femur length and head circumference with a correlation of determination of  $R^2 = 0.9962$  ( $P < 0.0001$ ) in Nigerian fetuses in Jos. The relationship is best described by the power regression equation  $y = 0.046x^{1.2897}$  where  $y$  is the femur length in millimeters and  $x$  is the head circumference in millimeters. Fig. 6.11 shows the relationship between fetal weight which is strongly correlated with fetal nutrition and head circumference. The relationship is best described by the exponential regression equation  $y = 57.144e^{0.012x}$  where  $y$  is the fetal weight in grams and  $x$  is the head circumference in millimeters.

Centile values for 5<sup>th</sup>, 50<sup>th</sup> and 95<sup>th</sup> are plotted as shown in Fig. 6.12. In Fig. 6.13, the 5<sup>th</sup>, 50<sup>th</sup> and 95<sup>th</sup> centile values of head circumference measurement are smoothed into a growth chart which can be utilized to determine growth and of course brain size development, strongly related to intelligence and wellness, using head circumference. Fig. 6. 14 is a graphical display showing the growth rate of the measured fetal head circumference with a quadratic polynomial mathematical model predictive formula  $y = 0.0008x^2 - 0.0095x + 2.1811$  ( $R^2 = 0.721$ ;  $p < 0.0001$ ); where  $y$  is the fetal head circumference growth rate in millimeters and  $x$  is the

gestational age in weeks. It is clear from this graph that growth rate is much higher in the early stages of development than the late ones which precede term.

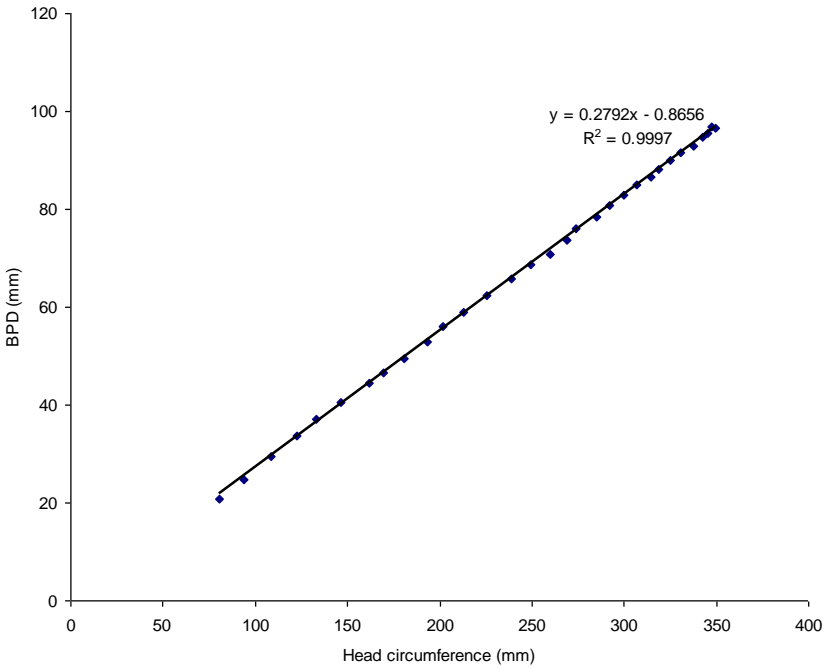


**Fig. 6.7** Correlation and regression equation of mean head circumference values in 13,740 Nigerian fetuses in Jos plotted against biparietal diameter.

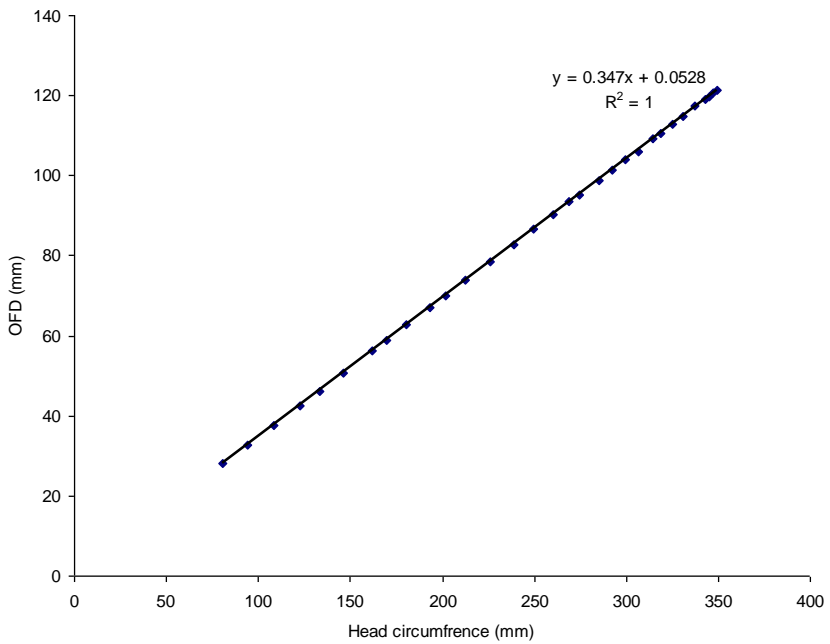


**Fig. 6.8** Correlation and regression equation of mean head circumference values in 13,740 Nigerian fetuses in Jos plotted against occipitofrontal diameter.

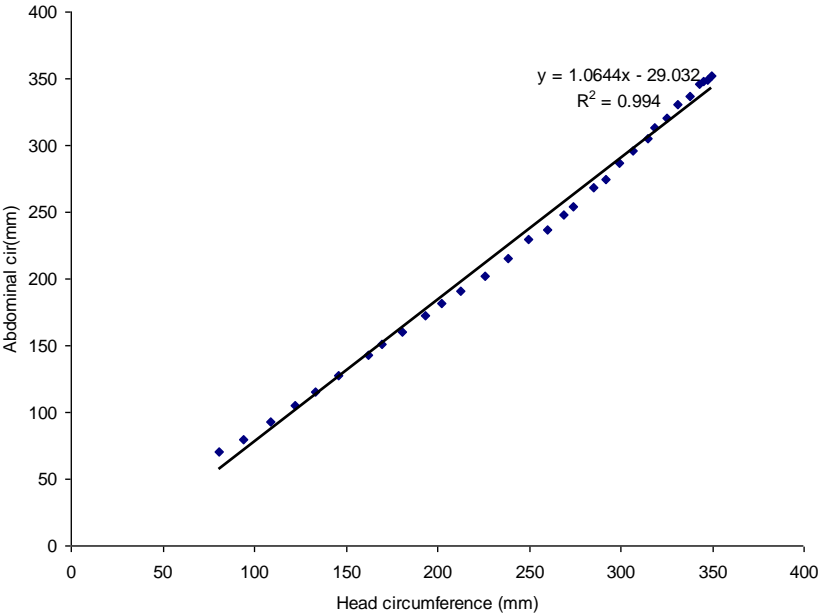


**Fig. 6.9** Correlation and regression equation of mean head circumference values in 13,740 Nigerian fetuses in Jos plotted against abdominal circumference.

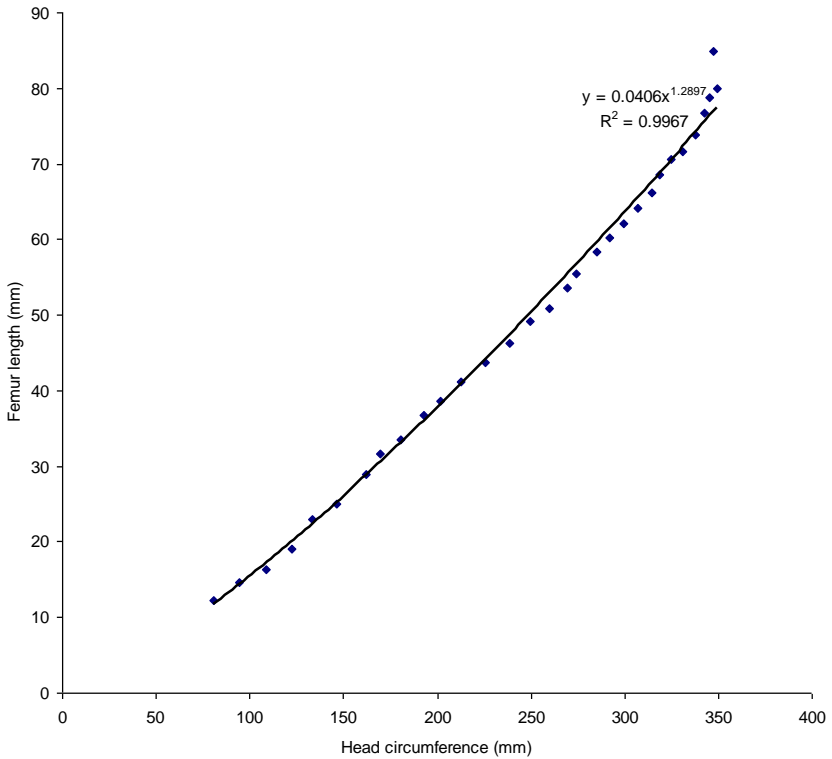


**Fig. 6.10** Correlation and regression equation of mean head circumference values in 13,740 Nigerian fetuses in Jos plotted against femur length.

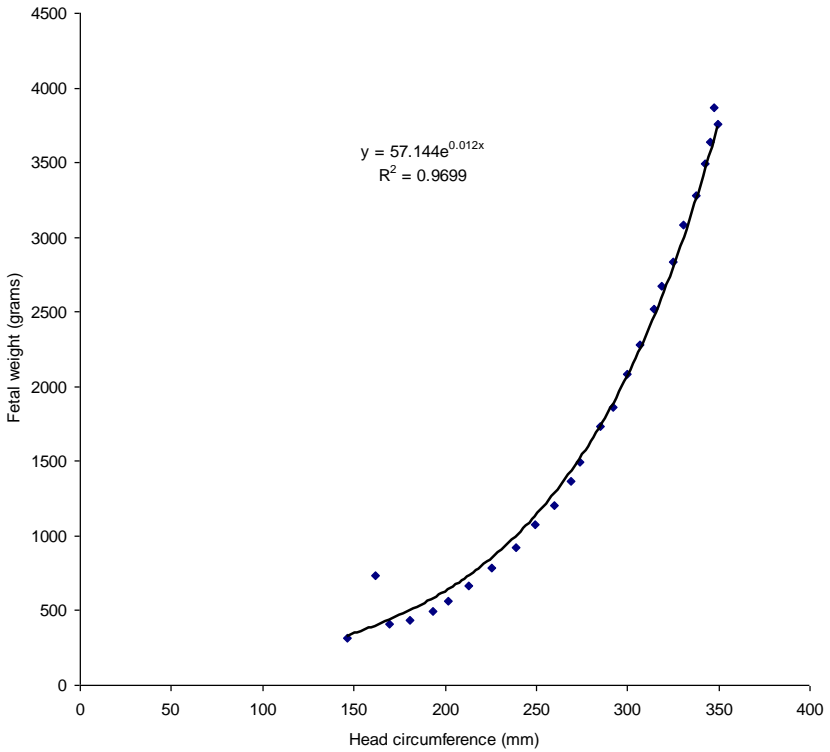


**Fig. 6.11** Correlation and regression equation of mean head circumference values in 13,740 Nigerian fetuses in Jos plotted against fetal weight.



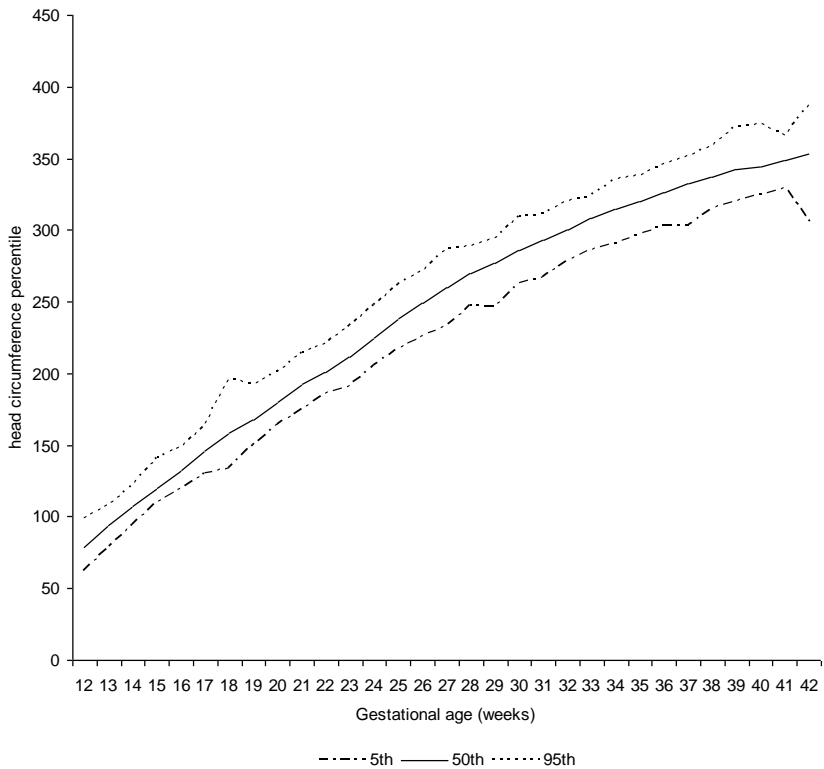


**Fig. 6.12** Fifth, 50th and 97th centiles for head circumference in 13,740 fetuses at different gestational ages from 12 to 42 weeks.

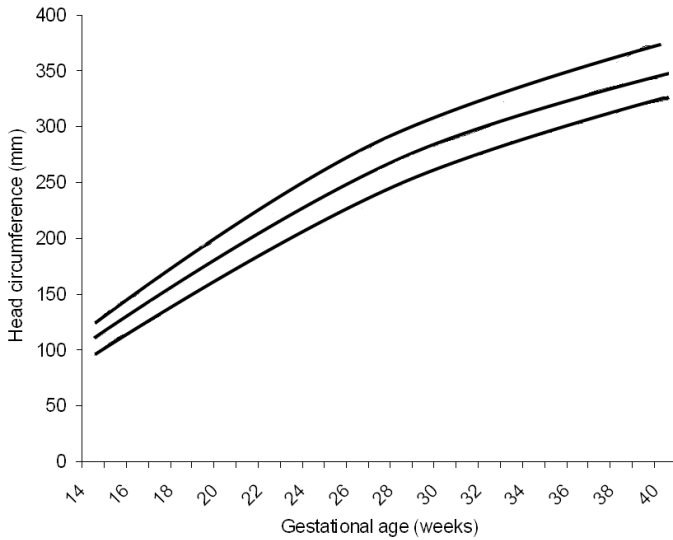


**Fig. 6.13** Curves created from 3rd, 50th and 97th fetal head circumference centiles.

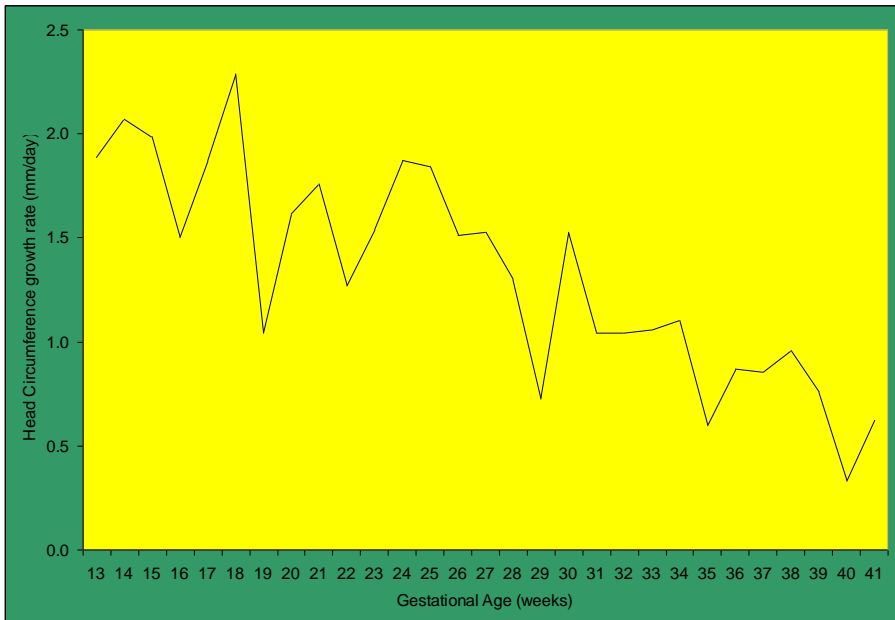


**Fig. 6.14** Growth velocity pattern of head circumference in 13,740 Nigerian fetuses in Jos.

## Biometrics of Fetal Biparietal Diameter

The fetal biparietal diameter measurements were classified into thirty one groups (Tab. 6.5). The group with the highest number of observations was from 34 to 34 + 6 while 42 to 42+6 group had the lowest number of observations. The measurements varied more at 18 to 18+6 group. The standard error of mean of BPD measurements is relatively small suggesting that the sample mean is very close to the population mean. For example, at 13 weeks gestation, the mean fetal biparietal diameter was 94.1mm while the standard error of mean was 0.5. This means that the difference between the mean biparietal diameters of the sample of fetuses at 13 weeks is just 0.5mm different from that of the population of fetuses at 13 weeks gestation.

The geometric means (Tab. 6.6) of all sets of measurements from 12 – 42 weeks are less than their arithmetic means but greater than their harmonic means indicating that all the values of fetal biparietal diameter measurements were not identical. Tab. 6.7 gives the centile values of fetal biparietal diameter measurements. This table gives the 3<sup>rd</sup>, 5<sup>th</sup>, 10<sup>th</sup>, 50<sup>th</sup>, 90<sup>th</sup>, 95<sup>th</sup>, and 97<sup>th</sup> centile values for fetal biparietal diameter measured at different gestational age ranging from 12 – 42 weeks. For example, it can be seen from the table that the 10<sup>th</sup> percentile of biparietal diameter at 20 to 20 + 6 weeks gestation is 48 millimeters. This means that 10% of the fetuses at 20 to 20 + 6 had a mean biparietal diameter less than 48 millimeters, while 90% had a mean biparietal diameter greater than 48 millimeters. Similarly, the 97<sup>th</sup> percentile of biparietal diameter at 36 to 36 + 6 is 94 millimeters. Hence 97% of fetuses at 36 to 36 + 6 had a mean biparietal diameter less than 94 millimeters while 3% had a mean biparietal diameter greater than 94 millimeters.

The standard score or z-score of biparietal diameter measurements in 13,740

fetuses ranging from 12 – 42 weeks of gestation is shown in Tab. 6.8. The z-score enables us to look at biparietal diameter measurements in each gestational age and see how they compare on the same standard; taking into account the mean and standard deviation of each gestational age. For example, biparietal diameter measurements at 15 weeks are 0.00133 standard deviations from the mean while measurements at 30 weeks are – 0.0407 standard deviations from the mean. Again, from the above z-score table, it can be seen that the biparietal diameter measurements at 38 weeks gestation are – 0.00499 standard deviations from the mean.

When biparietal diameter data of 13,740 fetuses was subjected to skewness analysis at different gestational age ranging from 12 – 42 weeks (Fig. 6.15), it can be seen that the distribution of biparietal diameter measurements has a longer “tail” to the left of the central maximum than to the right or is skewed to the left throughout pregnancy except at 14, 15, 18, 19, 20, 21 and 39 weeks where the distribution has a longer “tail” to the right of the central maximum than to the left or is skewed to the right.

When the biparietal diameter data was subjected to kurtosis analysis (Fig. 6.16), the analysis was found to be leptokurtic at 15, 18, 19, 22 and 29 weeks of gestation while at 12, 13, 16,17, 20, 21, 23, 24, 25, 26, 27, 28, 20, 31, 32,34, 35, 36, 39, 40, 41 and 42 weeks of gestation, the kurtosis was mesokurtic. The coefficient of dispersion of biparietal diameter data of 13,740 fetuses at different gestational age shows a decrease in value as gestational age advances except at 18, 20, 30 and 42 weeks where it peaks. At 25 weeks, it falls to zero before rising again (Fig. 6.17). The biparietal diameter scattergram in Fig. 6.18 shows that there are very few bad data points or outliers in the biparietal diameter measurements of 13,740 fetuses. The outliers are more from 26 – 42 weeks of gestation. This shows the pattern of growth recognized for neural tissue which suggests growth of brain.

**Tab. 6.5** Frequency Distribution Table of Fetal Biparietal Diameter Measurements Showing the Arithmetic mean, Standard Deviation and Standard Error of Mean from 12 – 42 weeks gestation.

GA (wks, days)	Fetuses (n)	BPD(mm)	SD	SEM
12 to 12+6	49	20.9	2.0	0.2
13 to 13+6	384	24.8	2.1	0.1
14 to 14+6	371	29.4	2.0	0.1
15 to 15+6	351	33.6	3.0	0.2
16 to 16+6	505	37.1	1.7	0.0
17 to 17+6	427	40.5	2.0	0.0
18 to 18+6	446	44.4	5.1	0.2
19 to 19+6	282	46.6	2.8	0.2
20 to 20+6	553	49.4	2.2	0.0
21 to 21+6	400	52.9	1.7	0.0
22 to 22+6	398	56.1	2.7	0.1
23 to 23+6	478	59.0	1.8	0.0
24 to 24+6	520	62.3	2.3	0.1
25 to 25+6	388	65.8	2.2	0.1
26 to 26+6	511	68.6	2.3	0.1
27 to 27+6	432	70.8	2.2	0.1
28 to 28+6	548	73.6	3.6	0.2
29 to 29+6	484	76.0	3.3	0.2
30 to 30+6	625	78.4	3.5	0.1
31 to 31+6	523	80.7	2.5	0.1
32 to 32+6	583	82.8	2.7	0.1
33 to 33+6	516	85.0	2.0	0.0
34 to 34+6	744	86.6	3.4	0.1
35 to 35+6	739	88.2	2.7	0.0
36 to 36+6	599	90.0	2.8	0.1
37 to 37+6	532	91.5	2.2	0.0
38 to 38+6	481	93.0	2.5	0.1
39 to 39+6	525	94.7	2.6	0.1
40 to 40+6	252	95.6	2.3	0.2
41 to 41+6	72	96.5	2.3	0.3
42 to 42+6	22	96.9	2.7	0.6
Total	13,740			

**Tab. 6.6** *Frequency distribution table of fetal head circumference measurements showing arithmetic mean, geometric mean and harmonic mean from 12 – 42 weeks gestation.*

<b>GA (week, days)</b>	<b>Number of fetuses (n)</b>	<b>Arithmetic mean (mm)</b>	<b>Geometric mean (mm)</b>	<b>Harmonic mean(mm)</b>
12 to 12+6	49	20.89796	20.8133	20.73384
13 to 13+6	384	24.79427	24.6967	24.58586
14 to 14+6	371	29.3504	29.27582	29.19156
15 to 15+6	351	33.60399	33.50901	33.43465
16 to 16+6	505	37.05941	37.01759	36.9743
17 to 17+6	427	40.52693	40.47596	40.42076
18 to 18+6	446	44.40359	44.19772	44.04385
19 to 19+6	282	46.61702	46.55173	46.4993
20 to 20+6	553	49.37613	49.33103	49.28833
21 to 21+6	400	52.9325	52.90432	52.87666
22 to 22+6	398	56.11055	56.05551	56.00847
23 to 23+6	478	59.03138	59.00269	58.97365
24 to 24+6	520	62.31538	62.27158	62.22575
25 to 25+6	388	65.84021	65.80398	65.76709
26 to 26+6	511	68.61644	68.57739	68.53812
27 to 27+6	432	70.84259	70.80765	70.77187
28 to 28+6	548	73.64051	73.49528	73.23101
29 to 29+6	484	75.98967	75.89696	75.77091
30 to 30+6	625	78.4288	78.34548	78.25781
31 to 31+6	523	80.73422	80.69387	80.65249
32 to 32+6	583	82.78902	82.73907	82.68323
33 to 33+6	516	84.98062	84.9576	84.93434
34 to 34+6	744	86.55645	86.48273	86.39934
35 to 35+6	739	88.15833	88.11768	88.07617
36 to 36+6	599	90.00835	89.96366	89.91594
37 to 37+6	532	91.49436	91.46841	91.44218
38 to 38+6	481	92.98753	92.95243	92.91693
39 to 39+6	525	94.74857	94.71294	94.67731
40 to 40+6	252	95.56349	95.53491	95.5063
41 to 41+6	72	96.45834	96.43224	96.40612
42 to 42+6	22	96.90909	96.87257	96.83514
<b>Total</b>	<b>13740</b>			

**Tab. 6.7** Fetal biparietal diameter centiles from 12 – 42 weeks.

GA (wks, days)	Biparietal diameter (mm)						
	3rd	5th	10th	50th	90th	95th	97th
12 to 12+6	19.0	19.0	19.0	20.0	24.0	25.5	26.0
13 to 13+6	20.0	22.0	22.5	25.0	27.0	27.0	27.0
14 to 14+6	26.2	27.0	28.0	29.0	31.0	31.0	32.0
15 to 15+6	31.0	31.0	32.0	34.0	35.0	35.0	35.4
16 to 16+6	33.0	34.0	35.0	37.0	39.0	39.0	39.0
17 to 17+6	37.0	38.0	38.8	41.0	42.0	42.0	43.2
18 to 18+6	41.0	41.0	42.0	44.0	45.0	46.0	47.0
19 to 19+6	44.0	44.2	45.0	46.0	47.0	49.0	50.0
20 to 20+6	46.0	47.0	48.0	49.0	51.0	52.0	53.4
21 to 21+6	49.0	50.0	51.0	53.0	54.0	55.0	56.0
22 to 22+6	53.0	53.0	54.0	56.0	57.0	59.0	60.0
23 to 23+6	55.0	56.0	57.0	59.0	61.0	61.0	62.0
24 to 24+6	56.6	58.0	60.0	63.0	64.0	65.0	67.0
25 to 25+6	62.0	63.0	64.0	66.0	68.0	69.0	70.0
26 to 26+6	63.0	64.0	66.0	69.0	70.0	72.0	74.0
27 to 27+6	64.0	66.0	68.0	71.0	72.7	74.0	75.0
28 to 28+6	69.0	71.0	72.0	74.0	75.1	77.0	78.0
29 to 29+6	70.7	73.0	74.0	76.0	78.0	78.8	79.0
30 to 30+6	71.0	72.0	74.0	79.0	81.0	84.0	85.0
31 to 31+6	74.7	76.0	78.0	81.0	83.0	84.0	84.3
32 to 32+6	77.0	78.0	80.0	83.0	85.0	87.0	87.0
33 to 33+6	80.0	82.0	82.0	85.0	87.0	88.0	88.0
34 to 34+6	80.4	82.0	83.5	87.0	89.0	91.0	92.0
35 to 35+6	82.0	83.0	85.0	89.0	91.0	92.0	93.0
36 to 36+6	84.0	85.0	87.0	90.0	92.0	93.0	94.0
37 to 37+6	87.0	87.0	89.0	92.0	94.0	94.0	95.0
38 to 38+6	88.0	89.0	90.0	93.0	96.0	97.0	98.0
39 to 39+6	90.0	91.0	92.0	94.0	98.0	99.0	99.0
40 to 40+6	91.0	91.0	93.0	95.0	98.7	100.0	100.0
41 to 41+6	91.2	92.0	93.0	96.0	100.0	101.0	101.0
42 to 42+6	91.0	91.0	91.0	98.0	99.0	99.0	99.0

**Tab. 6.8** Standard score (z-score) of biparietal diameter measurements in 13,740 Nigerian fetuses in Jos ranging from 12 – 42 weeks gestation.

Gestational age (weeks)	Fetuses (n)	Mean z-score
12 to 12+6	49	-2.71565
13 to 13+6	384	-2.73E-03
14 to 14+6	371	-2.48E-02
15 to 15+6	351	1.33E-03
16 to 16+6	505	-2.39E-02
17 to 17+6	427	3.47E-03
18 to 18+6	446	7.03E-04
19 to 19+6	282	6.08E-03
20 to 20+6	553	-1.08E-02
21 to 21+6	400	1.91E-02
22 to 22+6	398	3.91E-03
23 to 23+6	478	1.74E-02
24 to 24+6	520	6.69E-03
25 to 25+6	388	1.83E-02
26 to 26+6	511	7.15E-03
27 to 27+6	432	1.94E-02
28 to 28+6	548	1.13E-02
29 to 29+6	484	-3.13E-03
30 to 30+6	625	-4.89E-02
31 to 31+6	523	1.52E-03
32 to 32+6	583	-4.07E-03
33 to 33+6	516	-9.69E-03
34 to 34+6	744	-1.41E-02
35 to 35+6	739	-1.54E-02
36 to 36+6	599	2.98E-03
37 to 37+6	532	-2.56E-03
38 to 38+6	481	-4.99E-03
39 to 39+6	525	1.87E-02
40 to 40+6	252	-1.59E-02
41 to 41+6	72	-1.81E-02
42 to 42+6	22	3.37E-03
Total	13740	



In Fig. 6.19, mean biparietal diameter is plotted against gestational age with error bars showing standard deviation. Arithmetic mean and standard deviation go together like star and satellite. With the mean, we have some idea of the kind of numbers it represents, but the whole story is still a mystery. To clear up the mystery of the hidden numbers that made up a mean, the standard deviation is necessary. For example, the mean  $\pm 1$  standard deviation will include about 2 out of 3 numbers in the group while the mean  $\pm 2$  standard deviations will include about 95 out of 100 numbers in the group and the mean  $\pm 3$  standard deviations will include 997 numbers out of 1,000. Mathematical modeling of fetal biparietal diameter data demonstrated that the best-fitted regression model to describe the relationship between biparietal diameter and gestational age is as shown in Fig. 6.20. There is a positive polynomial correlation between gestational age and biparietal diameter with a correlation of determination of  $R^2 = 0.9996$  ( $P < 0.0001$ ) in Nigerian fetuses in Jos.

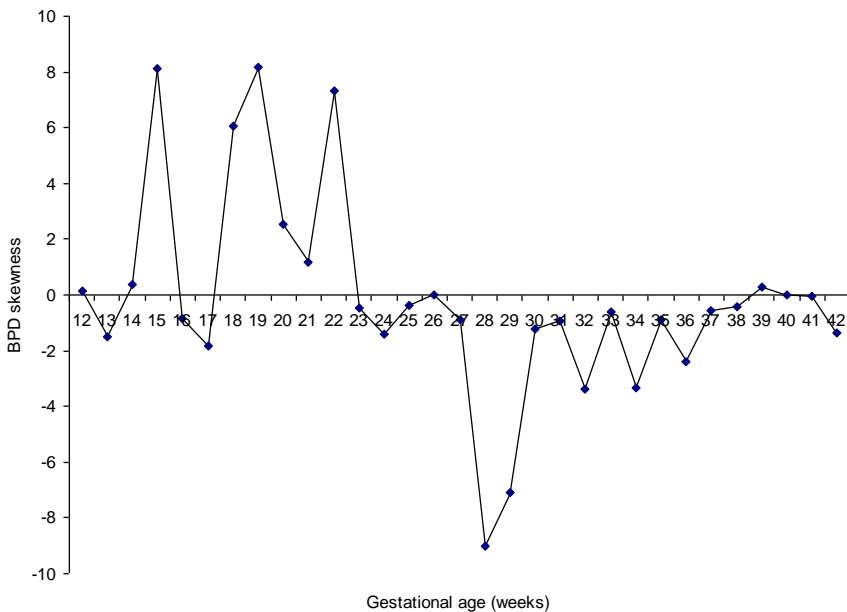


**Fig. 6.15** Biparietal diameter data of 13,740 fetuses subjected to Skewness analysis at different gestational age ranging from 12 – 42 weeks.

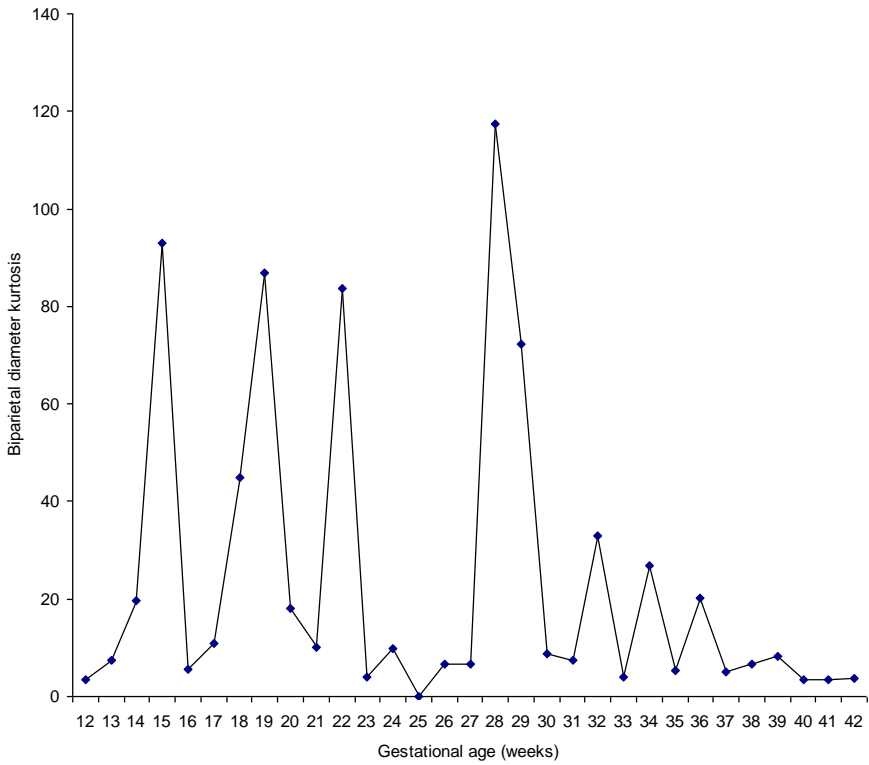


**Fig. 6.16** Biparietal diameter data of 13,740 fetuses subjected to kurtosis analysis at different gestational age ranging from 12 – 42 weeks.

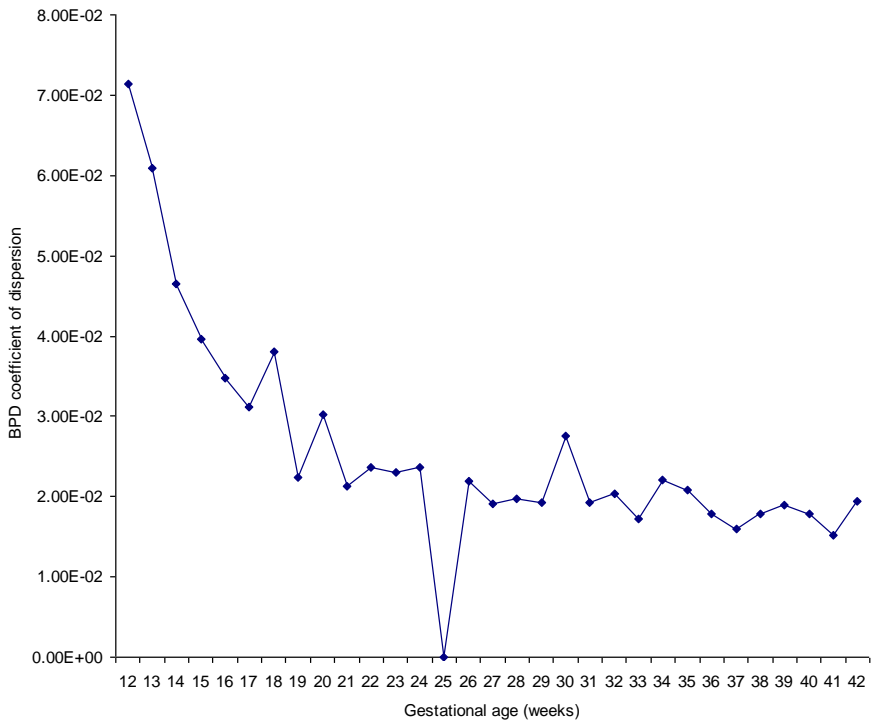


**Fig. 6.17** Biparietal diameter coefficient of dispersion in 13,740 fetuses of gestational ages between 12 to 42 weeks.

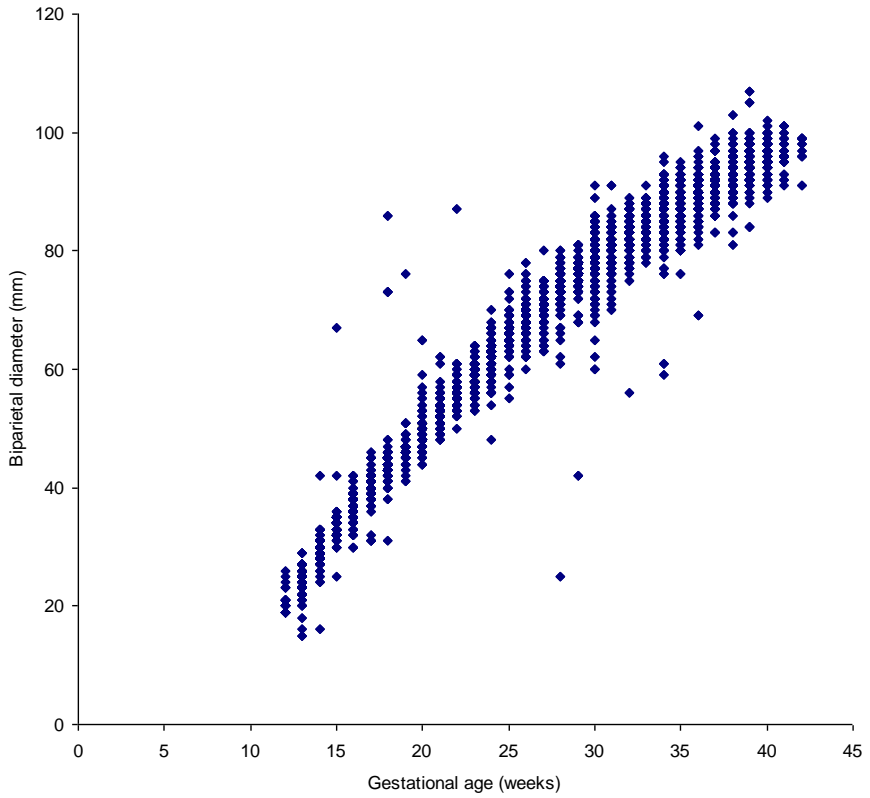


**Fig. 6.18** Scattergram of 13,740 fetal biparietal diameter measurements from 12 – 42 weeks gestation.

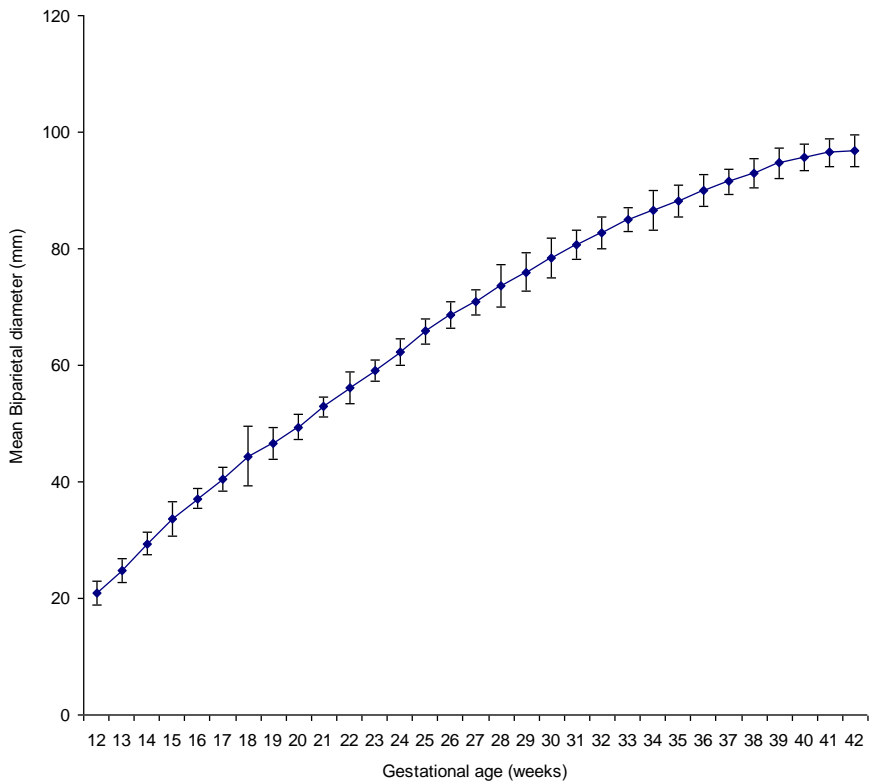


**Fig. 6.19** Mean fetal biparietal diameter values in 13,740 fetuses of women at different gestational ages between 12 – 42 weeks. The vertical bars show the values of  $\pm SD$ .

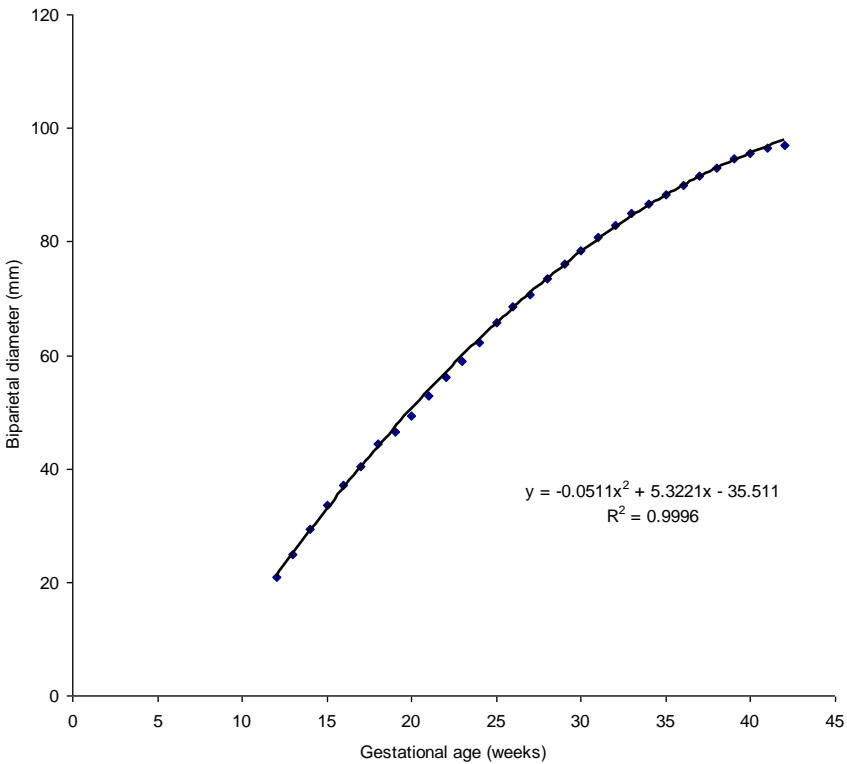


**Fig. 6.20** Correlation and regression equation of mean biparietal diameter values in 13,740 Nigerian fetuses in Jos plotted against gestational age in weeks.

The relationship is best described by the second order polynomial regression equation  $y = -0.0511x^2 + 5.3221x - 35.511$  where  $y$  is the biparietal diameter in millimeters and  $x$  is the gestational age in weeks. This means that biparietal diameter could predict the gestational age of fetuses by 99.99 percent ( $R^2 = 0.9999$ ) in 13,740 fetuses in this study. When other fetal anthropometric parameters like head circumference, occipitofrontal diameter, abdominal circumference, femur length and weight are plotted against biparietal diameter certain hidden relationships can be forced out. For example, Fig. 6.21 shows the relationship between biparietal diameter and head circumference. From the graph, it can be seen that there is a positive linear correlation between biparietal diameter and head

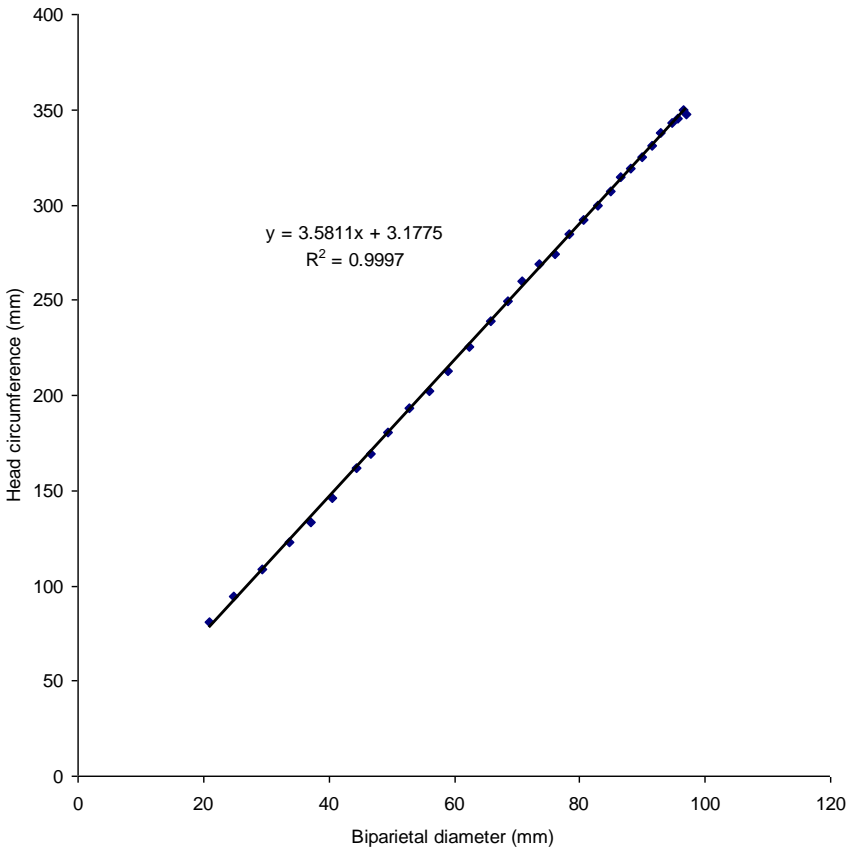
circumference with a correlation of determination of  $R^2 = 0.9997$  ( $P < 0.0001$ ) in Nigerian fetuses in Jos. The relationship is best described by the linear regression equation  $y = 3.5811x + 3.1775$  where  $x$  is the biparietal diameter in millimeters and  $y$  is the head circumference in millimeters.

Fig. 6.22 shows the relationship of biparietal diameter with occipitofrontal diameter. From the graph, it can be seen that there is a positive linear correlation between occipitofrontal diameter and biparietal diameter with a correlation of determination of  $R^2 = 0.9997$  ( $P < 0.0001$ ) in Nigerian fetuses in Jos. The relationship is best described by the linear regression equation  $y = 1.2425x + 1.1552$  where  $y$  is the occipitofrontal diameter in millimeters and  $x$  is biparietal diameter in millimeters.

Fig. 6.23 shows the relationship of biparietal diameter with abdominal circumference. From the graph, it can be seen that there is a positive linear correlation between abdominal circumference and biparietal diameter with a correlation of determination of  $R^2 = 0.9994$  ( $P < 0.0001$ ) in Nigerian fetuses in Jos. The relationship is best described by second order polynomial regression equation  $y = 0.0144x^2 + 2.0241x + 21.816$  where  $y$  is the abdominal circumference in millimeters and  $x$  is the biparietal diameter in millimeters.

Fig. 6.24 shows relationship between femur length and biparietal diameter. There is a positive power correlation between femur length and biparietal diameter with a correlation of determination of  $r^2 = 0.9986$  ( $P < 0.0001$ ) in Nigerian fetuses in Jos. The relationship is best described by the fourth order polynomial regression equation  $y = 5E-06x^4 - 0.0011x^3 + 0.0855x^2 - 2.0951x + 27.664$  where  $y$  is the femur length in millimeters and  $x$  is the biparietal diameter in millimeters. Fig. 6.25 shows the relationship between fetal weight which is strongly correlated with fetal nutrition and biparietal diameter. There is a positive exponential correlation between fetal weight and biparietal diameter with a correlation of determination of

$r^2 = 0.9988$  ( $P < 0.0001$ ) in Nigerian fetuses in Jos. The relationship is best described by the exponential regression equation  $y = 45.141e^{0.0461x}$  where  $y$  is the fetal weight in grams and  $x$  is the biparietal diameter in millimeters.



**Fig. 6.21** Correlation and regression equation of mean head circumference values in 13,740 Nigerian fetuses in Jos plotted against biparietal diameter.



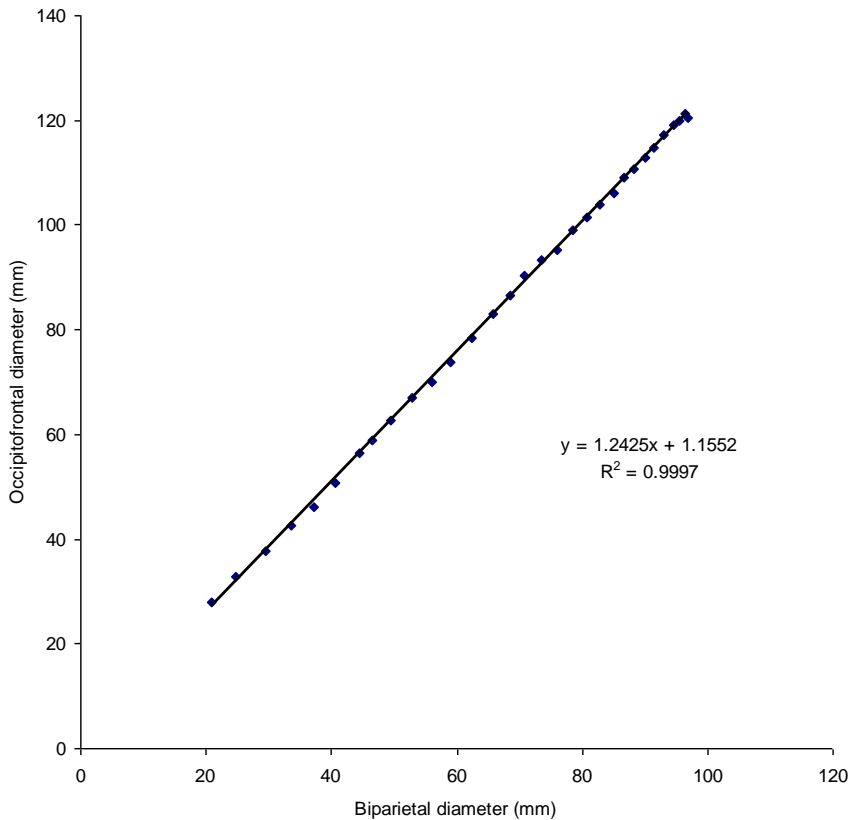


**Fig. 6.22** Correlation and regression equation of mean biparietal diameter values in 13,740 Nigerian fetuses in Jos plotted against occipitofrontal diameter.

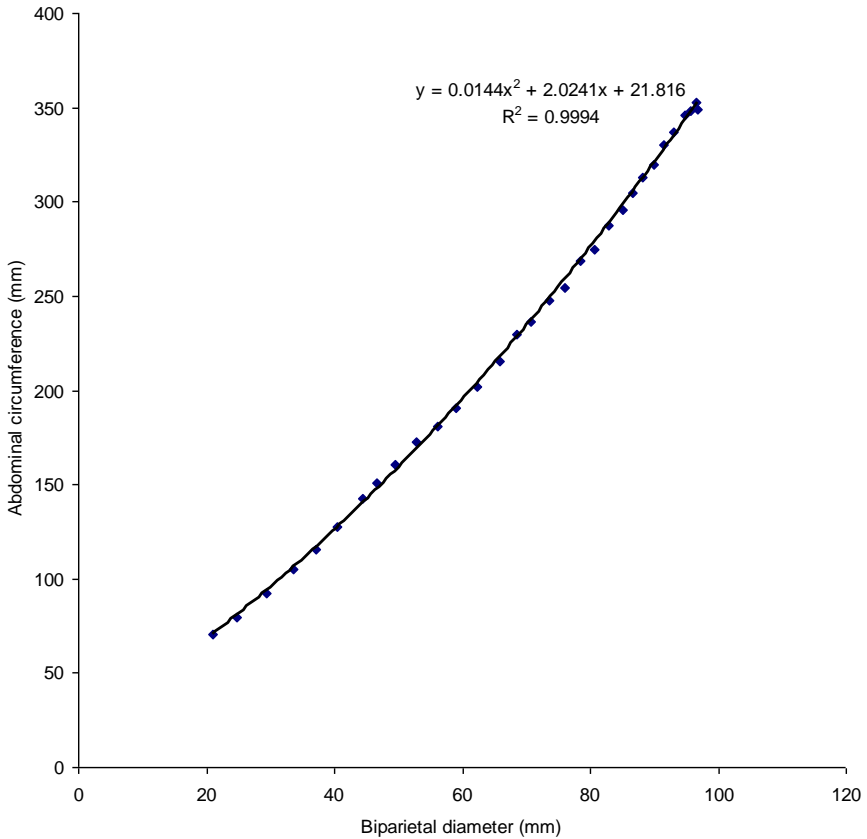


**Fig. 6.23** Correlation and regression equation of mean biparietal diameter values in 13,740 Nigerian fetuses in Jos plotted against abdominal circumference.

Centile values for 5<sup>th</sup>, 50<sup>th</sup> and 95<sup>th</sup> are plotted as shown in Fig. 6.26. In Fig. 6.27, the 3<sup>rd</sup>, 50<sup>th</sup> and 97<sup>th</sup> of biparietal diameter are smoothed into a growth chart which can be utilized to determine growth and of course brain size development, which is strongly related to intelligence and wellness, using biparietal diameter. Fig. 6.28 is a graphical display showing the growth rate of the measured fetal biparietal diameter. It is clear from this graph that growth rate is much higher in the early stages of development than the late ones which precede term.

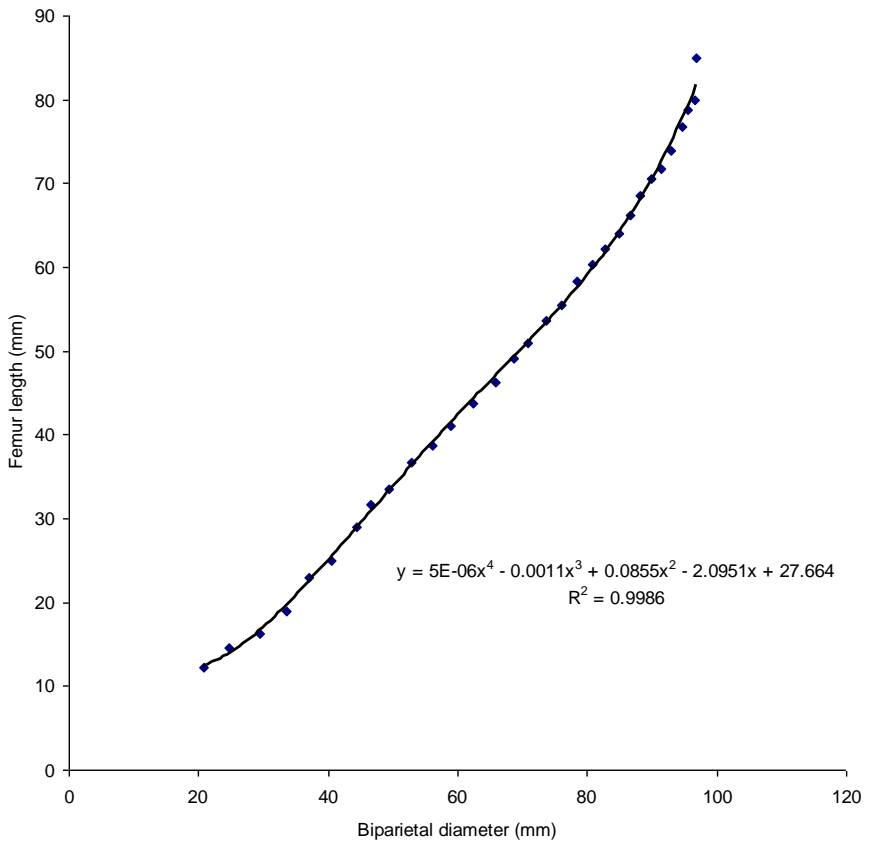


**Fig. 6.24** Correlation and regression equation of mean biparietal diameter values in 13,740 Nigerian fetuses in Jos plotted against femur length.

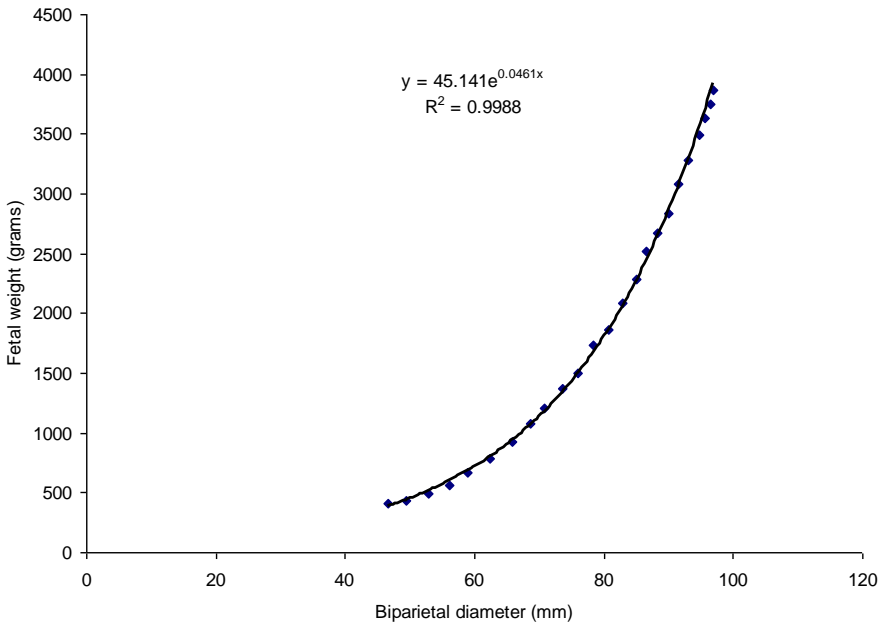


**Fig. 6.25** Correlation and regression equation of mean biparietal diameter values in 13,740 Nigerian fetuses in Jos plotted against fetal weight.

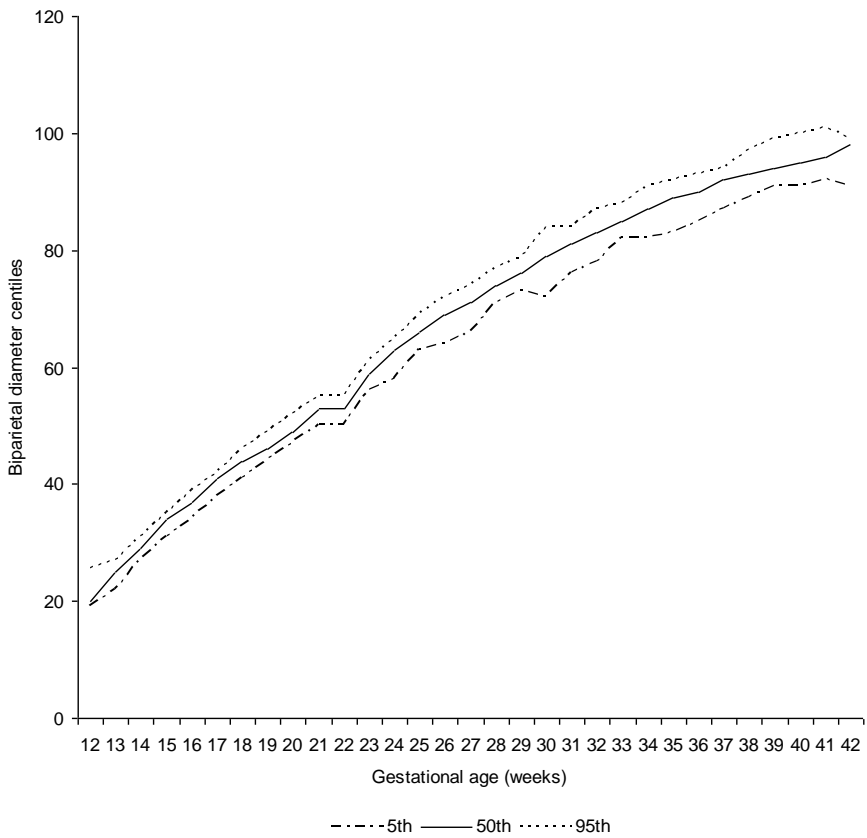


**Fig. 6.26** Fifth, 50th and 97th centiles for biparietal diameter in 13,740 fetuses at different gestational ages from 12 to 42 weeks.

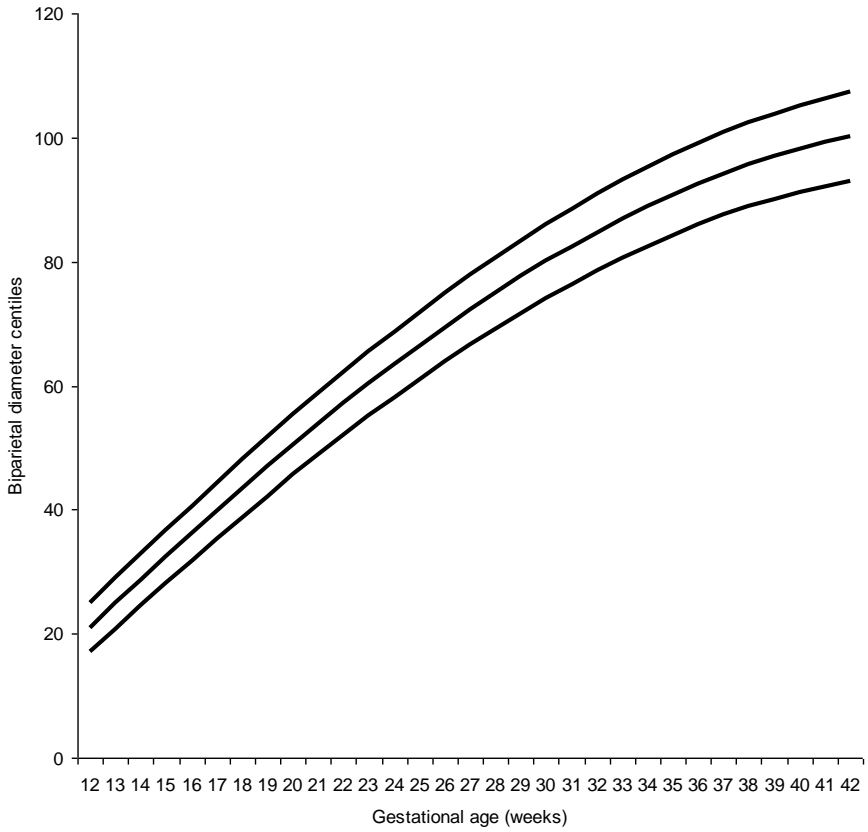


**Fig. 6.27** Curves created from 3rd, 50th and 97th fetal biparietal diameter centiles.

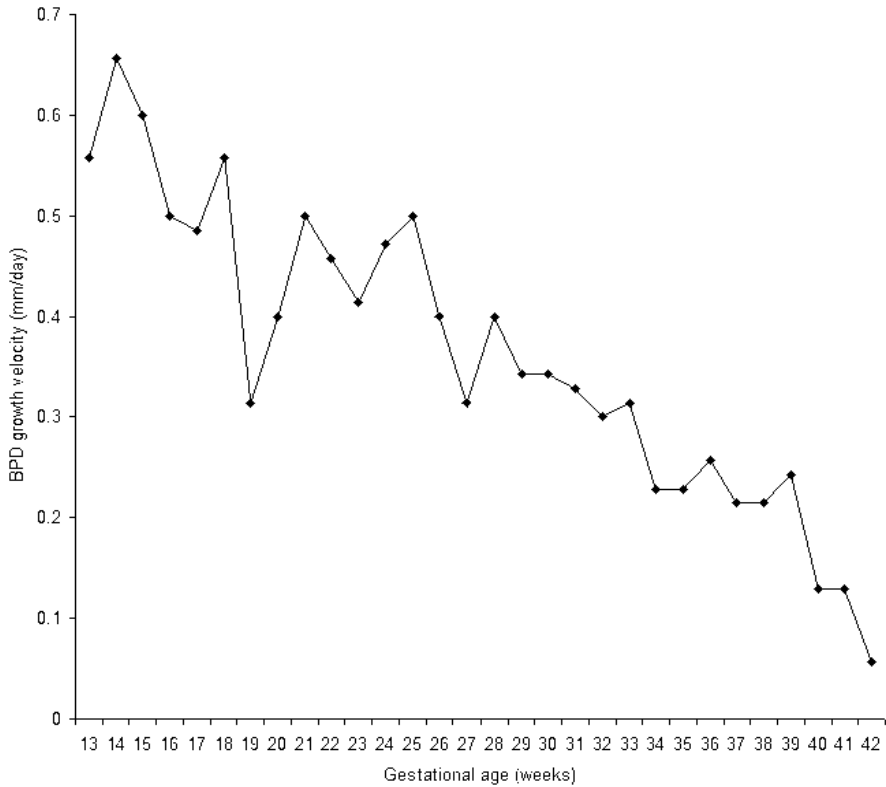


**Fig. 6.28** Growth velocity pattern of biparietal diameter in 13,740 Nigerian fetuses in Jos ranging from 12 – 42 weeks.

## Biometrics of Fetal Occipitofrontal Diameter

The mean fetal occipitofrontal diameter values at each week of gestation from 12 – 42 are as shown in Tab. 6.9. This table gives the mean values of fetal occipitofrontal diameter measurements for each gestational age in weeks from 12 – 42 weeks together with their corresponding standard deviations and standard errors of mean. The highest mean value was obtained at 42 weeks while the least mean value was gotten at 12 weeks. The range of variability was 3.7 and 5.3 for the minimum and maximum values respectively. With the arithmetic mean, one

has some idea of the kind of numbers it represents, but the whole story is still a mystery. To clear up the mystery of the hidden numbers that made up a mean, the standard deviation is necessary. For example, the mean occipitofrontal diameter at 19 weeks is 58.9mm plus 5.3mm or 58.9mm minus 5.3mm. This means 2 out of 3 measurements of occipitofrontal diameter at 19 weeks, approximately 188 occipitofrontal diameter measurements in a class of 282, should be between 53.6mm and 64.2mm. Since the standard error of mean at 19 weeks is 0.3mm, it is telling us that the real mean occipitofrontal diameter of fetuses in Jos at 19 weeks is probably between 58.6mm and 59.2mm (58.9mm plus or minus 0.3mm). It can also be seen that the standard error of mean for each week of gestation from 12 – 42 is very small suggesting that the sample mean is very close to the population mean. For example, at 13 weeks gestation, the mean fetal occipitofrontal diameter was 94.1mm while the standard error of mean was 0.5. This means that the difference between the mean occipitofrontal diameters of the sample of fetuses at 13 weeks is just 0.5mm different from that of the population of fetuses at 13 weeks gestation. The geometric means (Tab. 6.10) of all sets of measurements from 12 – 42 weeks are less than their arithmetic means but greater than their harmonic means indicating that all the values of fetal occipitofrontal diameter measurements were not identical. Tab.6.11 gives the centile values of fetal occipitofrontal diameter measurements. This table gives the 3<sup>rd</sup>, 5<sup>th</sup>, 10<sup>th</sup>, 50<sup>th</sup>, 90<sup>th</sup>, 95<sup>th</sup>, and 97<sup>th</sup> centile values for fetal occipitofrontal diameter measured at different gestational age ranging from 12 – 42 weeks. For example, it can be seen from the table that the 10<sup>th</sup> percentile of occipitofrontal diameter at 20 to 20 + 6 weeks gestation is 59 millimeters.



**Tab. 6.9** Frequency distribution table of fetal occipitofrontal diameter measurements showing arithmetic mean, standard deviation and standard error of mean from 12 – 42 weeks gestation.

GA (week, days)	Fetuses (n)	Mean OFD (mm)	SD	SEM
12 to 12+6	49	28	3.7	0.5
13 to 13+6	384	32.7	3.3	0.2
14 to 14+6	371	37.7	4.1	0.2
15 to 15+6	351	42.5	4.8	0.3
16 to 16+6	505	46.2	3.4	0.2
17 to 17+6	427	50.8	3.8	0.2
18 to 18+6	446	56.3	8.1	0.4
19 to 19+6	282	58.9	5.3	0.3
20 to 20+6	553	62.8	4.4	0.2
21 to 21+6	400	67.1	4.1	0.2
22 to 22+6	398	70.1	4	0.2
23 to 23+6	478	73.9	4.8	0.2
24 to 24+6	520	78.4	4.6	0.2
25 to 25+6	388	82.9	4.9	0.2
26 to 26+6	511	86.6	5.3	0.2
27 to 27+6	432	90.3	5.4	0.3
28 to 28+6	548	93.4	4.6	0.2
29 to 29+6	484	95.2	8.1	0.4
30 to 30+6	625	98.9	6	0.2
31 to 31+6	523	101.5	5.2	0.2
32 to 32+6	583	104	5.1	0.2
33 to 33+6	516	106	4.5	0.2
34 to 34+6	744	109.2	5.2	0.2
35 to 35+6	739	110.7	4.7	0.2
36 to 36+6	599	112.9	5.1	0.2
37 to 37+6	532	114.9	4.7	0.2
38 to 38+6	481	117.3	5.3	0.2
39 to 39+6	525	119	5	0.2
40 to 40+6	252	119.8	4.9	0.3
41 to 41+6	72	121.3	4.1	1.5
42 to 42+6	22	120.6	8.2	1.7
Total	13,740			

**Tab. 6.10** Frequency distribution table of fetal occipitofrontal diameter measurements showing arithmetic mean, geometric mean and harmonic mean from 12 – 42 weeks gestation.

GA (week, days)	Number of fetuses (n)	Arithmetic mean (mm)	Geometric mean (mm)	Harmonic mean (mm)
12 to 12+6	49	28.02041	27.7769	27.52186
13 to 13+6	384	32.67969	32.49849	32.30374
14 to 14+6	371	37.72507	37.5314	37.35426
15 to 15+6	351	42.54986	42.33276	42.14695
16 to 16+6	505	46.16832	46.04197	45.91577
17 to 17+6	427	50.77986	50.63799	50.49517
18 to 18+6	446	56.33184	55.87227	55.49466
19 to 19+6	282	58.88298	58.66893	58.47072
20 to 20+6	553	62.78843	62.64119	62.50017
21 to 21+6	400	67.08	66.95792	66.83591
22 to 22+6	398	70.07789	69.969	69.86189
23 to 23+6	478	73.86192	73.70367	73.54012
24 to 24+6	520	78.375	78.24005	78.10592
25 to 25+6	388	82.89433	82.74525	82.58868
26 to 26+6	511	86.55968	86.39996	86.24117
27 to 27+6	432	90.25926	90.09711	89.93079
28 to 28+6	548	93.44526	93.32742	93.20554
29 to 29+6	484	95.21694	94.65898	93.60843
30 to 30+6	625	98.8752	98.68735	98.48719
31 to 31+6	523	101.4646	101.321	101.1645
32 to 32+6	583	104.0069	103.8739	103.7304
33 to 33+6	516	106.5562	106.456	106.3478
34 to 34+6	744	109.2218	109.0918	108.9546
35 to 35+6	739	110.7172	110.6159	110.5123
36 to 36+6	599	112.8781	112.7592	112.6352
37 to 37+6	532	114.9004	114.802	114.7024
38 to 38+6	481	117.2599	117.1476	117.0403
39 to 39+6	525	119.0152	118.9098	118.8046
40 to 40+6	252	119.8294	119.7336	119.6402
41 to 41+6	72	121.2639	121.1941	121.1232
42 to 42+6	22	120.6364	120.3676	120.0943
Total	13740			

**Tab. 6.11** *Fetal occipitofrontal diameter centiles from 12 – 42 weeks.*

Occipitofrontal diameter centiles (mm)							
Gestational age (weeks, days)	3rd	5th	10th	50th	90th	95th	97th
12 to 12+6	19.0	21.0	24.0	27.0	33.0	34.0	35.0
13 to 13+6	26.0	27.0	28.0	33.0	37.0	38.0	38.0
14 to 14+6	32.0	33.0	33.0	38.0	41.0	42.0	44.0
15 to 15+6	36.0	38.0	39.0	42.0	47.0	49.0	54.0
16 to 16+6	40.0	41.0	42.0	46.0	50.0	52.0	52.0
17 to 17+6	42.8	45.0	47.0	51.0	55.0	57.0	59.0
18 to 18+6	45.0	47.0	51.0	55.0	59.6	68.0	70.0
19 to 19+6	49.0	52.0	54.3	58.0	64.0	66.9	69.5
20 to 20+6	56.0	57.0	59.0	63.0	68.0	70.0	73.0
21 to 21+6	59.0	61.0	63.0	67.0	72.0	74.0	77.0
22 to 22+6	63.0	65.0	66.0	70.0	75.0	76.1	77.0
23 to 23+6	64.0	66.0	69.0	74.0	79.0	81.0	83.0
24 to 24+6	69.0	71.0	74.0	78.0	83.0	86.0	87.0
25 to 25+6	72.1	75.0	78.0	83.0	88.0	90.6	92.0
26 to 26+6	76.0	78.0	81.0	86.0	92.0	94.0	97.0
27 to 27+6	79.9	81.0	83.3	90.0	97.0	100.0	101.0
28 to 28+6	84.0	86.0	89.0	94.0	99.0	100.0	101.0
29 to 29+6	79.8	85.3	90.0	96.0	101.0	102.0	105.0
30 to 30+6	87.0	91.0	93.0	99.0	104.0	107.0	109.2
31 to 31+6	88.0	93.0	96.0	102.0	107.0	108.0	109.0
32 to 32+6	95.0	97.0	99.0	104.0	110.0	111.0	112.0
33 to 33+6	97.0	99.0	102.0	107.0	111.0	113.0	114.0
34 to 34+6	99.0	101.0	104.0	109.0	115.0	116.0	118.0
35 to 35+6	101.0	103.0	105.0	111.0	116.0	117.0	118.0
36 to 36+6	105.0	105.0	106.0	113.0	118.0	120.0	122.0
37 to 37+6	104.0	105.0	108.3	116.0	119.7	122.0	124.0
38 to 38+6	108.0	109.0	111.0	117.0	122.0	125.0	126.0
39 to 39+6	110.0	111.0	113.6	119.0	125.0	129.0	131.0
40 to 40+6	112.0	112.7	115.0	119.0	125.0	129.4	132.8
41 to 41+6	110.0	114.0	116.0	121.0	127.0	127.0	127.8
42 to 42+6	106.0	106.0	106.0	123.0	134.0	134.0	134.0

This means that 10% of the fetuses at 20 to 20 + 6 had a mean occipitofrontal diameter less than 59 millimeters, while 90% had a mean occipitofrontal diameter greater than 59 millimeters. Similarly, the 97<sup>th</sup> percentile of

occipitofrontal diameter at 36 to 36 + 6 is 118 millimeters. Hence 97% of fetuses at 36 to 36 + 6 had a mean occipitofrontal diameter less than 118 millimeters while 3% had a mean occipitofrontal diameter greater than 118 millimeters. The standard score or z-score of occipitofrontal diameter measurements in 13,740 fetuses ranging from 12 – 42 weeks of gestation is shown in Tab.6.12. The z-score enables us to look at occipitofrontal diameter measurements in each gestational age and see how they compare on the same standard; taking into account the mean and standard deviation of each gestational age. For example, occipitofrontal diameter measurements at 15 weeks are 0.0104 standard deviations from the mean while measurements at 37 weeks are 0.0000 standard deviations from the mean. Again, from the above z-score table, it can be seen that the occipitofrontal diameter measurements at 38 weeks gestation are – 0.0075 standard deviations from the mean.

When occipitofrontal diameter data of 13,740 fetuses was subjected to skewness analysis at different gestational age ranging from 12 – 42 weeks (Fig. 6.29), it can be seen that the distribution of occipitofrontal diameter measurements has a longer “tail” to the right of the central maximum than to the left or is skewed to the right from 13 – 24, 26, 38, 39 and 40 weeks. From 12, 13, 25, 27 – 37, 41 and 42 weeks, the distribution has a longer “tail” to the left of the central maximum than to the right or is skewed to the left. By the time pregnancy reaches term, the distribution becomes skewed to the right before skewing again to the left as from 41 weeks. When the occipitofrontal diameter data was subjected to kurtosis analysis (Fig. 6.30), the analysis was found to be leptokurtic at 14, 15, 18, 19, 29 and 38 weeks of gestation while mesokurtic at the other weeks of gestation. The coefficient of dispersion of occipitofrontal diameter data of 13,740 fetuses at different gestational age shows a decrease in value as gestational age advances except at 18 and 42 weeks where it peaks (Fig. 6.31). The occipitofrontal diameter scattergram in Fig. 6.45 shows that there are very few bad data points or outliers in

the occipitofrontal diameter measurements of 13,740 fetuses. The outliers are more from 26 – 42 weeks of gestation. This shows the pattern of growth recognized for neural tissue which suggests growth of brain.

**Tab. 6.12** *Standard score (z-score) of occipitofrontal diameter measurements in 13,740 Nigerian fetuses in Jos ranging from 12 – 42 weeks gestation.*

GA (weeks, days)	Fetuses (n)	Mean z-score
12 to 12+6	49	5.52E-03
13 to 13+6	384	-6.16E-03
14 to 14+6	371	6.11E-03
15 to 15+6	351	1.04E-02
16 to 16+6	505	-9.32E-03
17 to 17+6	427	-5.30E-03
18 to 18+6	446	3.93E-03
19 to 19+6	282	-3.21E-03
20 to 20+6	553	-2.63E-03
21 to 21+6	400	-4.88E-03
22 to 22+6	398	-5.53E-03
23 to 23+6	478	-7.93E-03
24 to 24+6	520	-5.43E-03
25 to 25+6	388	-1.16E-03
26 to 26+6	511	-7.61E-03
27 to 27+6	432	-7.54E-03
28 to 28+6	548	9.84E-03
29 to 29+6	484	2.09E-03
30 to 30+6	625	-4.13E-03
31 to 31+6	523	-6.80E-03
32 to 32+6	583	-0.50846
33 to 33+6	516	-9.73E-03
34 to 34+6	744	-0.28427
35 to 35+6	739	3.66E-03
36 to 36+6	599	-4.29E-03
37 to 37+6	532	8.00E-05
38 to 38+6	481	-7.57E-03
39 to 39+6	525	3.05E-03
40 to 40+6	252	5.99E-03
41 to 41+6	72	-8.81E-03
42 to 42+6	22	4.43E-03
Total	13,740	

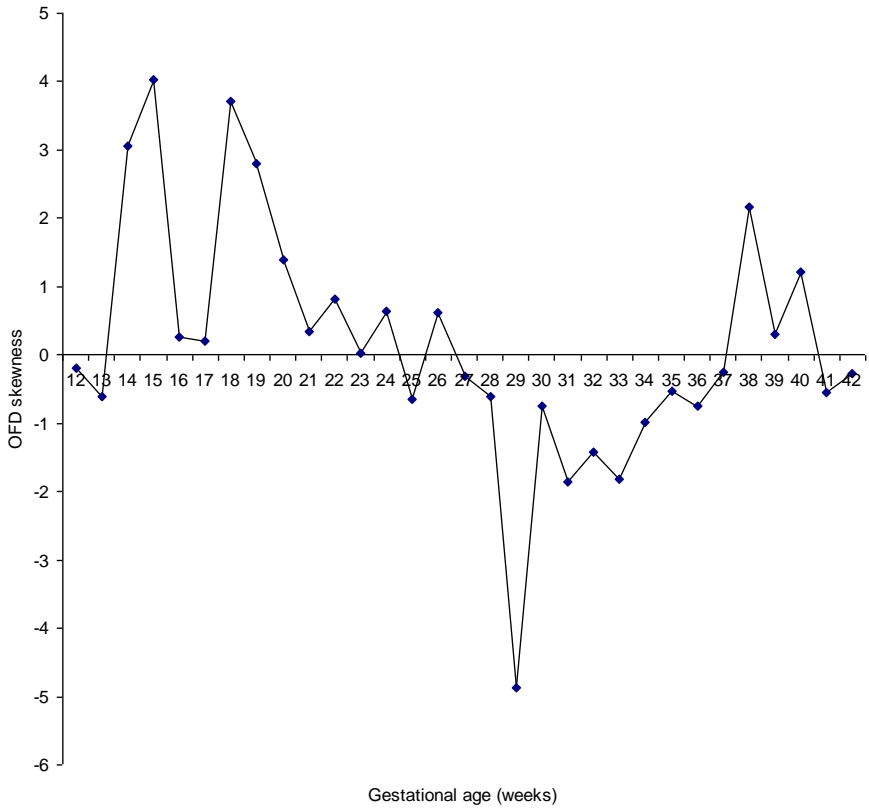


**Fig. 6.29** Occipitofrontal diameter data of 13,740 fetuses subjected to Skewness analysis at different gestational age ranging from 12 – 42 weeks.

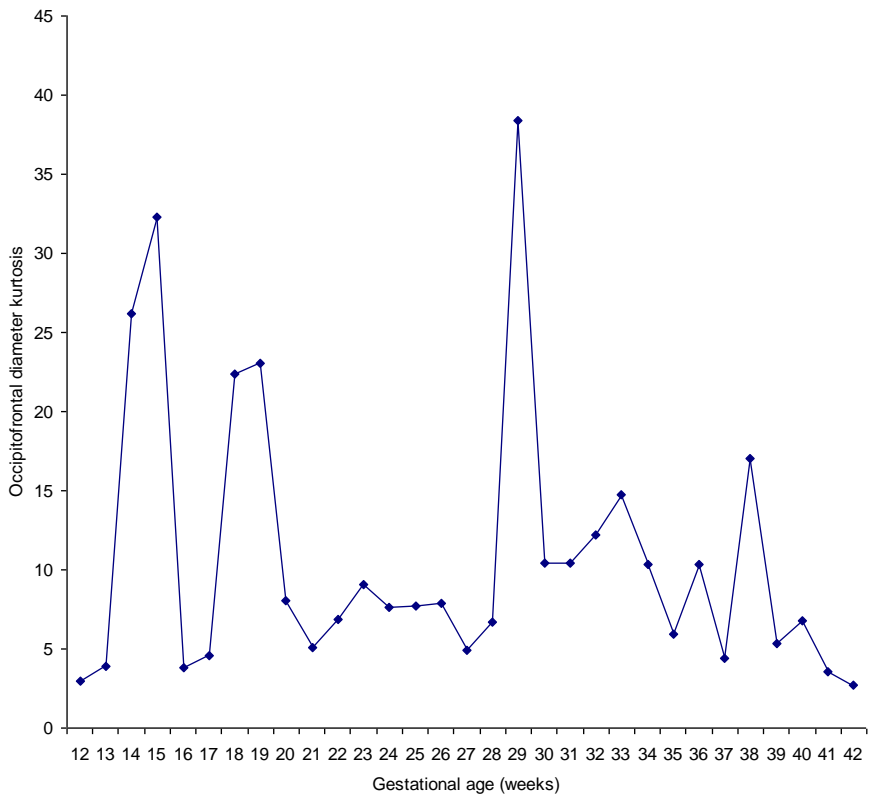


**Fig. 6.30** Occipitofrontal diameter data of 13,740 fetuses subjected to kurtosis analysis at different gestational age ranging from 12 – 42 weeks.

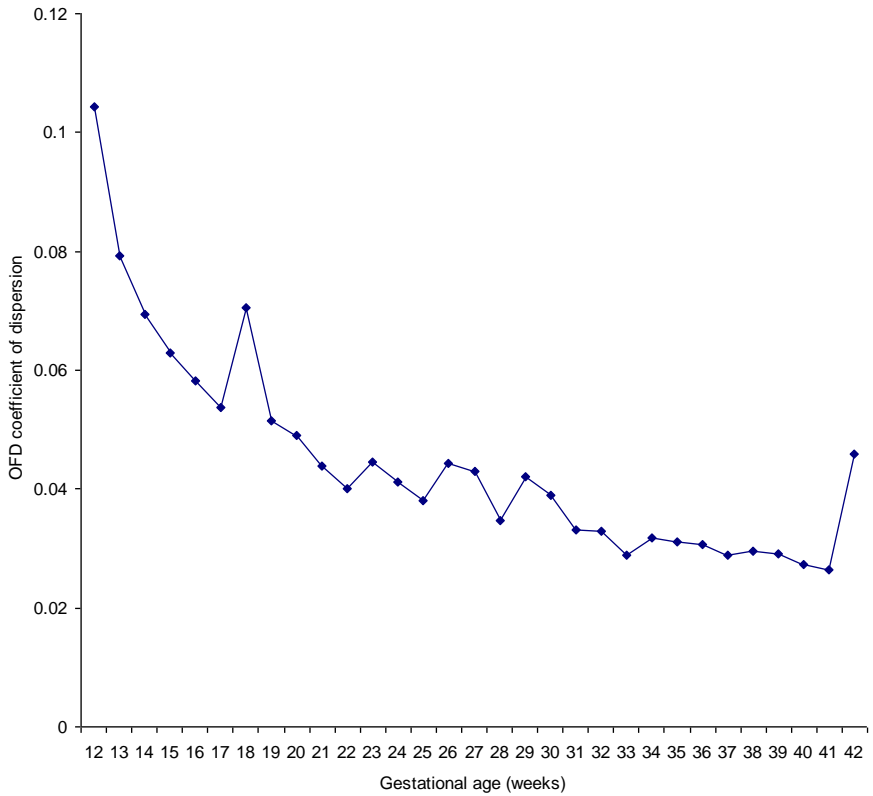


**Fig. 6.31** Occipitofrontal diameter coefficient of dispersion in 13,740 fetuses of gestational ages between 12 to 42 weeks.



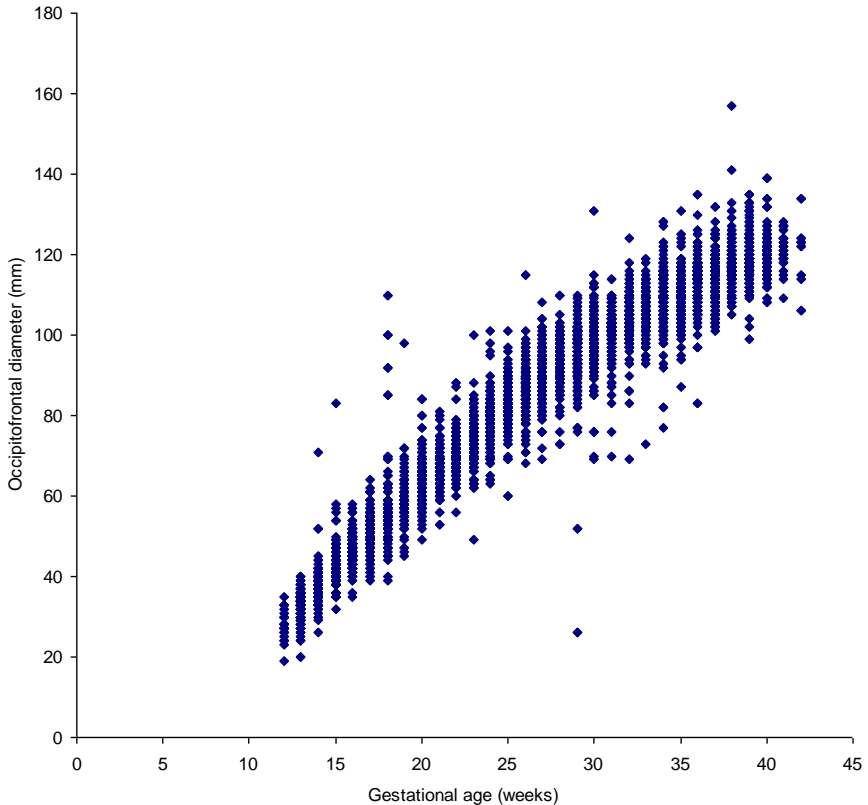


**Fig. 6.32** Scattergram of 13,740 fetal occipitofrontal diameter measurements from 12 – 42 weeks gestation.

In Fig. 6.33, mean occipitofrontal diameter is plotted against gestational age with error bars showing standard deviation. Mathematical modeling of occipitofrontal diameter data demonstrated that the best-fitted regression model is as shown in Fig. 6.34. There is a positive polynomial correlation between gestational age and occipitofrontal diameter with a correlation of determination of  $r^2 = 0.9996$  ( $P < 0.0001$ ) in Nigerian fetuses in Jos. The relationship is best described by the third order polynomial regression equation  $y = -0.001x^3 + 0.0137x^2 + 4.671x - 27.99$  where  $y$  is the occipitofrontal diameter in millimeters and  $x$  is the gestational age in weeks.

When monthly mean values of occipitofrontal diameter are plotted against gestational age in months, a positive polynomial correlation between gestational age and occipitofrontal diameter with a correlation of determination of  $r^2 = 0.9997$  ( $P < 0.0001$ ) in Nigerian fetuses in Jos was found (Fig. 6.35). The relationship is best described by the second order polynomial regression equation  $y = - 1.2964x^2 + 32.011x - 70.179$  where  $y$  is the occipitofrontal diameter in millimeters and  $x$  is the gestational age in months.

When other fetal anthropometric parameters like head circumference, biparietal diameter, abdominal circumference, femur length and weight are plotted against occipitofrontal diameter certain hidden relationships can be forced out. For example, Fig.6.36 shows the relationship of occipitofrontal diameter with biparietal diameter. From the graph, it can be seen that there is a positive linear correlation between biparietal diameter and occipitofrontal diameter with a correlation of determination of  $r^2 = 0.9997$  ( $P < 0.0001$ ) in Nigerian fetuses in Jos. The relationship is best described by the linear regression equation  $y = 0.8046x - 0.9072$  where  $y$  is the biparietal diameter in millimeters and  $x$  is the occipitofrontal diameter in millimeters. Fig. 6.37 shows relationship of occipitofrontal diameter with head circumference which has regression equation of  $y = 2.882x + 0.1487$ ;  $r^2 = 1$  ( $P < 0.0001$ ). Fig. 6.38 shows relationship of occipitofrontal diameter with abdominal circumference. From the graph, it can be seen that there is a positive polynomial correlation between abdominal circumference and occipitofrontal diameter with a correlation of determination of  $r^2 = 0.9993$  ( $P < 0.0001$ ) in Nigerian fetuses in Jos.

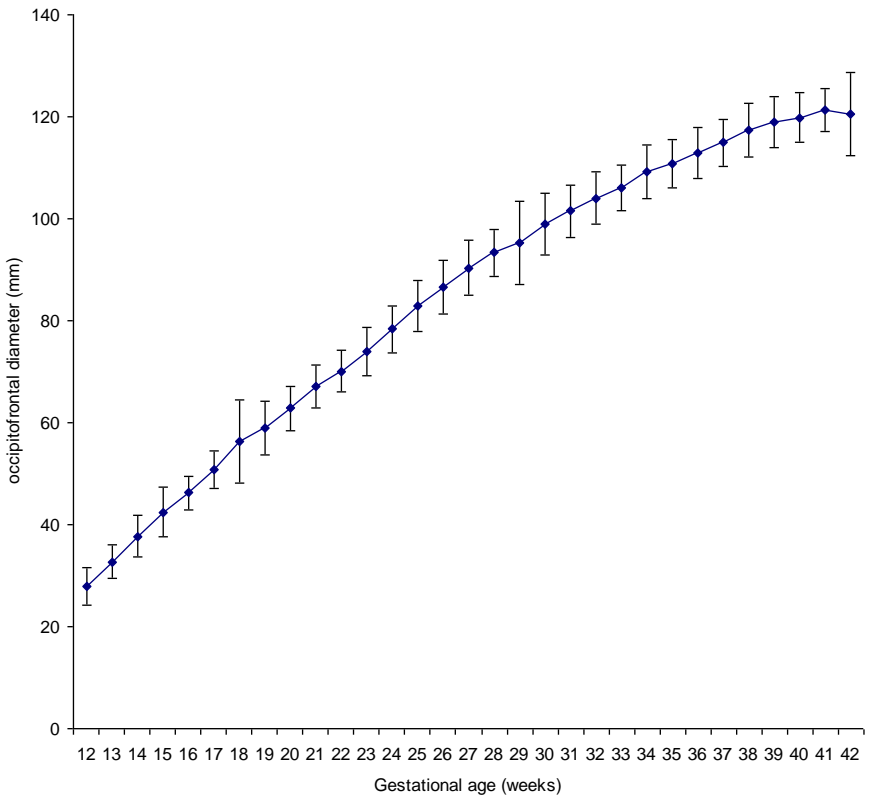


**Fig. 6.33** Mean fetal occipitofrontal diameter values in 13,740 fetuses of women at different gestational ages between 12 – 42 weeks. The vertical bars show the values of  $\pm SD$ .

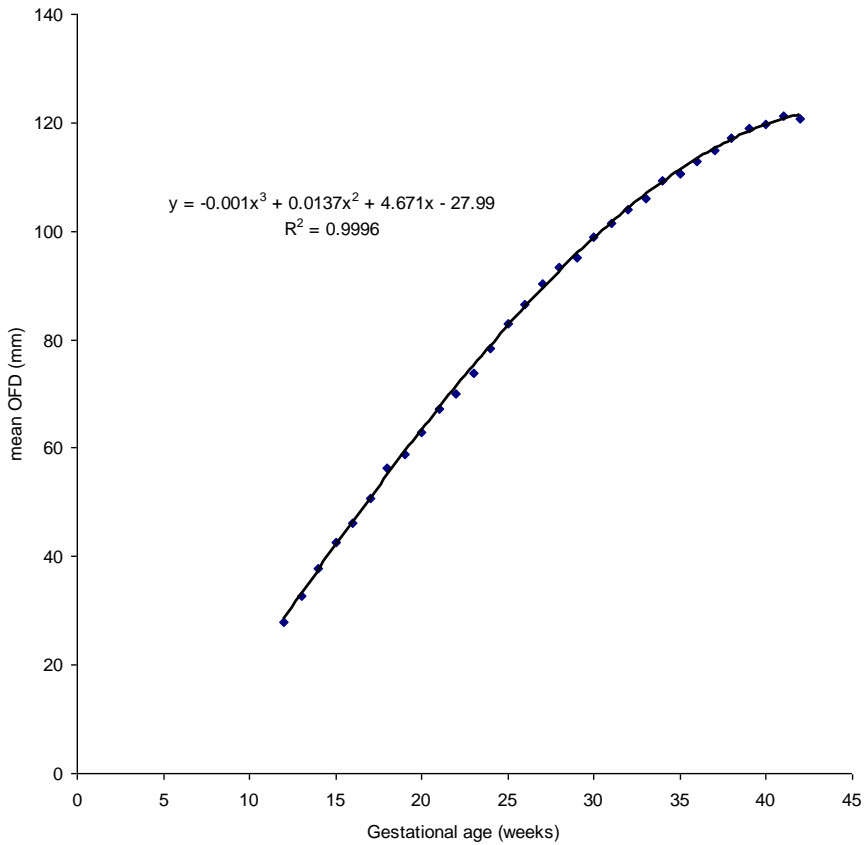


**Fig. 6.34** Correlation and regression equation of mean occipitofrontal diameter values in 13,740 Nigerian fetuses in Jos plotted against gestational age in weeks.

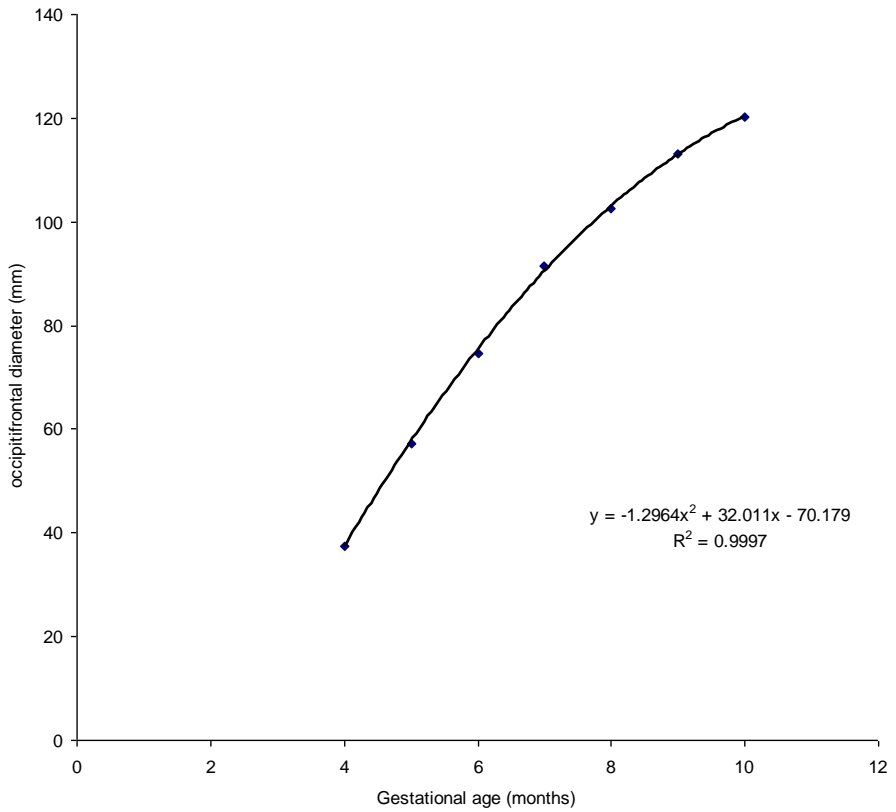


**Figure 6.35** Correlation and regression equation of mean occipitofrontal diameter values in 13,740 Nigerian fetuses in Jos plotted against gestational age in months.

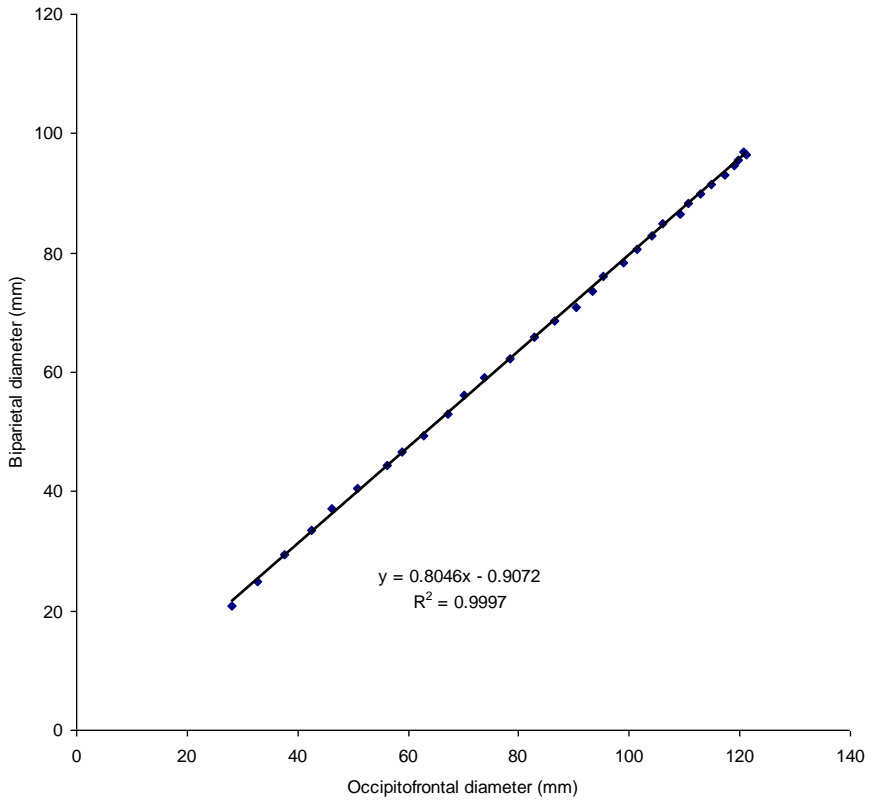


**Fig. 6.36** Correlation and regression equation of mean occipitofrontal diameter values in 13,740 Nigerian fetuses in Jos plotted against biparietal diameter.

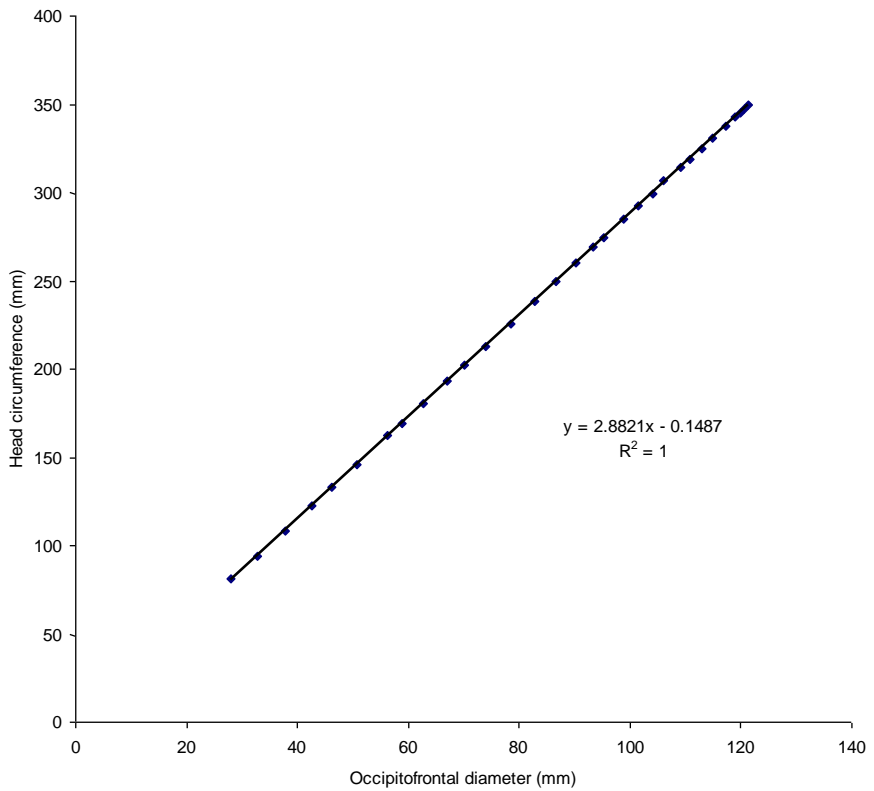


**Fig. 6.37** Correlation and regression equation of mean head circumference values in 13,740 Nigerian fetuses in Jos plotted against occipitofrontal diameter.

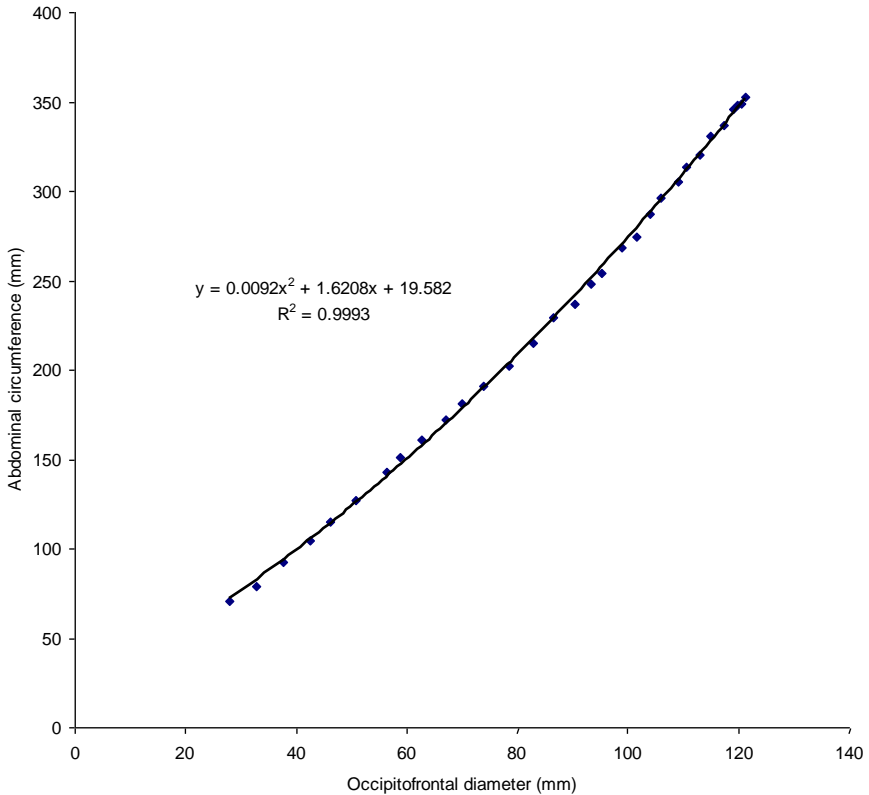


**Fig. 6.38** Correlation and regression equation of mean occipitofrontal diameter values in 13,740 Nigerian fetuses in Jos plotted against abdominal circumference.

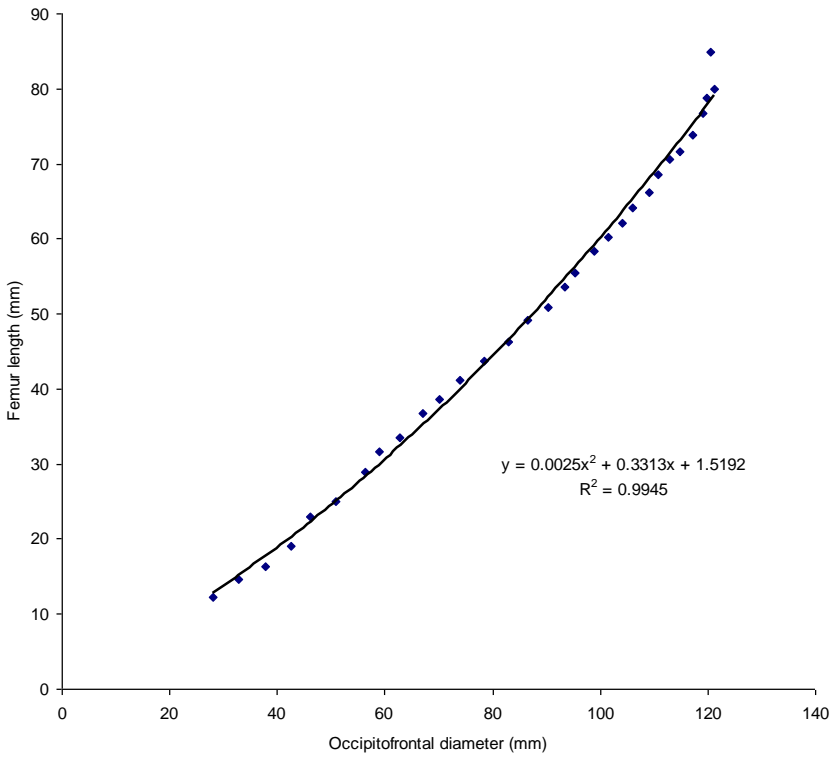
The relationship is best described by the quadratic regression equation  $y = 0.0092x^2 + 1.6208x + 19.582$  where  $y$  is the abdominal circumference in millimeters and  $x$  is the occipitofrontal diameter in millimeters.

Fig. 6.39 shows relationship between femur length and occipitofrontal diameter. There is a positive polynomial correlation between femur length and occipitofrontal diameter with a correlation of determination of  $r^2 = 0.9945$  ( $P < 0.0001$ ) in Nigerian fetuses in Jos. The relationship is best described by the quadratic regression equation  $y = 0.0025x^2 + 0.3313x + 1.5192$



where  $y$  is the femur length in millimeters and  $x$  is the occipitofrontal diameter in millimeters. Fig. 6.40 shows the relationship between fetal weight which is strongly correlated with fetal nutrition and occipitofrontal diameter. The graph shows that there is a positive polynomial correlation between fetal weight and occipitofrontal diameter with a correlation of determination of  $r^2 = 0.9989$  ( $P < 0.0001$ ) in Nigerian fetuses in Jos. The relationship is best described by the third order regression equation  $y = 0.0071x^3 - 1.0218x^2 + 57.868x - 925.93$  where  $y$  is the fetal weight in grams and  $x$  is the occipitofrontal diameter in millimeters.

Occipitofrontal diameter centile values for 5<sup>th</sup>, 50<sup>th</sup> and 95<sup>th</sup> are plotted as shown in Fig. 6.41. In Fig. 6.42, the 3<sup>rd</sup>, 50<sup>th</sup> and 97<sup>th</sup> are smoothed into a growth chart which can be utilized to determine occipitofrontal diameter growth and of course brain size development, which is strongly related to intelligence and wellness, using occipitofrontal diameter. Fig. 6. 43 is a graphical display showing the growth rate of the measured fetal occipitofrontal diameter at gestational age ranging from 12 – 42 weeks. It is clear from this graph that growth rate is much higher in the early stages of development than the late ones which precede term.



**Fig. 6.39** Correlation and regression equation of mean occipitofrontal diameter values in 13,740 Nigerian fetuses in Jos plotted against femur length.

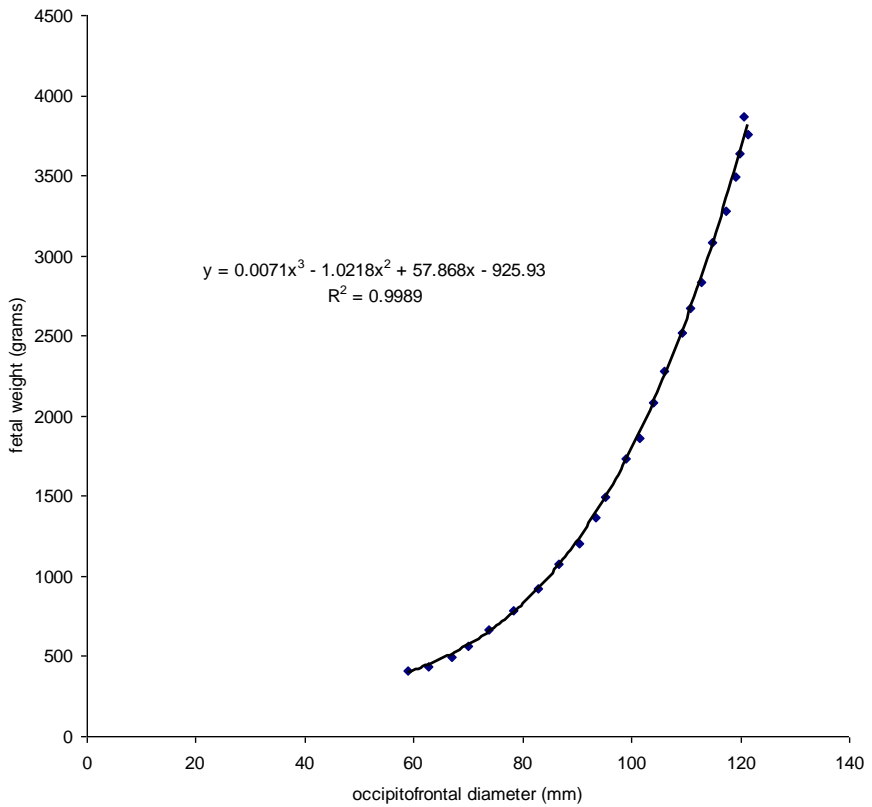


**Fig. 6.40** Correlation and regression equation of mean occipitofrontal diameter values in 13,740 Nigerian fetuses in Jos plotted against fetal weight.

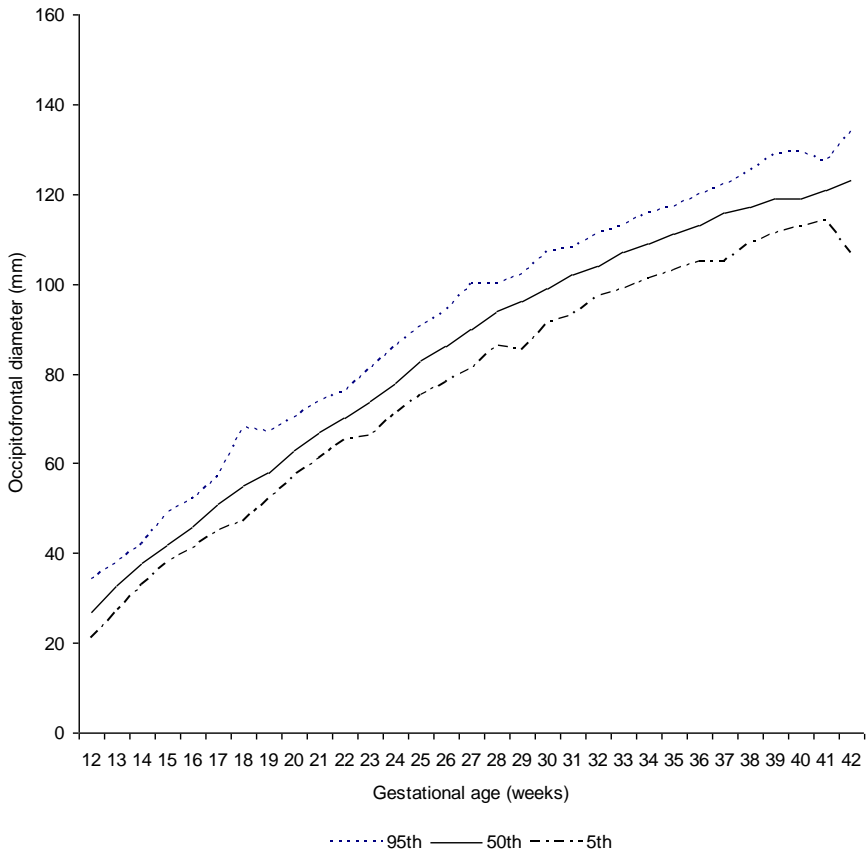


**Fig. 6.41** Fifth, 50th and 97th centiles for occipitofrontal diameter in 13,740 fetuses at different gestational ages from 12 to 42 weeks.

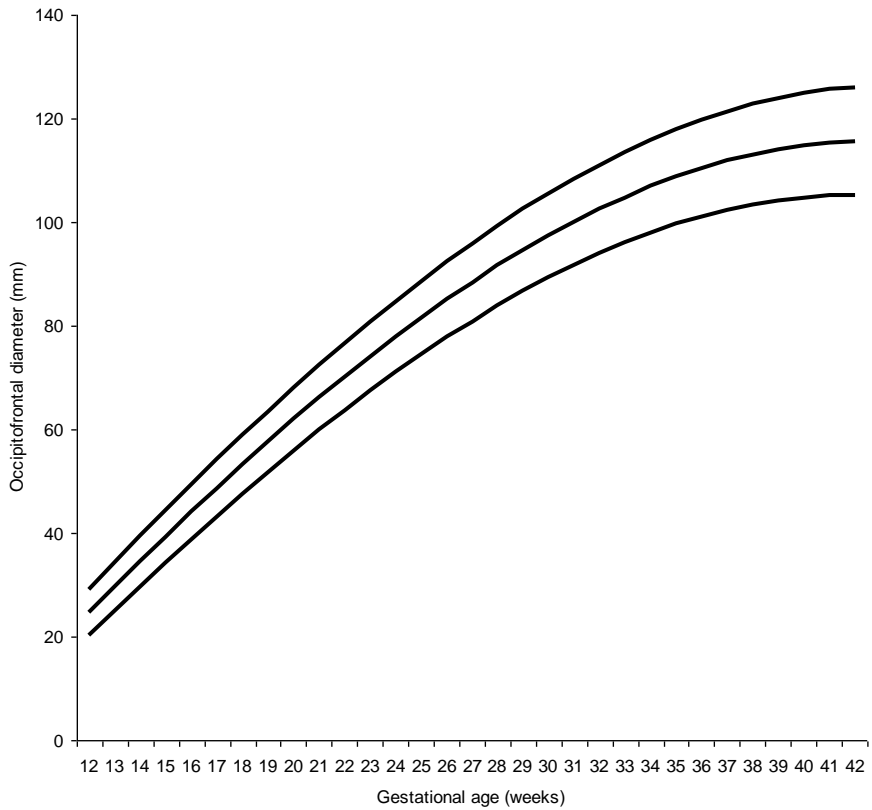


**Fig. 6.42** Curves created from 3rd, 50th and 97th fetal occipitofrontal diameter centiles.

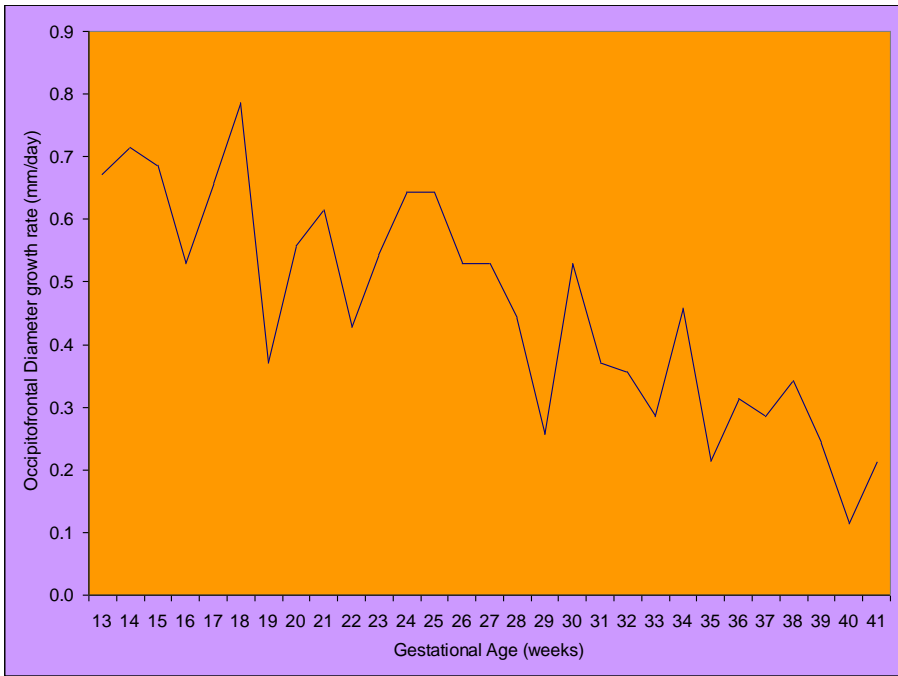


*Fig. 6.43* Growth velocity pattern of occipitofrontal diameter in 13,740 Nigerian fetuses in Jos ranging from 12 – 42 weeks.

## Biometrics of Fetal Abdominal Circumference

The mean fetal abdominal circumference values at each week of gestation from 12 – 42 are as shown in Tab. 6.13. This table gives the mean values of fetal abdominal circumference measurements for each gestational age in weeks from 12 – 42 weeks together with their corresponding standard deviations and standard errors of mean.

Variation in the measurements of fetal abdominal circumference was found to be 2mm and above at weeks 18, 21, 31, 35, 39 and 42. The highest mean abdominal circumference was achieved at 42 weeks and the lowest mean abdominal circumference was at 12 weeks. With the arithmetic mean, one has

some idea of the kind of numbers it represents, but the whole story is still a mystery. To clear up the mystery of the hidden numbers that made up a mean, the standard deviation is necessary. For example, the mean abdominal circumference at 36 weeks is 320.0mm plus 1.8mm or 320.0mm minus 1.8mm. This means 2 out of 3 measurements of abdominal circumference at 36 weeks, approximately 399 abdominal circumference measurements in a class of 599, should be between 318.2mm and 321.8mm. Since the standard error of mean at 36 weeks is 0.0mm, it is telling us that the real mean abdominal circumference of fetuses in Jos at 41 weeks is 320.0mm (320.0mm plus or minus 0.0mm). It can also be seen that the standard error of mean for each week of gestation from 12 – 42 is very small suggesting that the sample mean is very close to the population mean. For example, at 13 weeks gestation, the mean fetal abdominal circumference was 79.2mm while the standard error of mean was 1.2. This means that the difference between the mean abdominal circumferences of the sample of fetuses at 13 weeks is just 1.2mm different from that of the population of fetuses at 13 weeks gestation. The geometric means (Tab. 6.14) of all sets of measurements from 12 – 42 weeks are less than their arithmetic means but greater than their harmonic means indicating that all the values of fetal abdominal circumference measurements were not identical.

Tab. 6.15 gives the centile values of fetal abdominal circumference measurements. This table gives the 3<sup>rd</sup>, 5<sup>th</sup>, 10<sup>th</sup>, 50<sup>th</sup>, 90<sup>th</sup>, 95<sup>th</sup>, and 97<sup>th</sup> centile values for fetal abdominal circumference measured at different gestational age ranging from 12 – 42 weeks. For example, it can be seen from the table that the 5<sup>th</sup> percentile of abdominal circumference at 26 to 26 + 6 weeks gestation is 20.7 centimeters.

**Tab. 6.13** *Frequency distribution table of fetal abdominal circumference measurements showing the arithmetic mean, standard deviation and standard error of mean from 12 – 42 weeks gestation.*

<b>GA (week, days)</b>	<b>Fetuses (n)</b>	<b>Mean AC (mm)</b>	<b>SD</b>	<b>SE</b>
12 to 12+6	49	70.4	1.5	0.2
13 to 13+6	384	79.2	1.2	0.0
14 to 14+6	371	92.5	1.2	0.0
15 to 15+6	351	104.8	1.3	0.0
16 to 16+6	505	115.3	1.3	0.0
17 to 17+6	427	127.4	1.7	0.0
18 to 18+6	446	142.7	2.4	0.1
19 to 19+6	282	151.1	1.7	0.1
20 to 20+6	553	160.7	1.6	0.0
21 to 21+6	400	172.5	2.3	0.1
22 to 22+6	398	181.2	1.5	0.1
23 to 23+6	478	190.7	1.8	0.0
24 to 24+6	520	202.0	1.6	0.0
25 to 25+6	388	215.4	1.7	0.0
26 to 26+6	511	229.3	1.8	0.0
27 to 27+6	432	236.7	2.0	0.0
28 to 28+6	548	248.0	1.7	0.0
29 to 29+6	484	254.3	1.9	0.0
30 to 30+6	625	268.7	1.9	0.0
31 to 31+6	523	274.7	2.0	0.0
32 to 32+6	583	287.1	1.6	0.0
33 to 33+6	516	296.0	1.9	0.0
34 to 34+6	744	305.0	1.9	0.0
35 to 35+6	739	313.2	2.0	0.0
36 to 36+6	599	320.0	1.8	0.0
37 to 37+6	532	330.5	1.8	0.1
38 to 38+6	481	336.8	1.7	0.0
39 to 39+6	525	345.6	2.2	0.0
40 to 40+6	252	348.4	1.9	0.1
41 to 41+6	72	352.4	1.3	0.2
42 to 42+6	22	349.0	2.2	0.5
<b>Total</b>	<b>13,740</b>			



**Tab. 6.14** Frequency distribution table of fetal abdominal circumference measurements showing arithmetic mean, geometric mean and harmonic mean from 12 – 42 weeks gestation.

GA (week, days)	Number of fetuses (n)	Arithmetic mean (mm)	Geometric mean (mm)	Harmonic mean (mm)
12 to 12+6	49	7.042857	6.900781	6.770617
13 to 13+6	384	7.923438	7.82983	7.733103
14 to 14+6	371	9.249057	9.171251	9.087093
15 to 15+6	351	10.47692	10.40627	10.34549
16 to 16+6	505	11.5299	11.46782	11.41118
17 to 17+6	427	12.737	12.65461	12.57686
18 to 18+6	446	14.26883	14.11921	13.99722
19 to 19+6	282	15.11277	15.02775	14.94986
20 to 20+6	553	16.06546	15.98812	15.91212
21 to 21+6	400	17.2465	17.11336	16.98076
22 to 22+6	398	18.11658	18.05408	17.99383
23 to 23+6	478	19.06862	18.97901	18.8767
24 to 24+6	520	20.20365	20.13879	20.0751
25 to 25+6	388	21.53918	21.47404	21.40784
26 to 26+6	511	22.92955	22.86071	22.79436
27 to 27+6	432	23.6669	23.58506	23.50435
28 to 28+6	548	24.79635	24.74141	24.68774
29 to 29+6	484	25.42975	25.34406	25.23957
30 to 30+6	625	26.86768	26.80438	26.74241
31 to 31+6	523	27.474	27.39667	27.31487
32 to 32+6	583	28.70892	28.66116	28.6117
33 to 33+6	516	29.60368	29.54634	29.48943
34 to 34+6	744	30.50054	30.43813	30.37043
35 to 35+6	739	31.31651	31.25593	31.19619
36 to 36+6	599	31.99683	31.94766	31.89678
37 to 37+6	532	33.04906	32.99531	32.93646
38 to 38+6	481	33.68129	33.63824	33.59433
39 to 39+6	525	34.55905	34.48941	34.41487
40 to 40+6	252	34.83611	34.78634	34.73609
41 to 41+6	72	35.23889	35.2147	35.19038
42 to 42+6	22	34.90454	34.83539	34.7663
Total	13740			

**Tab. 6.15** *Fetal abdominal circumference centiles from 12 – 42 weeks.*

Abdominal circumference centiles (cm)							
Gestational age (weeks, days)	3rd	5th	10th	50th	90th	95th	97th
12 to 12+6	5.3	5.4	5.4	6.5	9.5	10.1	10.1
13 to 13+6	5.8	5.9	6.2	7.9	9.5	9.9	10.1
14 to 14+6	7.1	7.5	8.0	9.2	10.7	11.2	11.8
15 to 15+6	8.7	9.1	9.3	10.3	11.8	12.4	13.3
16 to 16+6	9.9	10.0	10.2	11.3	13.1	13.5	14.3
17 to 17+6	10.4	10.7	11.3	12.4	14.5	15.8	16.8
18 to 18+6	11.6	12.0	12.6	13.8	15.8	17.9	19.1
19 to 19+6	12.4	12.9	13.7	14.9	16.9	17.8	18.2
20 to 20+6	13.4	13.6	14.3	15.9	18.0	19.0	19.4
21 to 21+6	14.9	14.9	15.3	17.0	19.1	20.0	20.8
22 to 22+6	15.9	16.2	16.5	17.9	20.0	20.8	21.4
23 to 23+6	15.9	16.6	17.2	19.0	21.3	21.8	22.8
24 to 24+6	17.0	17.6	18.5	20.0	22.1	23.0	23.7
25 to 25+6	18.7	19.2	19.4	21.4	23.7	24.5	25.1
26 to 26+6	20.0	20.7	21.0	22.6	25.1	26.1	26.8
27 to 27+6	20.4	20.9	21.6	23.5	26.2	27.3	28.2
28 to 28+6	21.8	22.6	23.0	24.6	26.7	27.9	28.5
29 to 29+6	22.5	22.6	23.3	25.4	27.8	28.3	28.5
30 to 30+6	23.9	24.1	24.7	26.7	29.1	29.8	30.2
31 to 31+6	22.9	24.1	25.5	27.6	29.7	30.0	30.5
32 to 32+6	25.9	26.3	26.8	28.6	30.5	31.1	31.9
33 to 33+6	26.1	26.4	27.4	29.6	31.6	32.0	32.9
34 to 34+6	27.3	27.8	28.4	30.5	32.6	33.2	33.9
35 to 35+6	28.1	28.3	29.0	31.3	33.4	34.2	35.5
36 to 36+6	29.1	29.4	29.9	32.0	34.0	35.0	35.4
37 to 37+6	29.5	30.2	31.0	33.2	35.1	35.9	36.6
38 to 38+6	30.9	31.2	31.8	33.6	35.9	36.4	36.9
39 to 39+6	30.5	31.0	32.3	34.7	36.9	38.2	38.8
40 to 40+6	30.5	31.4	33.1	34.6	37.8	38.4	38.5
41 to 41+6	32.3	32.9	33.7	35.1	37.0	37.3	37.3
42 to 42+6	30.9	30.9	31.5	34.9	38.7	38.7	38.7

This means that 5% of the fetuses at 26 to 26 + 6 had a mean abdominal circumference less than 20.7 centimeters, while 95% had a mean abdominal circumference greater than 20.7 centimeters. Similarly, the 90<sup>th</sup> percentile of

abdominal circumference at 33 to 33 + 6 weeks is 31.6 centimeters. Hence 90% of fetuses at 33 to 33 + 6 weeks had a mean abdominal circumference less than 31.6 centimeters while 10% had a mean abdominal circumference greater than 31.6 centimeters.

The standard score or z-score of abdominal circumference measurements in 13,740 fetuses ranging from 12 – 42 weeks of gestation is shown in Tab. 6.16. The z-score enables one to look at abdominal circumference measurements at each gestational age and see how they compare on the same standard; taking into account the mean and standard deviation of each gestational age. For example, abdominal circumference measurements at 28 weeks are – 0.0215 standard deviations from the mean while measurements at 36 weeks are – 0.0175 standard deviations from the mean. Again, from the above z-score table, it can be seen that the abdominal circumference measurements at 38 weeks gestation are 0.00758 standard deviations from the mean.

When abdominal circumference data of 13,740 fetuses was subjected to skewness analysis at different gestational age ranging from 12 – 42 weeks (Fig. 6.44), it can be seen that the distribution of abdominal circumference measurements has a longer “tail” to the right of the central maximum than to the left or is skewed to the right from 12, 14, 15, 18, 19, 20, 21, 22 and 39 weeks. In the remaining weeks, the distribution has a longer “tail” to the left of the central maximum than to the right or is skewed to the left. By the time pregnancy reaches term, the distribution becomes skewed to the right before skewing again to the left as from 41 weeks. When the abdominal circumference data was subjected to kurtosis analysis (Fig.6. 45), the analysis was found to be leptokurtic at 15, 18, 19 and 21 weeks of gestation while at other weeks of gestation, the distribution was mesokurtic. The coefficient of dispersion (fig 46) of abdominal circumference data of 13,740 fetuses at different gestational age shows a relatively constant

pattern except at 20 weeks where it peaks. The abdominal circumference scattergram in Fig.6.47 shows that there are very few bad data points or outliers in the abdominal circumference measurements of 13,740 fetuses.

**Tab. 6.16** Standard score (z-score) of abdominal circumference measurements in 13,740 Nigerian fetuses in Jos ranging from 12 – 42 weeks gestation.

GA (weeks, days)	Fetuses (n)	Mean z-score
12 to 12+6	49	-2.71565
13 to 13+6	384	-1.75942
14 to 14+6	371	-7.86E-03
15 to 15+6	351	-2.37E-02
16 to 16+6	505	-7.62E-04
17 to 17+6	427	-2.00E-02
18 to 18+6	446	-4.86E-03
19 to 19+6	282	1.63E-02
20 to 20+6	553	-2.84E-02
21 to 21+6	400	-2.47E-02
22 to 22+6	398	-2.28E-02
23 to 23+6	478	-7.67E-03
24 to 24+6	520	2.28E-02
25 to 25+6	388	-4.85E-03
26 to 26+6	511	-2.50E-03
27 to 27+6	432	-1.55E-02
28 to 28+6	548	-2.15E-02
29 to 29+6	484	-1.30E-03
30 to 30+6	625	-1.22E-02
31 to 31+6	523	2.00E-02
32 to 32+6	583	-6.75E-03
33 to 33+6	516	1.94E-02
34 to 34+6	744	2.83E-03
35 to 35+6	739	-1.75E-02
36 to 36+6	599	-1.76E-02
37 to 37+6	532	0.272556
38 to 38+6	481	7.58E-03
39 to 39+6	525	-4.54E-03
40 to 40+6	252	-2.05E-02
41 to 41+6	72	-8.55E-03
42 to 42+6	22	2.07E-02
Total	13,740	

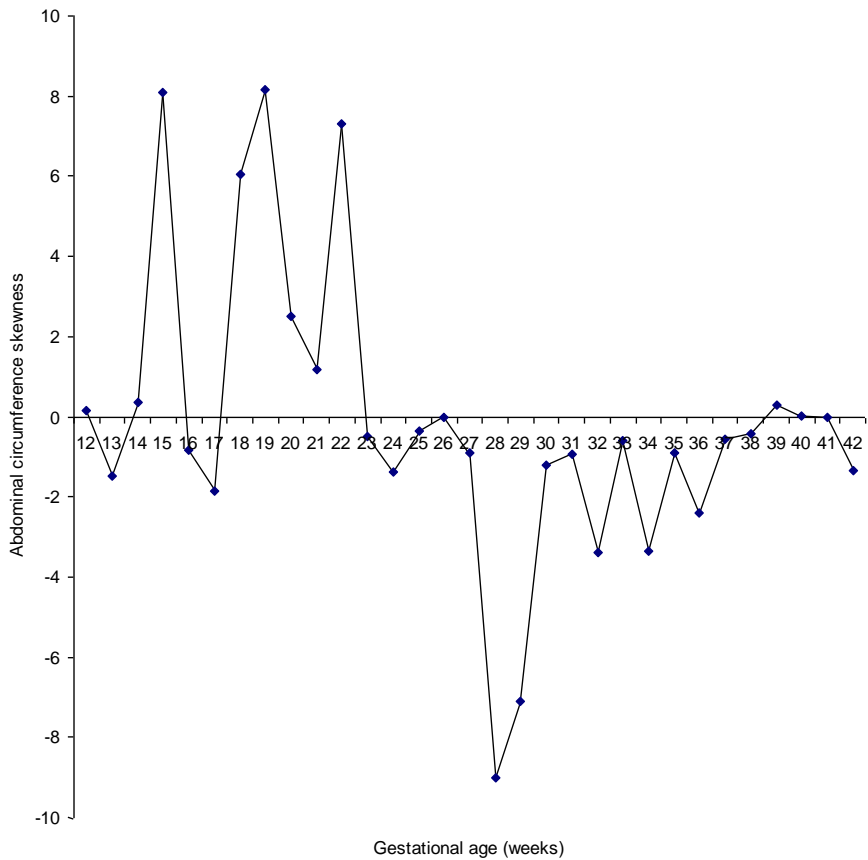


**Fig. 6.44** Abdominal circumference data of 13,740 fetuses subjected to Skewness analysis at different gestational age ranging from 12 – 42 weeks.

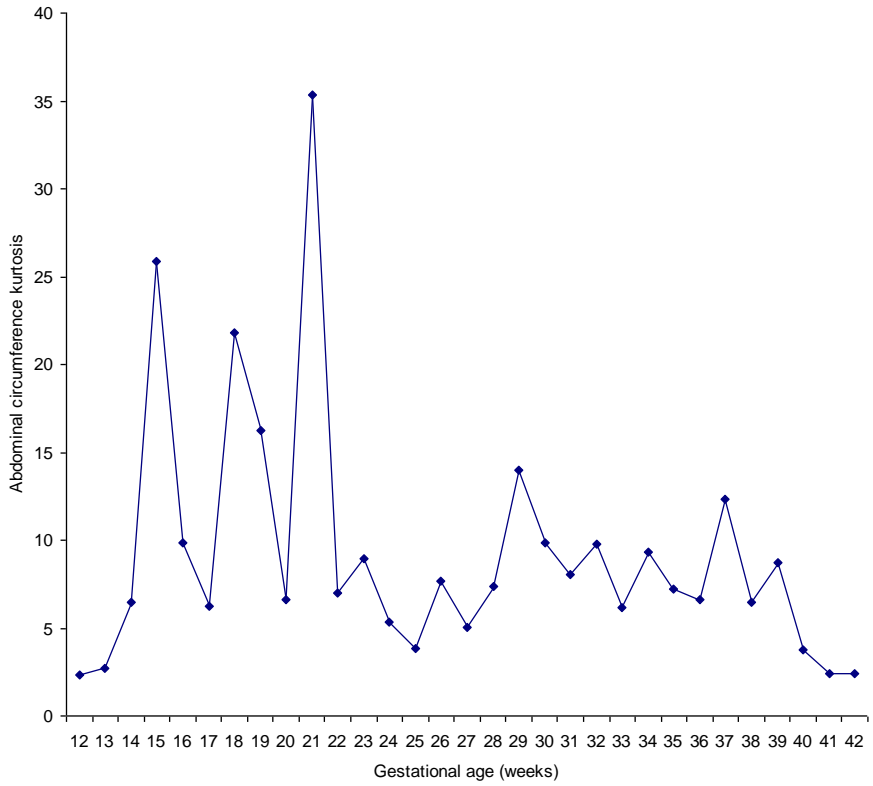


**Fig. 6.45** Abdominal circumference data of 13,740 fetuses subjected to kurtosis analysis at different gestational age ranging from 12 – 42 weeks.

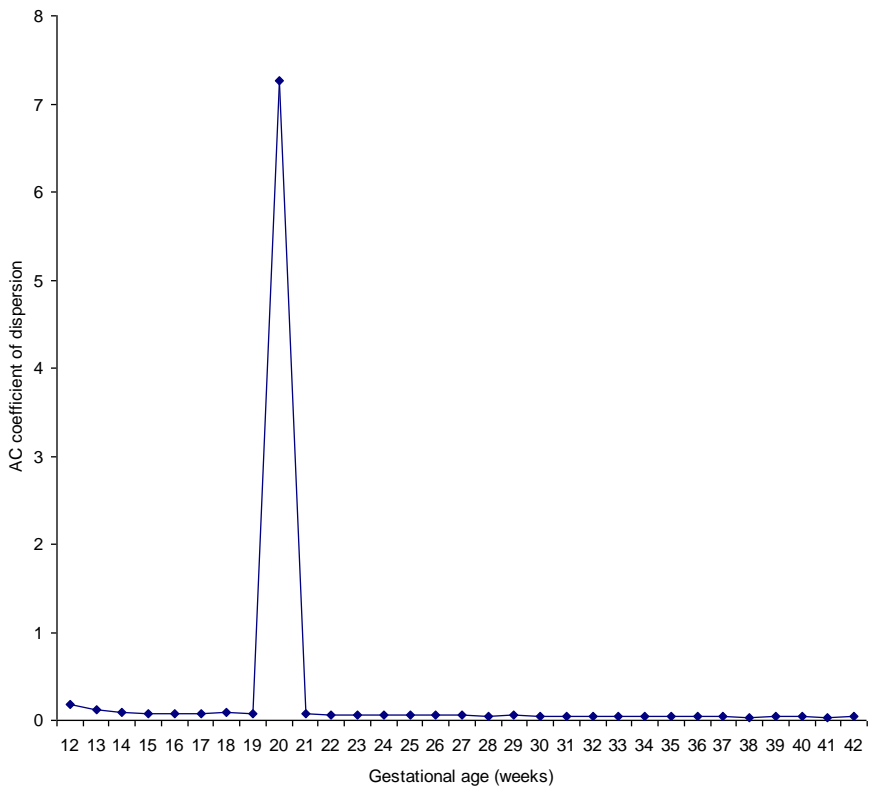


**Fig. 6.46** Abdominal circumference coefficient of dispersion in 13,740 fetuses of gestational ages between 12 to 42 weeks.

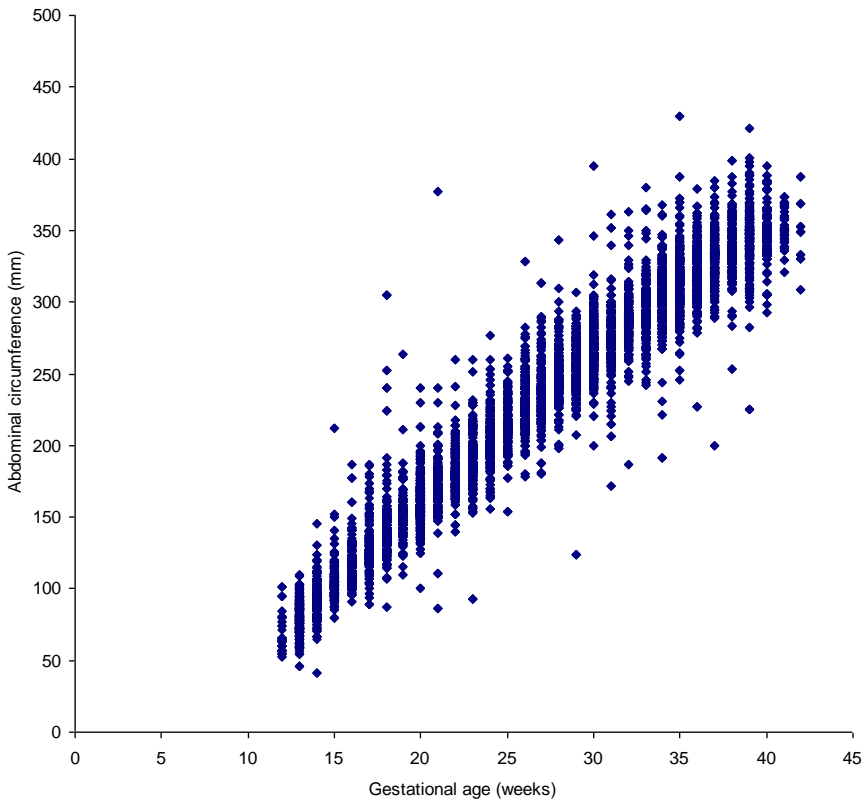


**Fig. 6.47** Scattergram of 13,740 fetal abdominal circumference measurements from 12 – 42 weeks gestation.

In Fig. 6.48, mean abdominal circumference is plotted against gestational age with error bars showing standard deviation. Mathematical modeling of abdominal circumference data demonstrated that the best-fitted regression model is that shown in Fig. 6.49. From this graph, it can be seen that there is a positive polynomial correlation between gestational age and abdominal circumference with a correlation of determination of  $r^2 = 0.9995$  ( $P < 0.0001$ ) in Nigerian fetuses in Jos. The relationship is best described by the fourth order polynomial regression equation  $y = -0.0004x^4 + 0.0349x^3 - 1.2485x^2 + 30.598x - 172.02$  where  $y$  is the abdominal circumference in millimeters and  $x$  is the gestational



age in weeks. The relationship is best described by the second order polynomial regression equation  $y = -2.1893x^2 + 73.861x - 168.99$  where  $y$  is the abdominal circumference in millimeters and  $x$  is the gestational age in months.

When other fetal anthropometric parameters like head circumference, biparietal diameter, occipitofrontal diameter, femur length and weight are plotted against abdominal circumference certain hidden relationships can be forced out. For example, Fig. 6.50 shows the relationship of abdominal circumference with biparietal diameter. From the graph, it can be seen that there is a positive polynomial correlation between biparietal diameter and abdominal circumference with a correlation of determination of  $r^2 = 0.9995$  ( $P < 0.0001$ ) in Nigerian fetuses in Jos. The relationship is best described by the quadratic regression equation  $y = -0.0003x^2 + 0.3777x - 3.6302$  where  $y$  is the biparietal diameter in millimeters and  $x$  is the abdominal circumference in millimeters. Fig. 6.51 shows relationship of abdominal circumference with occipitofrontal diameter. From the graph, it can be seen that there is a positive polynomial correlation between occipitofrontal diameter and abdominal circumference with a correlation of determination of  $r^2 = 0.9996$  ( $P < 0.0001$ ) in Nigerian fetuses in Jos.

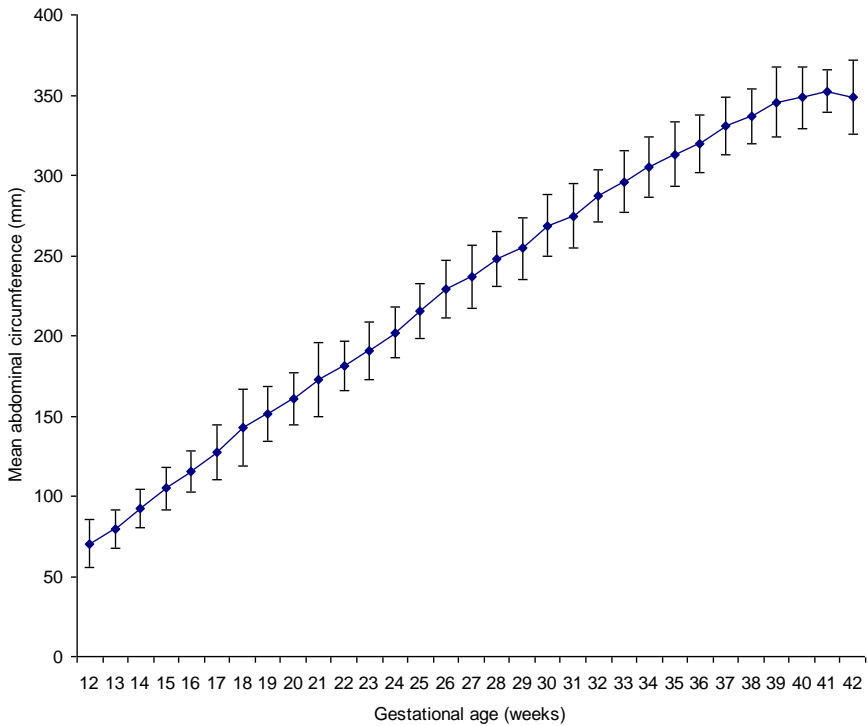


**Fig. 6.48** Mean fetal abdominal circumference values in 13,740 fetuses of women at different gestational ages between 12 – 42 weeks. The vertical bars show the values of  $\pm SD$ .

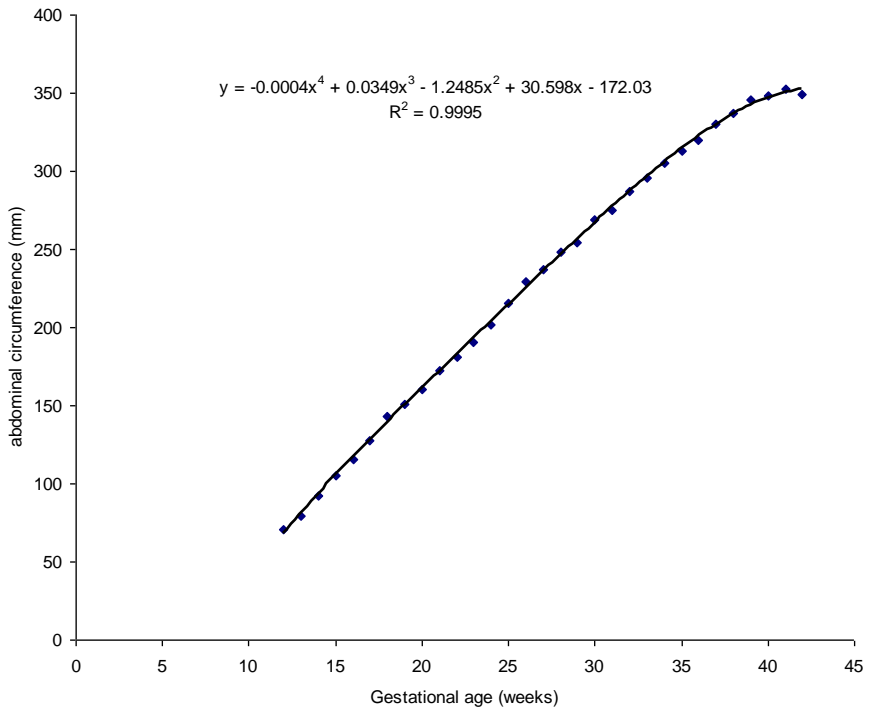


**Fig. 6.49** Correlation and regression equation of mean abdominal circumference values in 13,740 Nigerian fetuses in Jos plotted against gestational age in weeks.

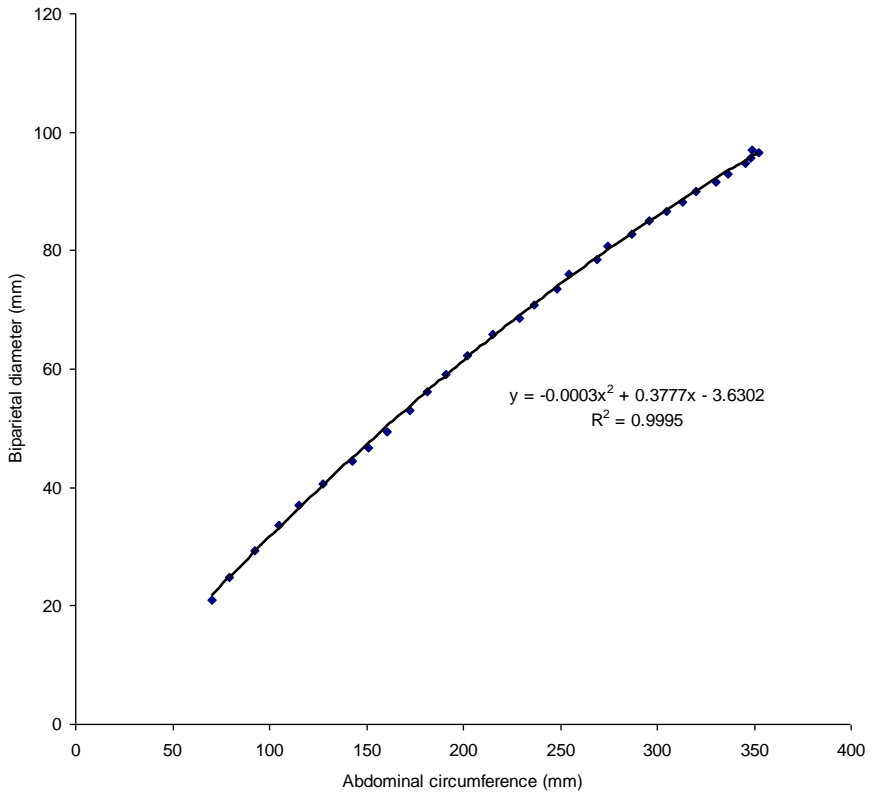


**Fig. 6.50** Correlation and regression equation of mean abdominal circumference values in 13,740 Nigerian fetuses in Jos plotted against biparietal diameter.

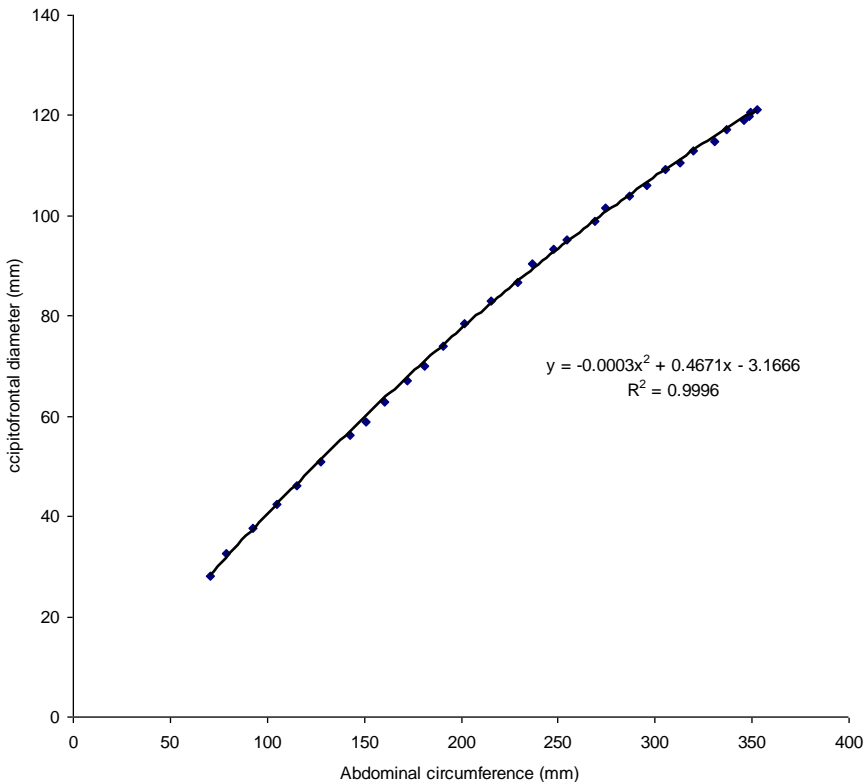


**Fig. 6.51** Correlation and regression equation of mean abdominal circumference values in 13,740 Nigerian fetuses in Jos plotted against occipitofrontal diameter.

The relationship is best described by the quadratic regression equation  $y = -0.0003x^2 + 0.4671x - 3.1666$  where  $y$  is the biparietal diameter in millimeters and  $x$  is the abdominal circumference in millimeters. Fig. 6.52 shows relationship of abdominal circumference with head circumference. From the graph, it can be seen that there is a positive polynomial correlation between abdominal circumference and head circumference with a correlation of determination of  $r^2 = 0.9996$  ( $P < 0.0001$ ) in Nigerian fetuses in Jos. The relationship is best described by the quadratic regression equation  $y = -0.0009x^2 + 1.3431x - 9.0021$  where  $y$  is the head circumference in millimeters and  $x$  is the abdominal circumference in millimeters. Fig. 6.53 shows

relationship between femur length and abdominal circumference. There is a positive linear correlation between femur length and abdominal circumference with a correlation of determination of  $r^2 = 0.9952$  ( $P < 0.0001$ ) in Nigerian fetuses in Jos. The relationship is best described by the linear regression equation  $y = 0.2381x - 5.0199$  where  $y$  is the femur length in millimeters and  $x$  is the abdominal circumference in millimeters.

Fig. 6.54 shows the relationship between fetal weight which is strongly correlated with fetal nutrition and abdominal circumference. From this graph, it can be seen that there is a positive polynomial correlation between fetal weight and abdominal circumference with a correlation of determination of  $r^2 = 0.9982$  ( $P < 0.0001$ ) in Nigerian fetuses in Jos. The relationship is best described by the second order regression equation  $y = 0.065x^2 - 16.072x + 1355.5$  where  $y$  is the fetal weight in grams and  $x$  is the abdominal circumference in millimeters. Abdominal circumference centile values for 5<sup>th</sup>, 50<sup>th</sup> and 95<sup>th</sup> centiles are plotted as shown in Fig. 6.55. In Fig. 6.56, 3<sup>rd</sup>, 50<sup>th</sup>, and 97<sup>th</sup> centiles are smoothed into a growth chart which can be utilized to determine growth of fetal abdominal circumference. Fig. 6.57 is a graphical display showing the growth rate of the measured fetal abdominal circumference. It is clear from this graph that growth rate fluctuates throughout the period of intrauterine life.

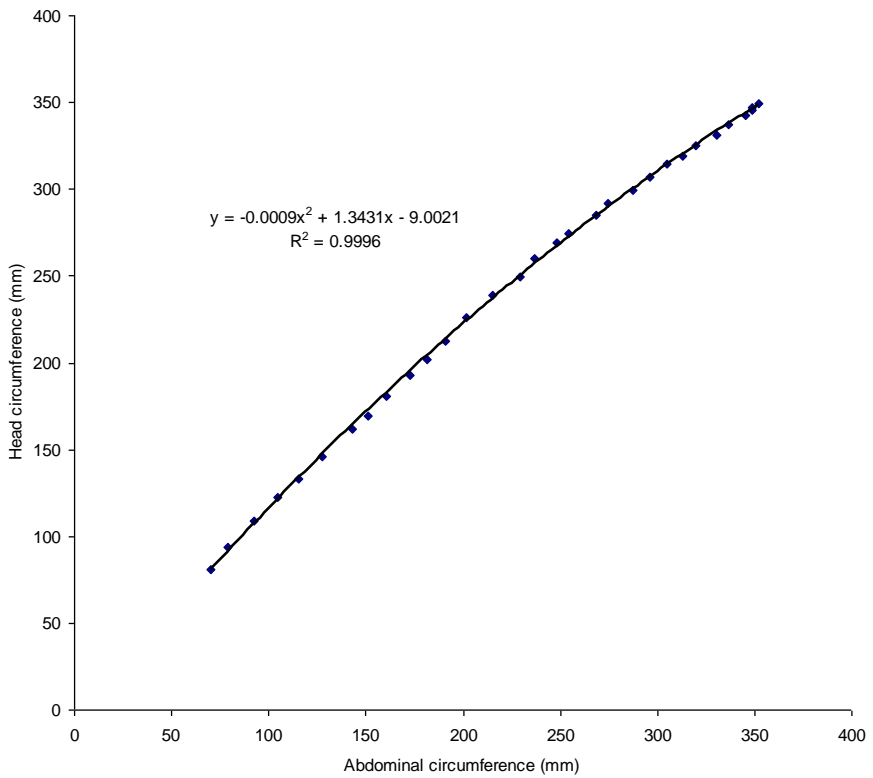


**Fig. 6.52** Correlation and regression equation of mean abdominal circumference values in 13,740 Nigerian fetuses in Jos plotted against abdominal circumference.

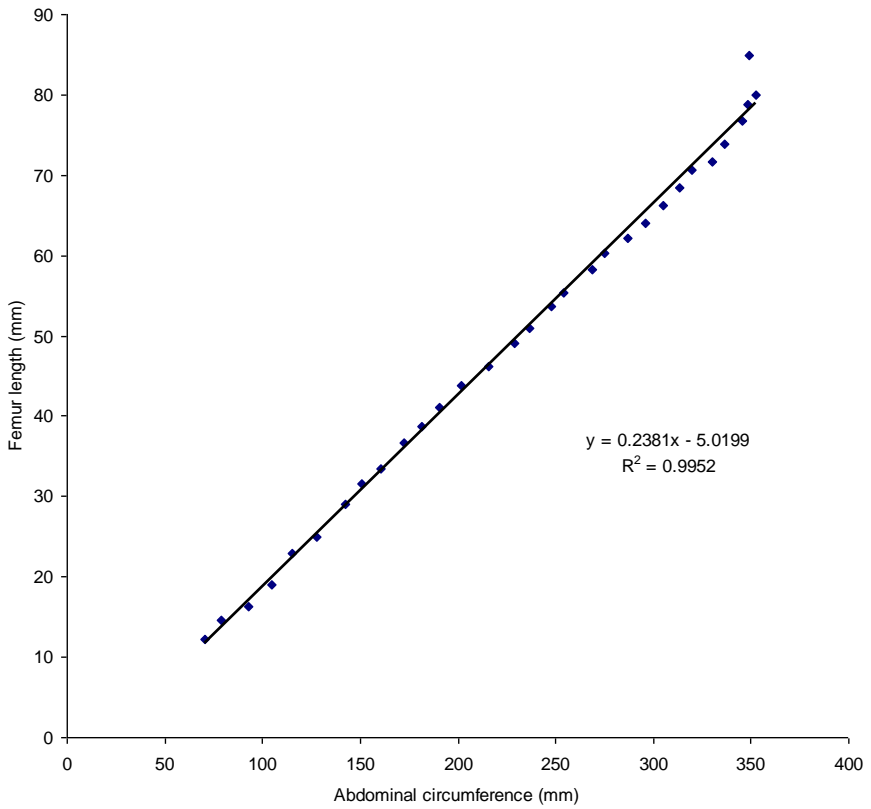


**Fig. 6.53** Correlation and regression equation of mean abdominal circumference values in 13,740 Nigerian fetuses in Jos plotted against femur length.



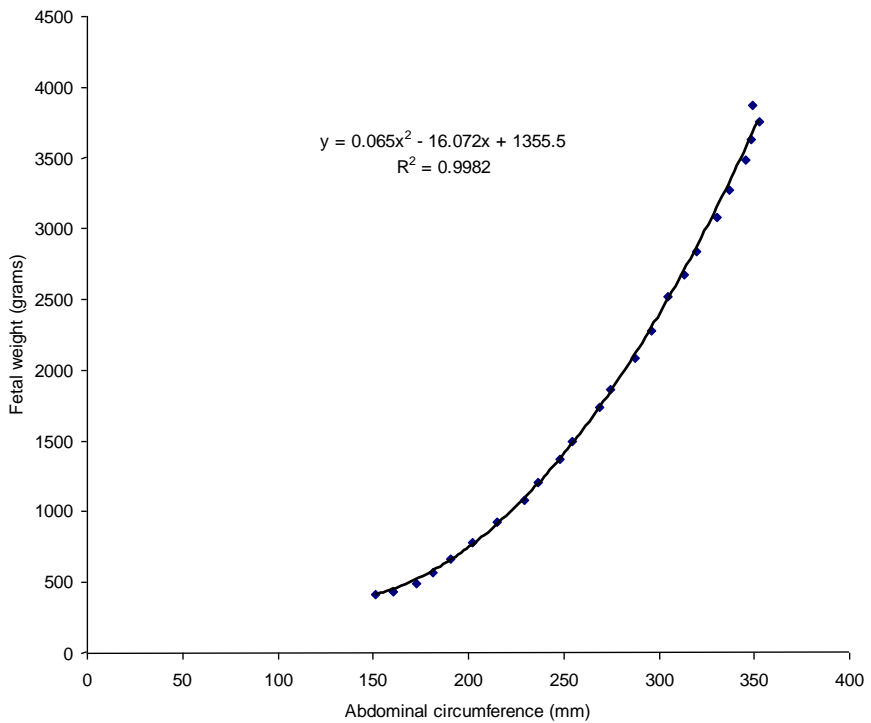


**Fig. 6.54** Correlation and regression equation of mean abdominal circumference values in 13,740 Nigerian fetuses in Jos plotted against fetal weight.

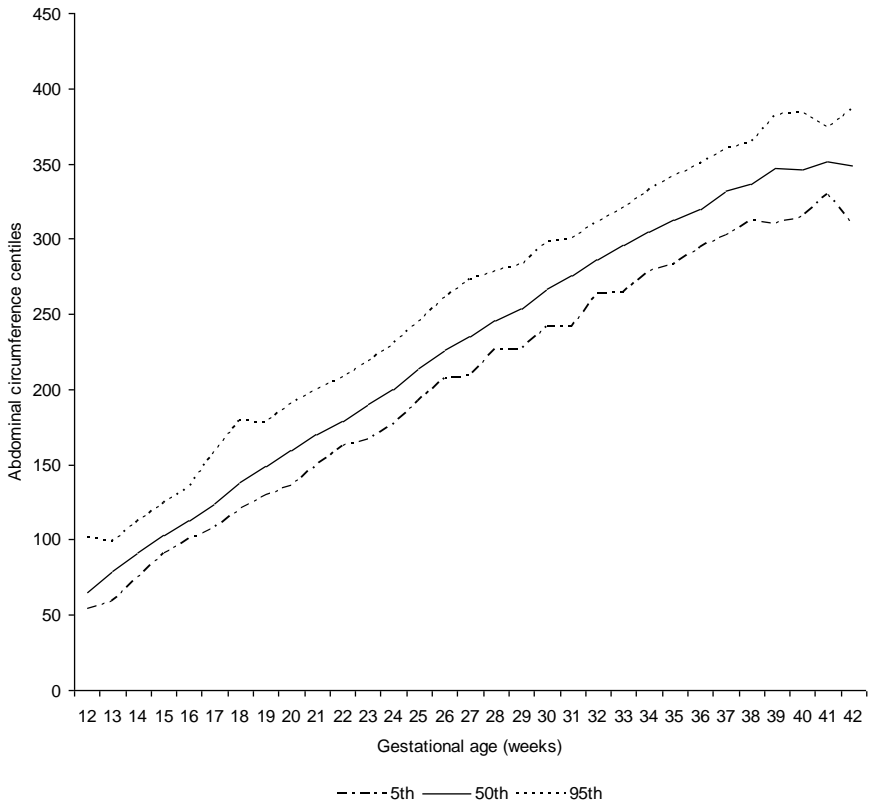


**Fig. 6.55** Fifth, 50th and 95th centiles for abdominal circumference in 13,740 fetuses at different gestational ages from 12 to 42 weeks.

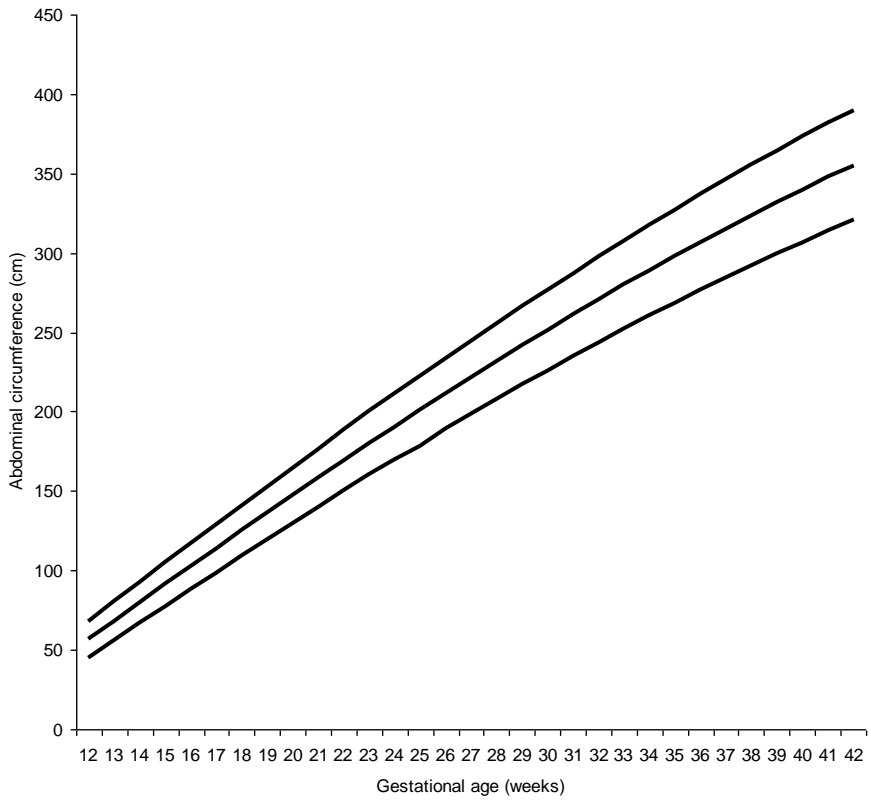


**Fig. 6.56** Curves created from 3rd, 50th and 97th fetal abdominal circumference centiles.

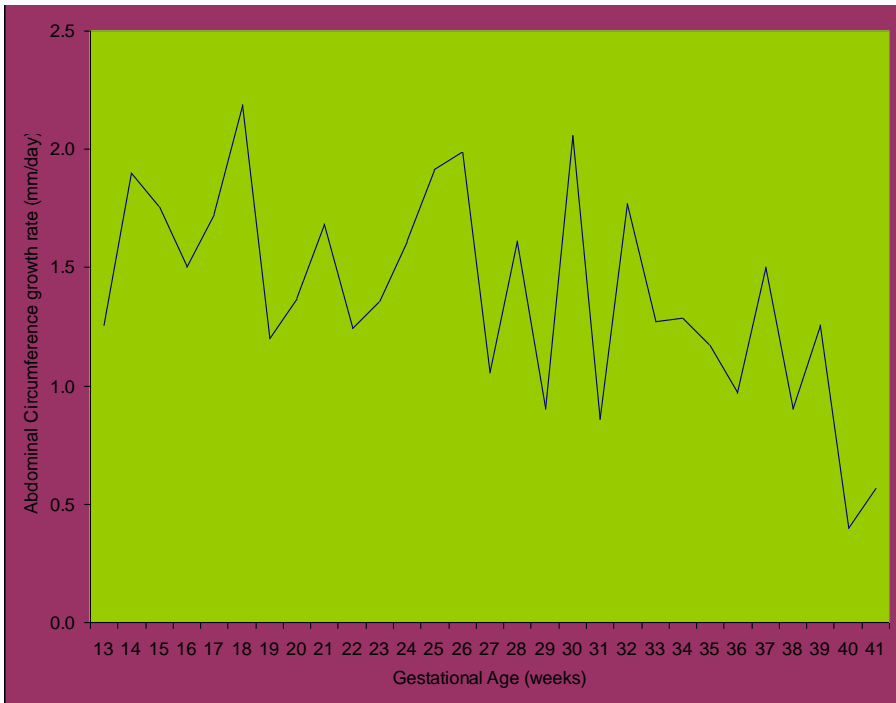


*Fig. 6.57 Growth velocity pattern of abdominal circumference in 13,740 Nigerian fetuses in Jos ranging from 12 – 42 weeks.*

## **Biometrics of Fetal Femur Length**

Fetal femur length measurements were classified into thirty one groups. The mean values at each week of gestation from 12 – 42 are as shown in Tab. 6.17. This table gives the mean values of fetal femur length measurements for each gestational age in weeks from 12 – 42 weeks together with their corresponding standard deviations and standard errors of mean. Variability of measurements was marked at weeks 16, 18, 37, 38 and 41 with the highest at 16 weeks. The standard error is found to be less than 1 throughout the period of gestation except at 42 weeks where it is 2.6 millimeters. With the arithmetic mean, one has some idea of the kind of numbers it represents, but the whole story is still a mystery. To

clear up the mystery of the hidden numbers that made up a mean, the standard deviation is necessary. For example, the mean femur length at 28 weeks is 53.6mm plus 3.4mm or 53.6mm minus 3.4mm. This means 2 out of 3 measurements of femur length at 28 weeks, approximately 365 femur length measurements in a class of 548, should be between 50.2mm and 57.0mm. Since the standard error of mean at 28 weeks is 0.1mm, it is telling us that the real mean femur length of fetuses in Jos at 28 weeks is probably between 53.5mm and 53.7mm (53.6mm plus or minus 0.1mm). It can also be seen that the standard error of mean for each week of gestation from 12 – 42 is very small suggesting that the sample mean is very close to the population mean. For example, at 33 weeks gestation, the mean fetal femur length was 64.1mm while the standard error of mean was 2.4. This means that the difference between the mean femur lengths of the sample of fetuses at 33 weeks is just 2.4mm different from that of the population of fetuses at 13 weeks gestation. The geometric means (Tab. 6.18) of all sets of measurements from 12 – 42 weeks are less than their arithmetic means but greater than their harmonic means indicating that all the values of fetal femur length measurements were not identical. Tab. 6. 19 gives the centile values of fetal femur length measurements. This table gives the 3<sup>rd</sup>, 5<sup>th</sup>, 10<sup>th</sup>, 50<sup>th</sup>, 90<sup>th</sup>, 95<sup>th</sup>, and 97<sup>th</sup> centile values for fetal femur length measured at different gestational age ranging from 12 – 42 weeks. For example, it can be seen from the table that the 5<sup>th</sup> percentile of femur length at 26 to 26 + 6 weeks gestation is 44 millimeters. This means that 5% of the fetuses at 26 to 26 + 6 had a mean femur length less than 44 millimeters, while 95% had a mean femur length greater than 44 mm. The 90<sup>th</sup> percentile of femur length at 33 to 33 + 6 weeks is 65 millimeters.

**Tab. 6.17** *Frequency distribution table of fetal femur length measurements showing the arithmetic mean, standard deviation and standard error of mean from 12 – 42 weeks gestation.*

<b>GA (weeks, days)</b>	<b>Fetuses (n)</b>	<b>Mean FL (mm)</b>	<b>SD</b>	<b>SE</b>
12 to 12+6	49	12.2	2.1	0.3
13 to 13+6	384	14.6	8	0.4
14 to 14+6	371	16.3	4.8	0.2
15 to 15+6	351	19.0	3.1	0.2
16 to 16+6	505	22.9	6.3	0.3
17 to 17+6	427	25.0	2.9	0.1
18 to 18+6	446	29.0	5.2	0.2
19 to 19+6	282	31.6	4.3	0.3
20 to 20+6	553	33.5	3.8	0.2
21 to 21+6	400	36.7	3.9	0.2
22 to 22+6	398	38.7	3.5	0.2
23 to 23+6	478	41.1	2.9	0.1
24 to 24+6	520	43.8	3	0.1
25 to 25+6	388	46.2	3.8	0.2
26 to 26+6	511	49.1	3.6	0.1
27 to 27+6	432	50.9	2.3	0.1
28 to 28+6	548	53.6	3.4	0.1
29 to 29+6	484	55.4	3.8	0.2
30 to 30+6	625	58.3	3.5	0.1
31 to 31+6	523	60.3	3.4	0.1
32 to 32+6	583	62.1	3.3	0.1
33 to 33+6	516	64.1	2.4	0.1
34 to 34+6	744	66.2	3.4	0.1
35 to 35+6	739	68.5	2.4	0
36 to 36+6	599	70.6	3.3	0.1
37 to 37+6	532	71.7	5.5	0.2
38 to 38+6	481	73.9	4.7	0.2
39 to 39+6	525	76.7	3	0.1
40 to 40+6	252	78.8	3.7	0.2
41 to 41+6	72	79.9	5.4	0.6
42 to 42+6	22	84.9	12	2.6
Total	13,740			

**Tab. 6.18** Frequency distribution table of fetal femur length measurements showing arithmetic mean, geometric mean and harmonic mean from 12 – 42 weeks gestation.

GA (week, days)	Number of fetuses (n)	Arithmetic mean (mm)	Geometric mean (mm)	Harmonic mean (mm)
12 to 12+6	49	12.20408	12.04776	11.9039
13 to 13+6	384	14.64063	13.85937	13.48663
14 to 14+6	371	16.34232	15.98908	15.74245
15 to 15+6	351	19.0114	18.78066	18.55452
16 to 16+6	505	22.93465	22.45429	22.13357
17 to 17+6	427	24.97424	24.80889	24.64348
18 to 18+6	446	29.00897	28.66378	28.37964
19 to 19+6	282	31.59575	31.33629	31.08744
20 to 20+6	553	33.4991	33.29572	33.09573
21 to 21+6	400	36.7075	36.50051	36.28643
22 to 22+6	398	38.72613	38.56079	38.38766
23 to 23+6	478	41.14675	41.04465	40.94054
24 to 24+6	520	43.77735	43.66936	43.5484
25 to 25+6	388	46.18299	46.00735	45.79766
26 to 26+6	511	49.08806	48.96292	48.84365
27 to 27+6	432	50.90278	50.84937	50.79458
28 to 28+6	548	53.55109	53.44577	53.34311
29 to 29+6	484	55.42355	55.26376	55.05746
30 to 30+6	625	58.2512	58.15721	58.06916
31 to 31+6	523	60.25813	60.16758	60.08173
32 to 32+6	583	62.0566	61.96439	61.86463
33 to 33+6	516	64.1376	64.08805	64.03426
34 to 34+6	744	64.1376	64.08805	64.03426
35 to 35+6	739	68.51151	68.47121	68.43069
36 to 36+6	599	70.5793	70.50031	70.41488
37 to 37+6	532	71.7124	71.26648	69.96014
38 to 38+6	481	73.88982	73.64711	73.19981
39 to 39+6	525	76.70477	76.64517	76.58453
40 to 40+6	252	78.78175	78.69141	78.59788
41 to 41+6	72	79.93056	79.76249	79.60353
42 to 42+6	22	84.90909	84.10523	83.32234
Total	13,740			

**Tab. 6.19** *Fetal femur length centiles from 12 – 42 weeks.*

GA (weeks, days)	Femur Length percentiles (mm)						
	3rd	5th	10th	50th	90th	95th	97th
12 to 12+6	9.0	9.5	10.0	12.0	14.0	17.0	19.0
13 to 13+6	10.0	10.0	11.0	14.0	16.0	18.0	20.5
14 to 14+6	12.0	12.0	13.0	16.0	19.0	21.0	21.0
15 to 15+6	13.6	14.0	16.0	19.0	22.0	23.4	24.0
16 to 16+6	17.0	18.0	19.0	22.0	26.0	27.0	28.0
17 to 17+6	20.0	20.0	21.0	25.0	27.0	30.0	31.0
18 to 18+6	22.0	23.0	25.0	29.0	31.0	33.0	37.0
19 to 19+6	26.0	27.0	28.0	31.0	36.0	37.8	42.6
20 to 20+6	26.6	27.0	29.0	34.0	38.0	39.0	40.0
21 to 21+6	29.0	30.0	32.0	37.0	40.0	41.0	42.0
22 to 22+6	30.0	32.0	34.0	39.0	42.0	43.0	44.0
23 to 23+6	35.0	36.0	37.0	42.0	44.0	46.0	46.0
24 to 24+6	38.0	39.0	40.0	44.0	47.0	48.0	49.0
25 to 25+6	39.7	41.0	42.9	46.0	49.0	52.0	53.0
26 to 26+6	42.0	44.0	46.0	49.0	52.8	55.0	56.0
27 to 27+6	46.0	47.0	48.3	51.0	54.0	54.4	55.0
28 to 28+6	48.0	49.0	50.0	54.0	57.0	58.0	59.0
29 to 29+6	50.0	51.0	52.5	55.0	59.0	61.0	62.0
30 to 30+6	52.0	53.3	56.0	58.0	61.0	63.0	65.0
31 to 31+6	55.0	55.0	57.0	60.0	62.0	64.0	66.0
32 to 32+6	56.0	57.0	59.0	62.0	64.0	65.0	66.0
33 to 33+6	59.0	60.0	62.0	64.0	65.0	66.0	67.0
34 to 34+6	60.0	62.0	64.0	66.5	68.0	69.0	70.0
35 to 35+6	63.0	65.0	66.0	69.0	70.0	70.0	72.0
36 to 36+6	65.0	66.0	68.0	71.0	72.0	72.0	73.0
37 to 37+6	64.0	65.0	69.0	73.0	74.0	74.0	75.0
38 to 38+6	66.0	69.0	71.0	75.0	76.0	76.0	77.0
39 to 39+6	70.0	71.3	73.0	77.0	79.0	80.0	81.0
40 to 40+6	69.7	72.0	74.0	80.0	83.0	83.4	84.4
41 to 41+6	73.0	73.0	74.3	79.0	88.0	92.0	96.9
42 to 42+6	71.0	71.0	71.6	81.0	99.0	99.0	99.0

Hence 90% of fetuses at 33 to 33 + 6 weeks had a mean femur length less than 65 millimeters while 10% had a mean femur length greater than 65 millimeters.



The standard score or z-score of femur length measurements in 13,740 fetuses ranging from 12 – 42 weeks of gestation is shown in Tab. 6.33. The z-score enables one to look at femur length measurements at each gestational age and see how they compare on the same standard; taking into account the mean and standard deviation of each gestational age. For example, femur length measurements at 20 weeks are 0.0000 standard deviations from the mean while measurements at 36 weeks are – 0.0014 standard deviations from the mean. Again, from the above z-score table, it can be seen that the femur length measurements at 38 weeks gestation are – 0.00067 standard deviations from the mean. When femur length data of 13,740 fetuses was subjected to skewness analysis at different gestational age ranging from 12 – 42 weeks (Fig. 6.58), it can be seen that the distribution of femur length measurements has a longer “tail” to the right of the central maximum than to the left or is skewed to the right from 13 – 21 weeks and then at 26, 28, 30, 31, 32, 35, and 41 weeks. From 22 – 25 weeks and then at 27, 29, 33, 34, 36, 37, 38, 39 and 40 weeks, the distribution has a longer “tail” to the left of the central maximum than to the right or is skewed to the left. By the time pregnancy reaches term, the distribution becomes skewed to the right before skewing again to the left as from 41 weeks. When the femur length data was subjected to kurtosis analysis (Fig. 6.59), the distribution was found to be leptokurtic at 13, 14, 16, 37 and 38 weeks of gestation while at other weeks of gestation, the distribution was mesokurtic. The coefficient of dispersion of femur length data of 13,740 fetuses at different gestational age shows a decrease in value as gestational age advances except at term where it peaks (Fig. 6.60). The femur length scattergram in Fig. 6.61 shows that there are very few bad data points or outliers in the femur length measurements of 13,740 fetuses. The outliers are more from 26 – 42 weeks of gestation. In Fig. 6.62, mean femur length is plotted against gestational age with error bars showing standard deviation. Arithmetic mean and standard deviation go together like star and satellite. With the mean, we have some idea of the kind of numbers it represents,

but the whole story is still a mystery. To clear up the mystery of the hidden numbers that made up a mean, the standard deviation is necessary.

**Tab. 6.20** *Standard score (z-score) of femur length measurements in 13,740 Nigerian fetuses in Jos ranging from 12 – 42 weeks gestation.*

GA (weeks, days)	Fetuses (n)	Mean z-score
12 to 12+6	49	3.89E-04
13 to 13+6	384	4.23E-03
14 to 14+6	371	3.59E-03
15 to 15+6	351	8.26E-04
16 to 16+6	505	3.57E-03
17 to 17+6	427	-2.36E-03
18 to 18+6	446	3.82E-04
19 to 19+6	282	-2.80E-04
20 to 20+6	553	-7.12E-05
21 to 21+6	400	6.41E-04
22 to 22+6	398	2.31E-03
23 to 23+6	478	3.49E-03
24 to 24+6	520	-1.45E-03
25 to 25+6	388	-1.22E-03
26 to 26+6	511	-7.85E-04
27 to 27+6	432	1.80E-04
28 to 28+6	548	-3.68E-03
29 to 29+6	484	1.01E-03
30 to 30+6	625	-2.87E-03
31 to 31+6	523	-2.81E-03
32 to 32+6	583	-2.95E-03
33 to 33+6	516	2.91E-03
34 to 34+6	744	2.44E-03
35 to 35+6	739	8.52E-04
36 to 36+6	599	-1.41E-03
37 to 37+6	532	9.06E-04
38 to 38+6	481	-6.75E-04
39 to 39+6	525	3.31E-04
40 to 40+6	252	-1.29E-03
41 to 41+6	72	2.59E-03
42 to 42+6	22	3.90E-04
Total	13,740	

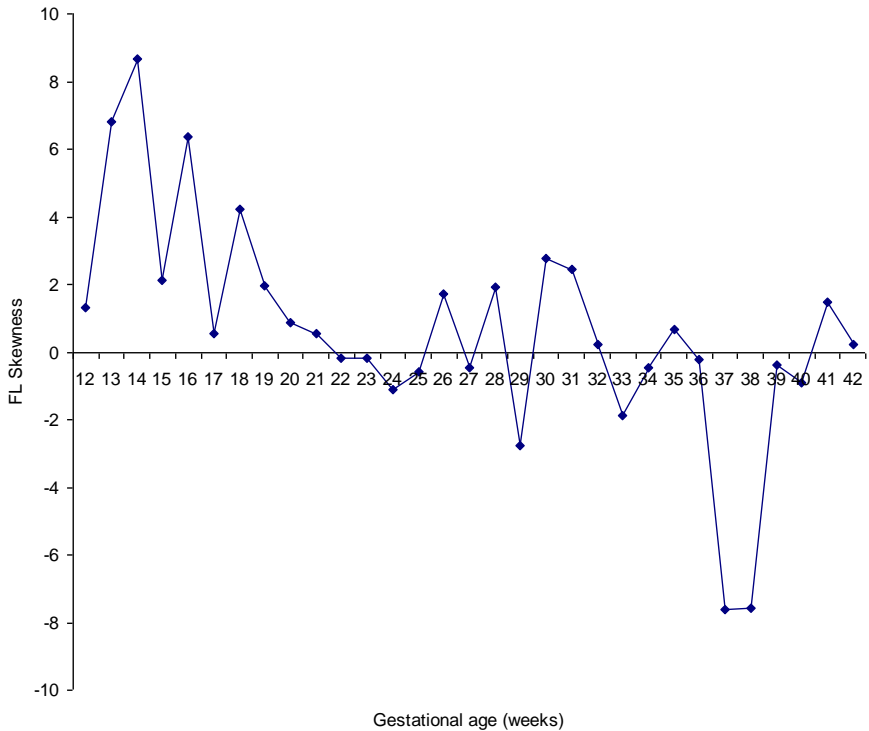


**Fig. 6.58** Femur length data of 13,740 fetuses subjected to Skewness analysis at different gestational age ranging from 12 – 42 weeks.

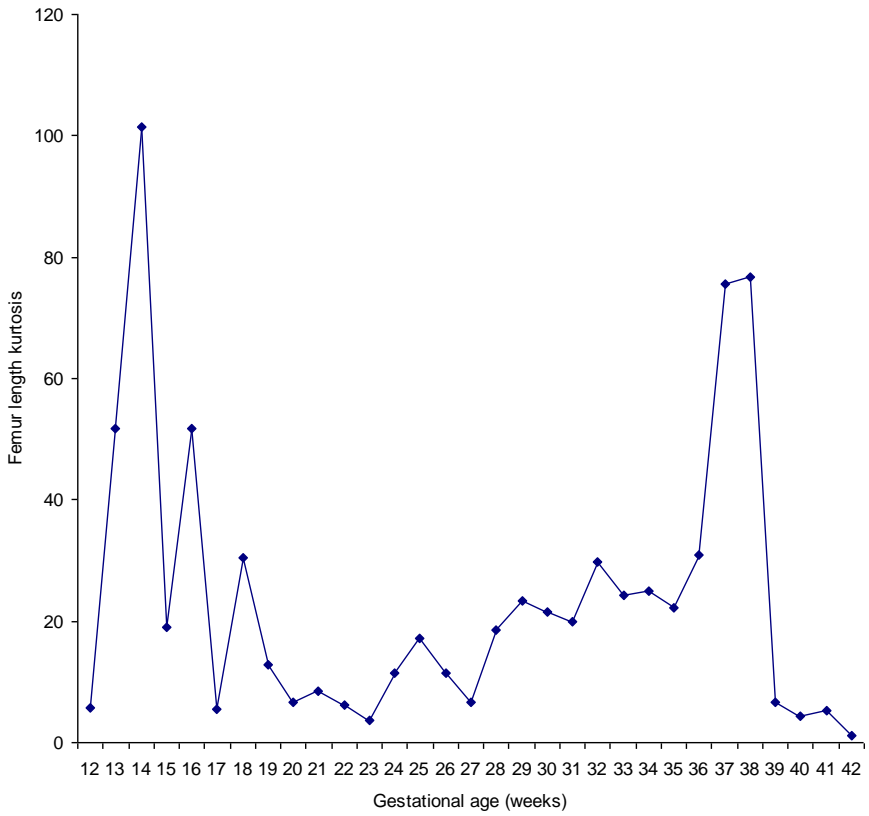


**Fig. 6.59** Femur length data of 13,740 fetuses subjected to kurtosis analysis at different gestational age ranging from 12 – 42 weeks.

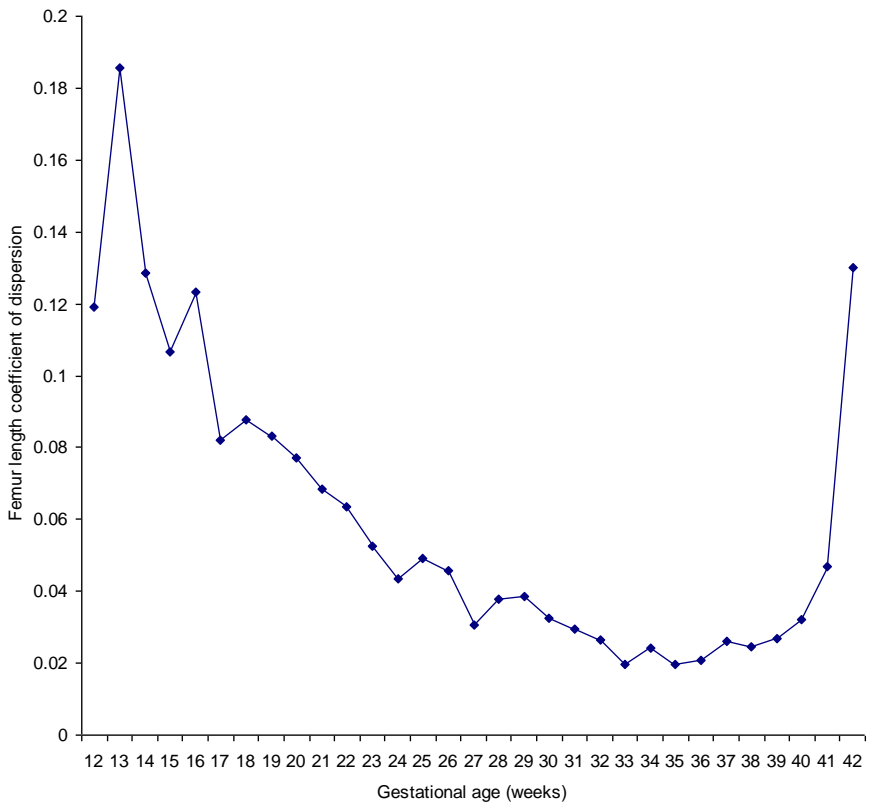


**Fig. 6.60** Femur length coefficient of dispersion in 13,740 fetuses of gestational ages between 12 to 42 weeks.

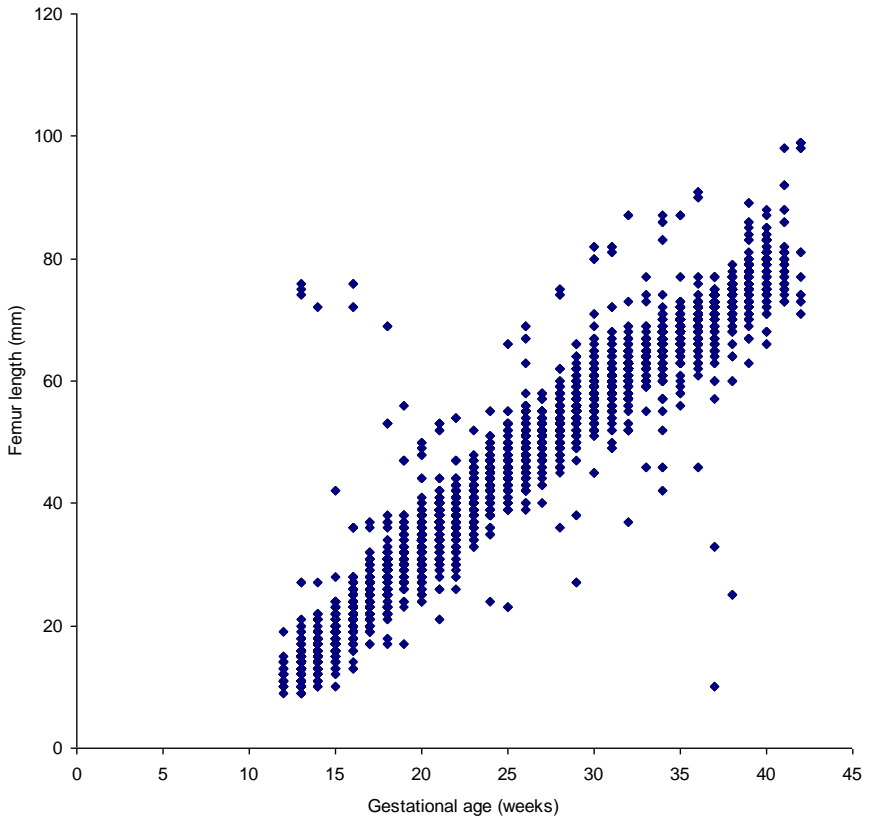


**Fig. 6.61** Scattergram of 13,740 fetal femur length measurements from 12 – 42 weeks gestation.

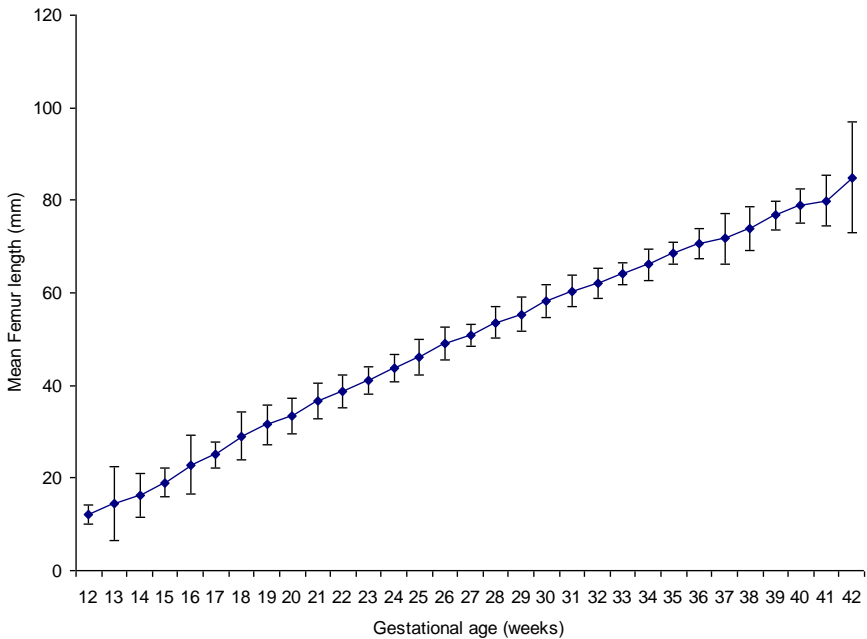


**Fig. 6.62** Mean fetal femur length values in 13,740 fetuses of women at different gestational ages between 12 – 42 weeks. The vertical bars show the values of  $\pm SD$ .

For example, the mean  $\pm 1$  standard deviation will include about 2 out of 3 numbers in the group while the mean  $\pm 2$  standard deviations will include about 95 out of 100 numbers in the group and the mean  $\pm 3$  standard deviations will include 997 numbers out of 1,000. Mathematical modeling of data demonstrated that the best-fitted regression model (Fig. 6.63) to describe the relationship between femur length and gestational age was the second order polynomial regression equation  $y = -0.017x^2 + 3.2794x - 25.282$  with a correlation of determination of  $r^2 = 0.999$  ( $P < 0.0001$ ) where  $y$  is the femur length in millimeters and  $x$  is the gestational age in weeks. When monthly mean values of femur length are plotted against gestational age in months, a positive polynomial correlation between gestational age and femur length with a correlation of determination of  $r^2 = 0.9992$  ( $P < 0.0001$ ) in Nigerian fetuses in Jos was found

(Fig. 6.64). The relationship is best described by the second order polynomial regression equation  $y = -3.667x^2 + 15.462x - 38.6$  where  $y$  is the femur length in millimeters and  $x$  is the gestational age in months.

When other fetal anthropometric parameters like head circumference, biparietal diameter, occipitofrontal diameter, abdominal circumference and weight are plotted against femur length certain hidden relationships can be forced out. For example, Fig. 6.65 shows the relationship of femur length with biparietal diameter. From the graph, it can be seen that there is a positive polynomial correlation between femur length and biparietal diameter with a correlation of determination of  $r^2 = 0.9993$  ( $P < 0.0001$ ) in Nigerian fetuses in Jos. The relationship is best described by the fourth order polynomial regression equation  $y = -4E-06x^4 + 0.0006x^3 - 0.0414x^2 + 2.3555x - 1.7905$  where  $y$  is the biparietal diameter in millimeters and  $x$  is the femur length in millimeters. Fig. 6. 66 shows relationship of femur length with occipitofrontal diameter. There is a positive polynomial correlation between femur length and biparietal diameter. The relationship is best described by the quadratic regression equation of  $y = -0.007x^2 + 2.0251x + 4.2448$  with a correlation of determination of  $r^2 = 0.9973$  ( $P < 0.0001$ ) in Nigerian fetuses in Jos. Fig. 6.67 shows relationship of femur length with abdominal circumference.



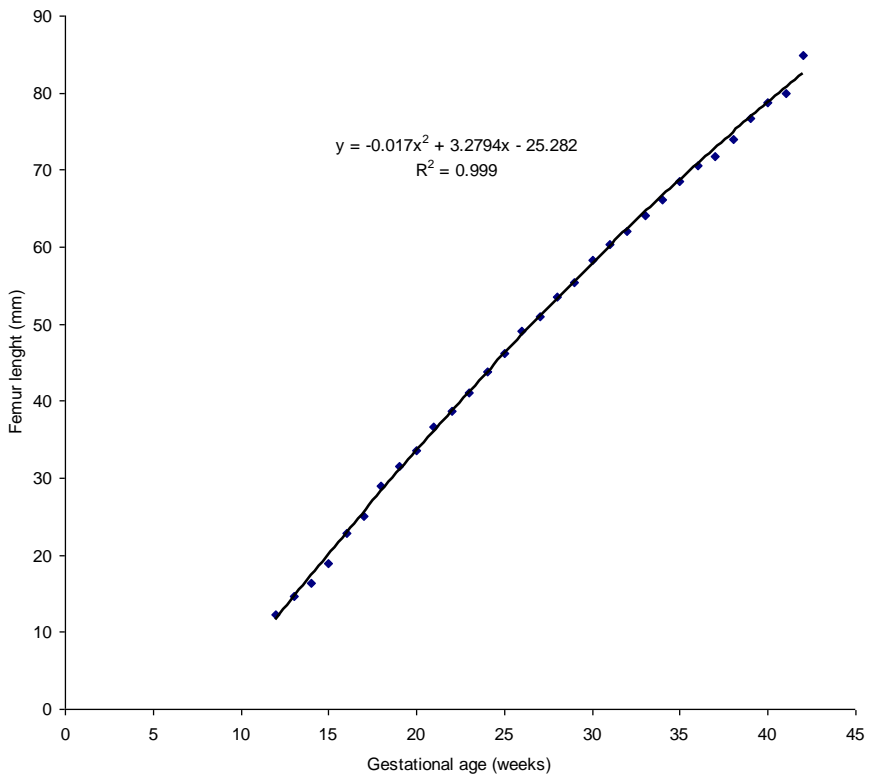


**Fig. 6.63** Correlation and regression equation of mean femur length values in 13,740 Nigerian fetuses in Jos plotted against gestational age in weeks.

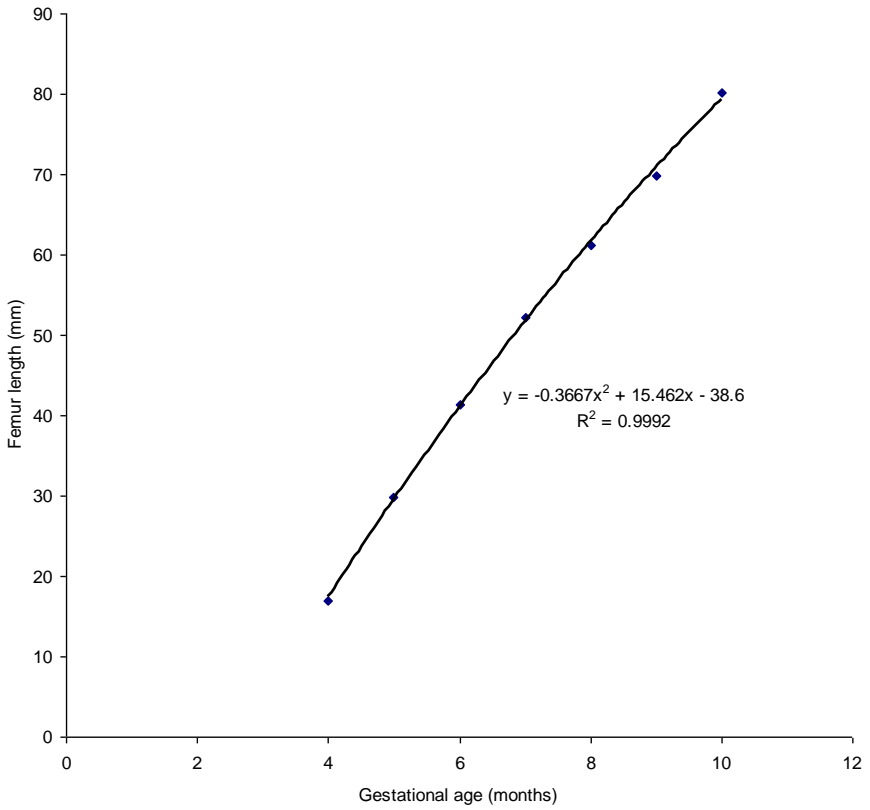


**Fig. 6.64** Correlation and regression equation of mean femur length values in 13,740 Nigerian fetuses in Jos plotted against gestational age in months.

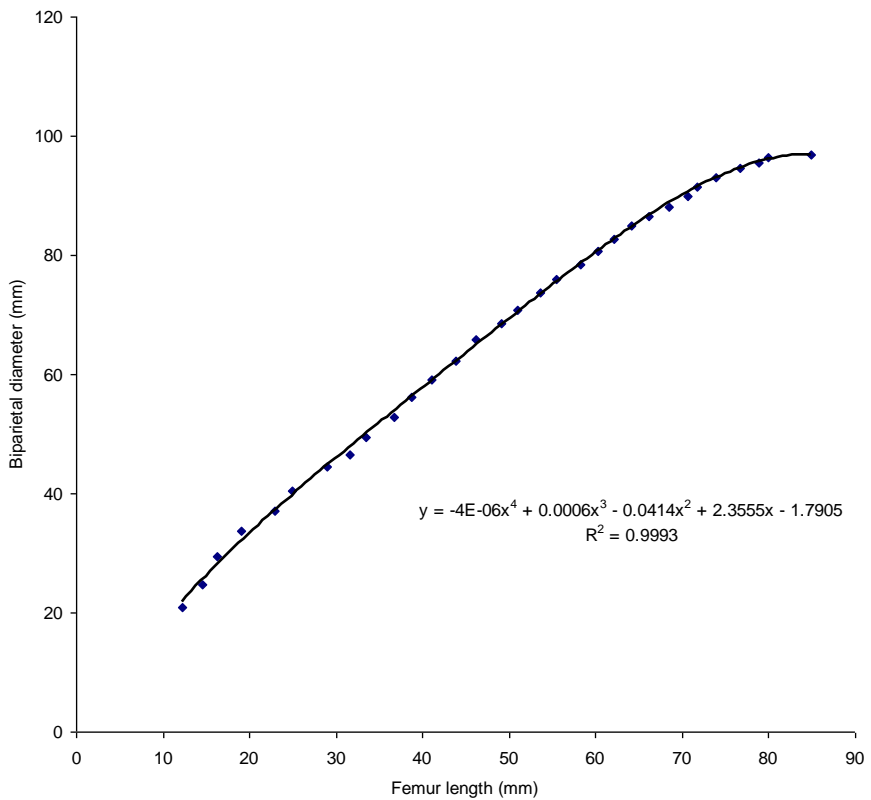


**Fig. 6.65** Correlation and regression equation of mean femur length values in 13,740 Nigerian fetuses in Jos plotted against biparietal diameter.

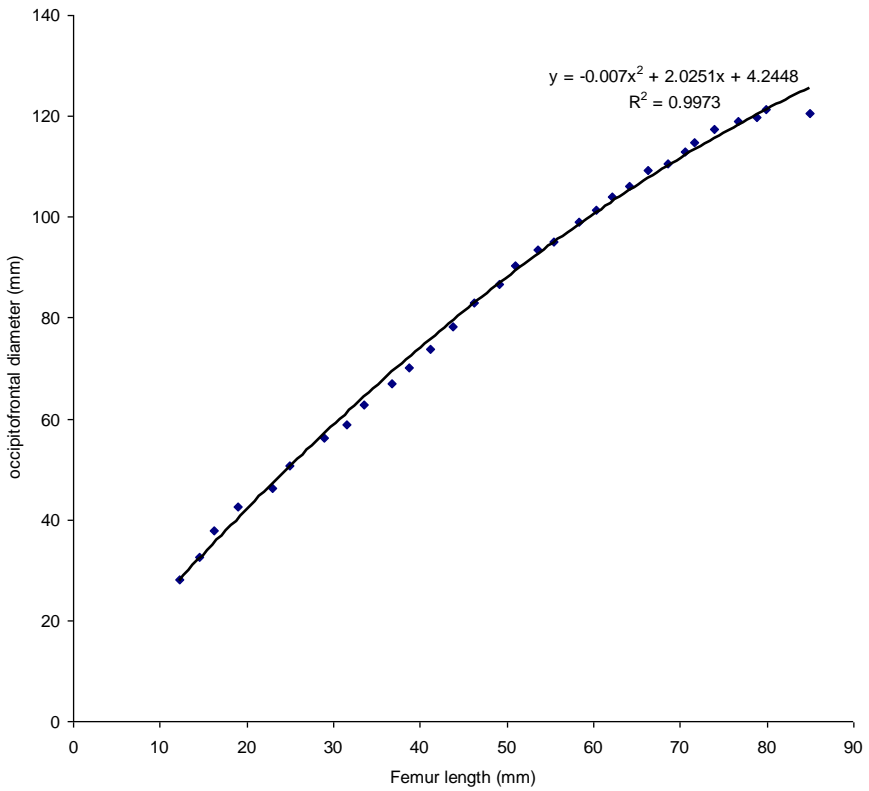


**Fig. 6.66** Correlation and regression equation of mean femur length values in 13,740 Nigerian fetuses in Jos plotted against occipitofrontal diameter.

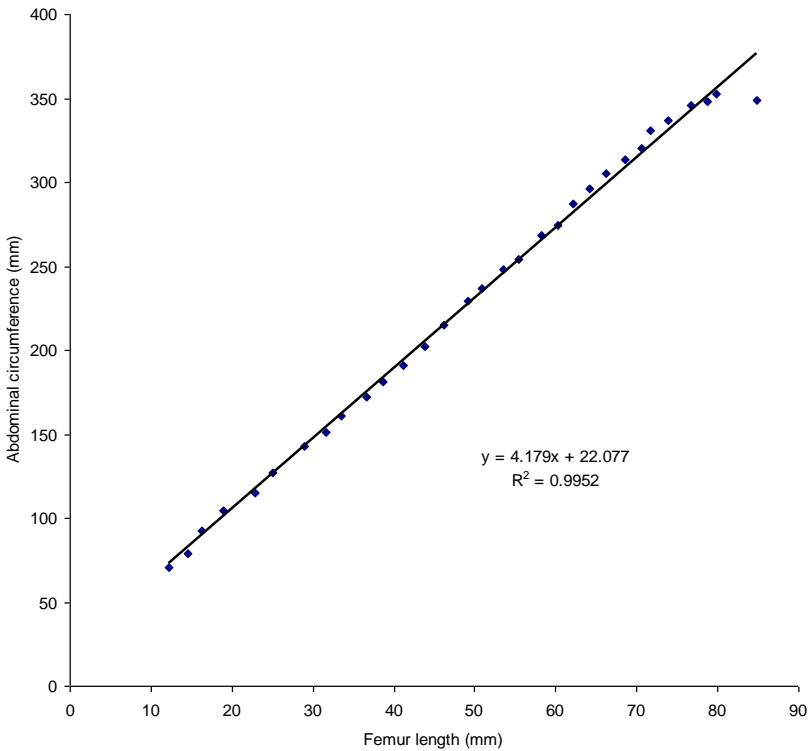


**Fig. 6.67** Correlation and regression equation of mean femur length values in 13,740 Nigerian fetuses in Jos plotted against femur length.

From the graph, it can be seen that there is a positive linear correlation between femur length and femur length with a correlation of determination of  $r^2 = 0.9952$  ( $P < 0.0001$ ) in Nigerian fetuses in Jos. The relationship is best described by the linear regression equation  $y = 4.179x + 22.077$  where  $y$  is the abdominal circumference in millimeters and  $x$  is the femur length in millimeters. Fig. 6.68 shows relationship between femur length and head circumference. There is a positive polynomial correlation between femur length and head circumference with a correlation of determination of  $r^2 = 0.9989$  ( $P < 0.0001$ ) in Nigerian fetuses in Jos. The relationship is best described by the third order regression equation  $y = -0.0004x^3 + 0.0429x^2 + 3.1567x + 43.238$  where  $y$  is the

head circumference in millimeters and  $x$  is the femur length in millimeters. Fig. 6.69 shows the relationship between fetal weight which is strongly correlated with fetal nutrition and femur length. From the graph, it can be seen that there is a positive power correlation between fetal weight and femur length with a correlation of determination of  $r^2 = 0.9944$  ( $P < 0.0001$ ) in Nigerian fetuses in Jos. The relationship is best described by the power regression equation  $y = 0.0575x^{2.534}$  where  $y$  is the fetal weight in grams and  $x$  is the femur length in millimeters. Femur length centiles values for 5<sup>th</sup>, 50<sup>th</sup> and 95<sup>th</sup> centiles are plotted as shown in Fig. 6.70. In Fig. 6.71, the 5<sup>th</sup>, 50<sup>th</sup> and 95<sup>th</sup> centiles are smoothed into a growth chart which can be utilized to determine growth of fetus using femur length. Fig. 6.72 is a graphical display showing the growth rate of the measured fetal femur length during intrauterine life.

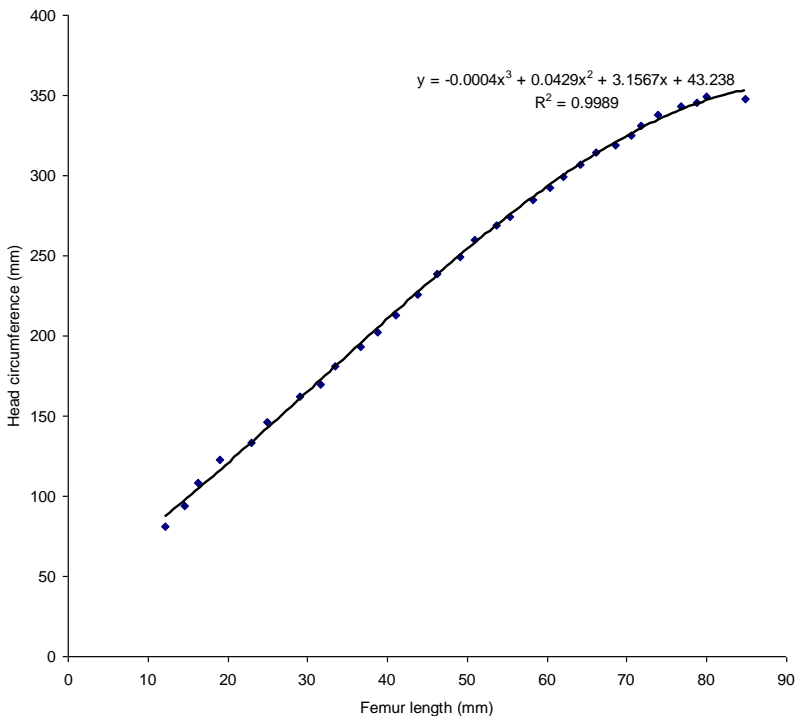


**Fig. 6.68** Correlation and regression equation of mean femur length values in 13,740 Nigerian fetuses in Jos plotted against femur length.

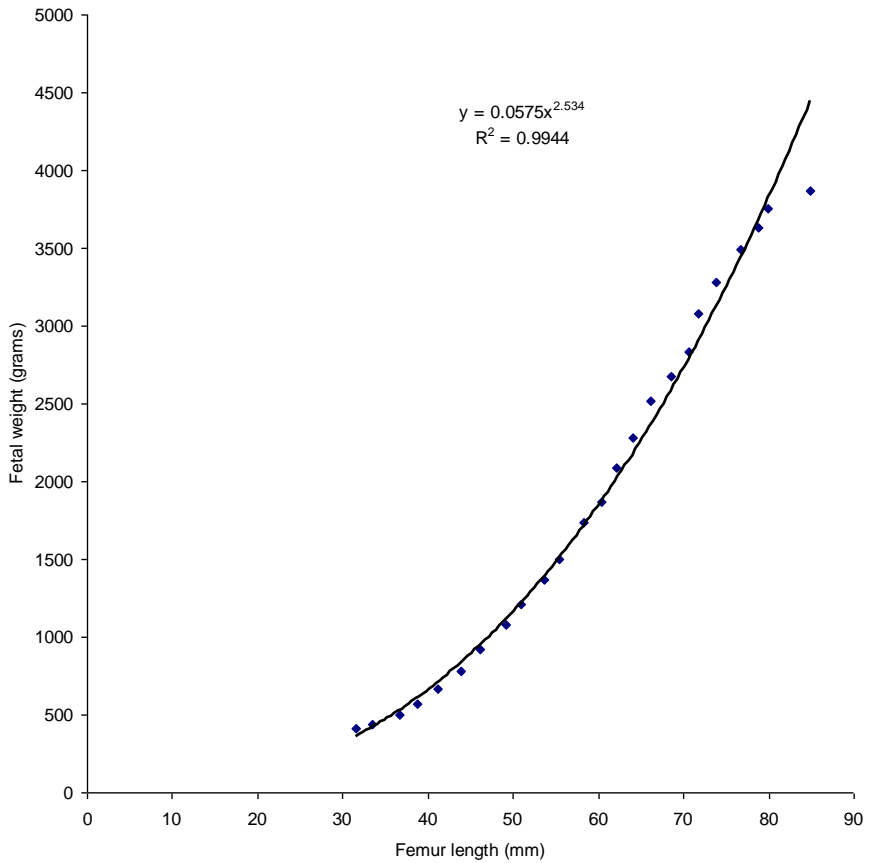


**Fig. 6.69** Correlation and regression equation of mean femur length values in 13,740 Nigerian fetuses in Jos plotted against fetal weight.

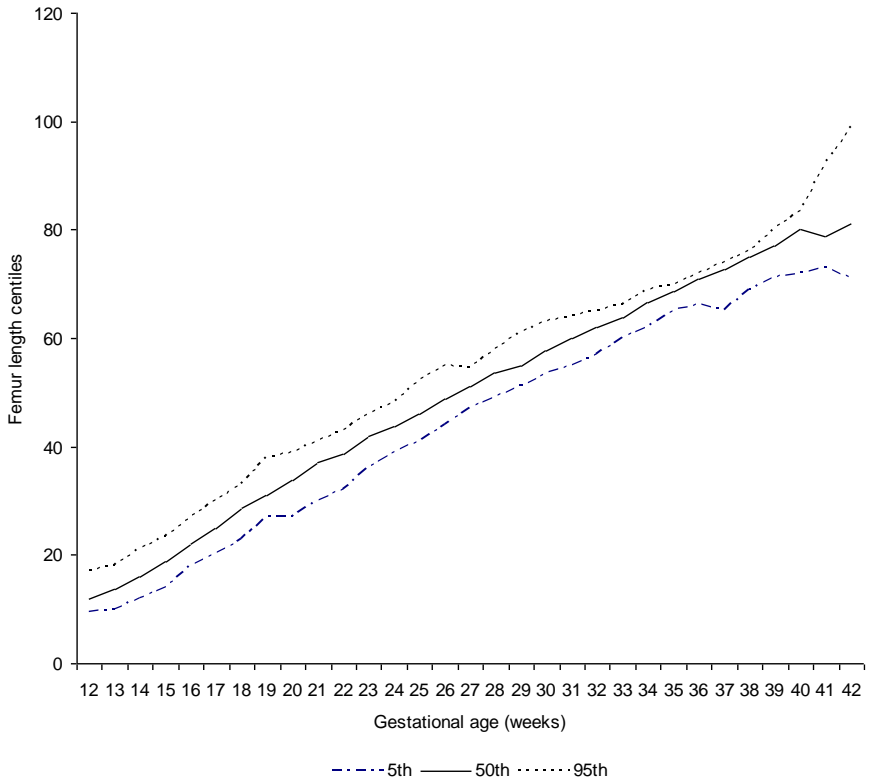


**Fig. 6.70** Fifth, 50th and 95th centiles for femur length in 13,740 fetuses at different gestational ages from 12 to 42 weeks.



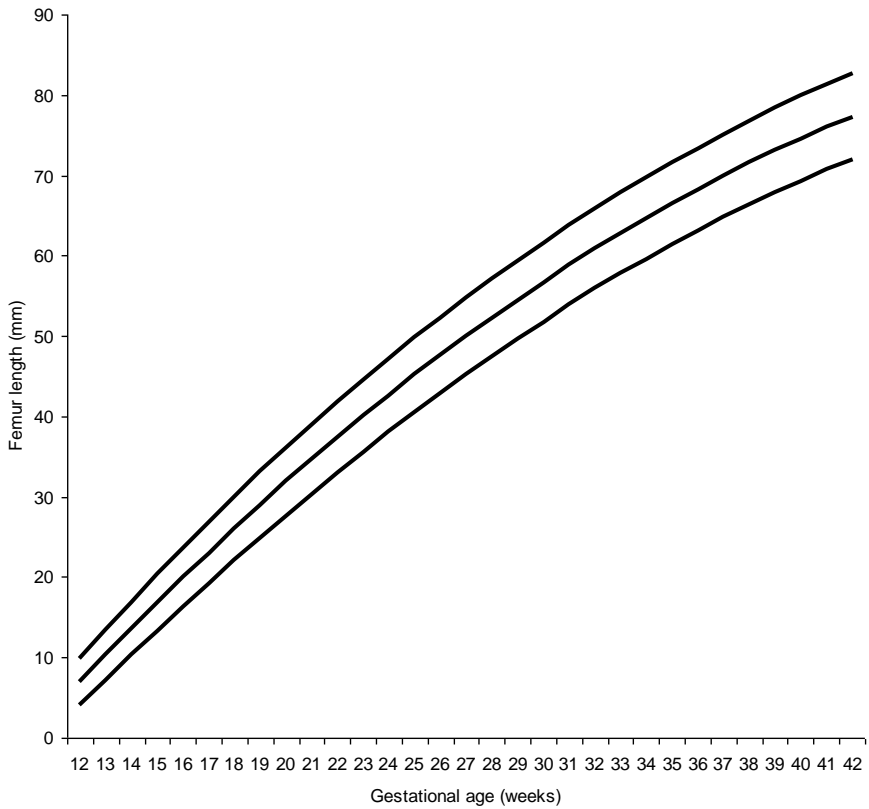


**Fig. 6.71** Curves created from 3rd, 50th and 97th fetal femur length centiles.

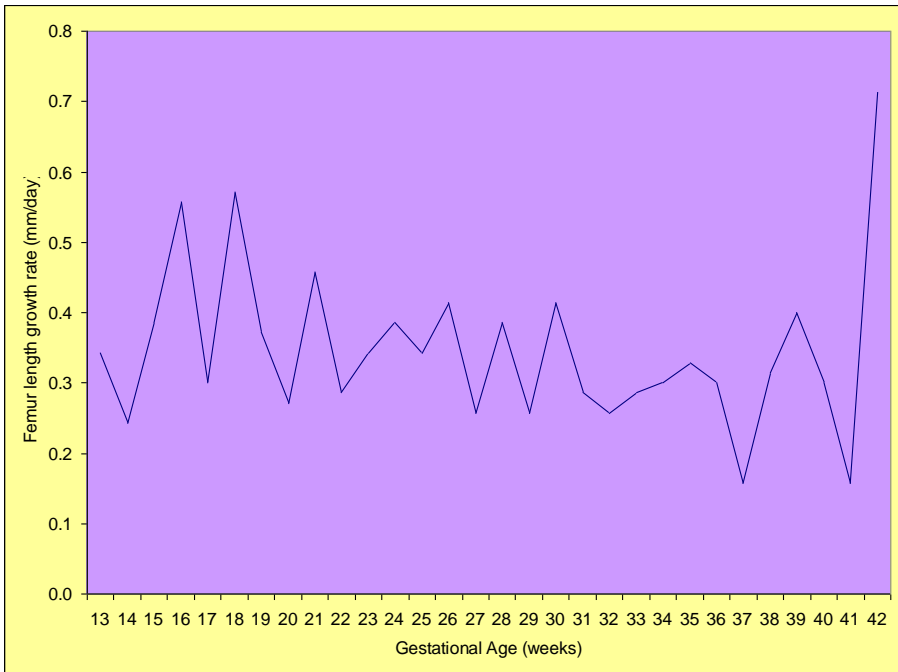


*Fig. 6.72 Growth velocity pattern of femur length in 13,740 Nigerian fetuses in Jos ranging from 12 – 42 weeks.*

## Biometrics of Fetal Weight

The fetal weight measurements were classified into twenty six groups. The mean weight values at each week of gestation from 17 – 42 are as shown in Tab. 6.21. This table gives the mean values of fetal weight measurements for each gestational age in weeks from 17 – 42 weeks together with their corresponding standard deviations and standard errors of mean. The standard deviation is necessary to clear up the mystery of the hidden numbers that made up a mean. For example, the mean weight at 39 weeks is 3490.8g plus 360.3g or 3490.8g minus 360.3g. This means 2 out of 3 measurements of weight at 39 weeks, approximately 350 weight measurements in a class of 525, should be between

3130.5g and 3851.1g. Since the standard error of mean at 39 weeks is 15.8g, it is telling us that the real mean weight of fetuses in Jos at 39 weeks is probably between 3475.0g and 3506.6g (3490.8g plus or minus 15.8g). The variability of the fetal weight measurements increases as gestational age increases. However, at week 18, there is marked variation up to 650 grams.

The geometric means (Tab. 6.22) of all sets of measurements from 17 – 42 weeks are less than their arithmetic means but greater than their harmonic means indicating that all the values of fetal weight measurements were not identical. Tab.6. 23 gives the 3<sup>rd</sup>, 5<sup>th</sup>, 10<sup>th</sup>, 50<sup>th</sup>, 90<sup>th</sup>, 95<sup>th</sup>, and 97<sup>th</sup> centile values for fetal weight measured at different gestational age ranging from 17 – 42 weeks. For example, it can be seen from the table that the 10<sup>th</sup> percentile of fetal weight at 20 to 20 + 6 weeks gestation is 300 grams. This means that 10% of the fetuses at 20 to 20 + 6 had a mean fetal weight less than 300 grams, while 90% had a mean fetal weight greater than 300 grams. Similarly, the 97<sup>th</sup> percentile of fetal weight at 36 to 36 + 6 is 3200 grams. Hence 97% of fetuses at 36 to 36 + 6 had a mean fetal weight less than 3200 grams while 3% had a mean fetal weight greater than 3200 grams.

When weight data of 12,080 fetuses was subjected to skewness analysis at different gestational age ranging from 17 – 42 weeks (Fig. 6.73), it can be seen that the distribution of weight measurements has a longer “tail” to the right of the central maximum than to the left or is skewed to the right from 17 – 31 weeks; and then later at 35, 39, 40 and 41 weeks. From 32, 33, 34, 36, 37, 38 and 42 weeks, the distribution has a longer “tail” to the left of the central maximum than to the right or is skewed to the left.

**Tab. 6.21** *Frequency distribution table of fetal weight measurements showing the arithmetic mean, standard deviation and standard error of mean from 12 – 42 weeks gestation.*

<b>GA (week, days)</b>	<b>Fetuses (n)</b>	<b>weight (g)</b>	<b>SD</b>	<b>SEM</b>
17 to 17+6	427	319.0	40.2	8.8
18 to 18+6	446	731.9	650.8	94.9
19 to 19+6	282	413.3	101.8	11.8
20 to 20+6	553	437.6	81.0	4.4
21 to 21+6	400	496.3	73.2	3.9
22 to 22+6	398	567.4	124.5	6.5
23 to 23+6	478	668.4	180.9	8.5
24 to 24+6	520	781.9	161.7	7.2
25 to 25+6	388	925.0	177.6	9.1
26 to 26+6	511	1077.6	217.9	9.7
27 to 27+6	432	1206.8	226.8	11.0
28 to 28+6	548	1370.2	227.7	9.8
29 to 29+6	484	1498.1	204.2	9.4
30 to 30+6	625	1733.8	297.7	12.0
31 to 31+6	523	1865.1	295.3	13.0
32 to 32+6	583	2086.1	276.3	11.5
33 to 33+6	516	2279.6	298.8	13.2
34 to 34+6	744	2516.0	333.0	12.4
35 to 35+6	739	2675.0	352.8	13.0
36 to 36+6	599	2837.0	341.3	14.1
37 to 37+6	532	3079.8	392.0	17.2
38 to 38+6	481	3276.7	351.3	16.2
39 to 39+6	525	3490.8	360.3	15.8
40 to 40+6	252	3634.9	419.8	26.4
41 to 41+6	72	3752.9	350.9	41.9
42 to 42+6	22	3868.2	599.5	127.8
Total	12,080			

**Tab. 6.22** Frequency distribution table of fetal weight measurements showing arithmetic mean, geometric mean and harmonic mean from 17 – 42 weeks gestation.

GA (week, days)	Number of fetuses (n)	Arithmetic mean (mm)	Geometric mean (mm)	Harmonic mean (mm)
17 to 17+6	427	319.0476	316.8977	315
18 to 18+6	446	731.9149	544.7203	447.3412
19 to 19+6	282	413.3333	406.0622	401.4273
20 to 20+6	553	437.574	431.6011	426.7036
21 to 21+6	400	496.3173	491.1159	485.939
22 to 22+6	398	567.3854	559.6849	554.3026
23 to 23+6	478	668.3516	654.8652	645.9038
24 to 24+6	520	781.8898	769.4403	759.0261
25 to 25+6	388	925.0000	911.0558	897.5364
26 to 26+6	511	1077.624	1061.000	1046.67
27 to 27+6	432	1206.792	1187.759	1169.68
28 to 28+6	548	1370.24	1353.363	1336.422
29 to 29+6	484	1498.105	1484.898	1472.064
30 to 30+6	625	1733.764	1710.785	1688.828
31 to 31+6	523	1865.125	1841.298	1815.473
32 to 32+6	583	2086.066	2065.578	2039.616
33 to 33+6	516	2279.648	2256.348	2225.095
34 to 34+6	744	2515.978	2490.586	2457.018
35 to 35+6	739	2674.966	2651.654	2627.941
36 to 36+6	599	2836.974	2813.571	2785.043
37 to 37+6	532	3079.808	3039.085	2949.43
38 to 38+6	481	3276.744	3255.992	3231.927
39 to 39+6	525	3490.822	3472.1	3453.111
40 to 40+6	252	3634.921	3611.771	3589.447
41 to 41+6	72	3752.857	3736.914	3721.155
42 to 42+6	22	3868.182	3822.286	3775.203
Total	12080			

**Tab. 6.23** Frequency distribution table of fetal weight measurements showing arithmetic mean, geometric mean and harmonic mean from 17 – 42 weeks gestation.

GA (week, days)	Number of fetuses (n)	Arithmetic mean (mm)	Geometric mean (mm)	Harmonic mean (mm)
17 to 17+6	427	319.0476	316.8977	315
18 to 18+6	446	731.9149	544.7203	447.3412
19 to 19+6	282	413.3333	406.0622	401.4273
20 to 20+6	553	437.574	431.6011	426.7036
21 to 21+6	400	496.3173	491.1159	485.939
22 to 22+6	398	567.3854	559.6849	554.3026
23 to 23+6	478	668.3516	654.8652	645.9038
24 to 24+6	520	781.8898	769.4403	759.0261
25 to 25+6	388	925.0000	911.0558	897.5364
26 to 26+6	511	1077.624	1061.000	1046.67
27 to 27+6	432	1206.792	1187.759	1169.68
28 to 28+6	548	1370.24	1353.363	1336.422
29 to 29+6	484	1498.105	1484.898	1472.064
30 to 30+6	625	1733.764	1710.785	1688.828
31 to 31+6	523	1865.125	1841.298	1815.473
32 to 32+6	583	2086.066	2065.578	2039.616
33 to 33+6	516	2279.648	2256.348	2225.095
34 to 34+6	744	2515.978	2490.586	2457.018
35 to 35+6	739	2674.966	2651.654	2627.941
36 to 36+6	599	2836.974	2813.571	2785.043
37 to 37+6	532	3079.808	3039.085	2949.43
38 to 38+6	481	3276.744	3255.992	3231.927
39 to 39+6	525	3490.822	3472.1	3453.111
40 to 40+6	252	3634.921	3611.771	3589.447
41 to 41+6	72	3752.857	3736.914	3721.155
42 to 42+6	22	3868.182	3822.286	3775.203
Total	12080			

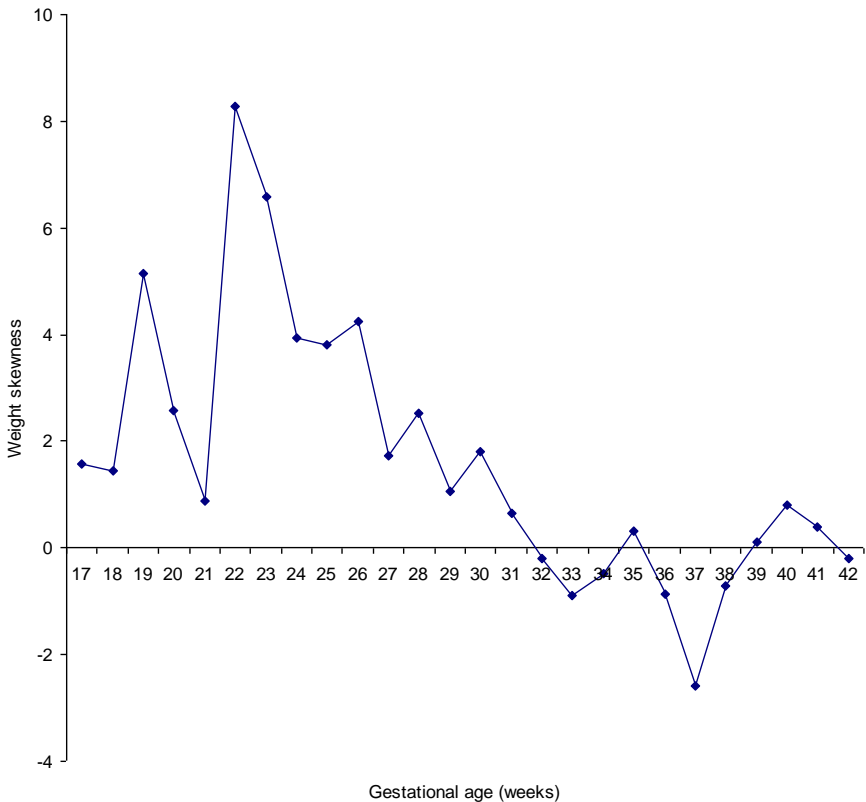


**Fig. 6.73** Weight data of 12,080 fetuses subjected to Skewness analysis at different gestational age ranging from 12 – 42 weeks.

When the weight data was subjected to kurtosis analysis (Fig. 6.74), the analysis was found to be leptokurtic at 19, 22, 23, 24, 25, 26, 28 and 37 weeks of gestation while at the other gestational ages, the distribution was found to be mesokurtic. The coefficient of dispersion of weight data of 12,080 fetuses at different gestational age shows a decrease in value as gestational age advances except at 18 weeks where it peaks (Fig. 6.75). In Fig. 6.76, mean weight is plotted against gestational age with error bars showing standard deviation. Mathematical modeling of data demonstrated that the best-fitted regression model (Fig. 6.77) to describe the relationship between weight and gestational age was the power

regression equation  $y = 0.038x^{3.1347}$  where  $y$  is the fetal weight in grams and  $x$  is the fetal age in weeks with a correlation of determination of  $r^2 = 0.9951$  ( $P < 0.0001$ ) in Nigerian fetuses in Jos.

When other fetal anthropometric parameters like head circumference, biparietal diameter, occipitofrontal diameter, abdominal circumference and femur length are plotted against weight, certain hidden relationships can be forced out. For example, Fig. 6.78 shows the relationship of weight with head circumference. From the graph, it can be seen that there is a positive polynomial correlation between head circumference and weight with a correlation of determination of  $r^2 = 0.9997$  ( $P < 0.0001$ ) in Nigerian fetuses in Jos. The relationship is best described by the fourth order polynomial regression equation  $y = 3E-12x^4 + 3E-08x^3 - 0.0001x^2 + 0.2173x + 106.44$  where  $y$  is the head circumference and  $x$  is the fetal weight in grams. Fig. 6.79 shows the relationship of fetal weight with occipitofrontal diameter which has regression equation of  $y = -9E-13x^4 + 1E-08x^3 - 4E-05x^2 + 0.0779x + 36.004$  where  $y$  is occipitofrontal diameter and  $x$  is the fetal weight in grams with a correlation of determination of  $r^2 = 0.9992$  ( $P < 0.0001$ ) in Nigerian fetuses in Jos. Fig. 6.80 shows the relationship between biparietal diameter and weight. The relationship is best described by the fourth order polynomial regression equation  $y = -3E-13x^4 + 4E-09x^3 - 2E-05x^2 + 0.0472x + 34.356$  where  $y$  is the biparietal diameter and  $x$  is the weight in grams with a correlation of determination of  $r^2 = 0.9994$  ( $P < 0.0001$ ) in Nigerian fetuses in Jos. Other relationships can be calculated outside the skull. Fig. 6.81 shows relationship of weight with abdominal circumference. From the graph, it can be seen that there is a positive polynomial correlation between abdominal circumference and weight with a correlation of determination of  $r^2 = 0.9993$  ( $P < 0.0001$ ) in Nigerian fetuses in Jos. The relationship is best described by the fourth order polynomial regression equation  $y = -3E-12x^4 + 2E-08x^3 - 9E-05x^2 + 0.1947x + 95.592$  where  $y$  is biparietal



diameter and  $x$  is the fetal weight in grams with a correlation of determination of  $r^2 = 0.9992$  ( $P < 0.0001$ ). Fig. 6.82 shows relationship between weight and femur length. There is a positive polynomial correlation between weight and femur length with a correlation of determination of  $r^2 = 0.9972$  ( $P < 0.0001$ ) in Nigerian fetuses in Jos. The relationship is best described by the fourth order polynomial regression equation  $y = 1E-12x^4 - 8E-09x^3 + 2E-05x^2 - 0.009x + 43.172$  where  $y$  is femur length and  $x$  is the fetal weight in grams.

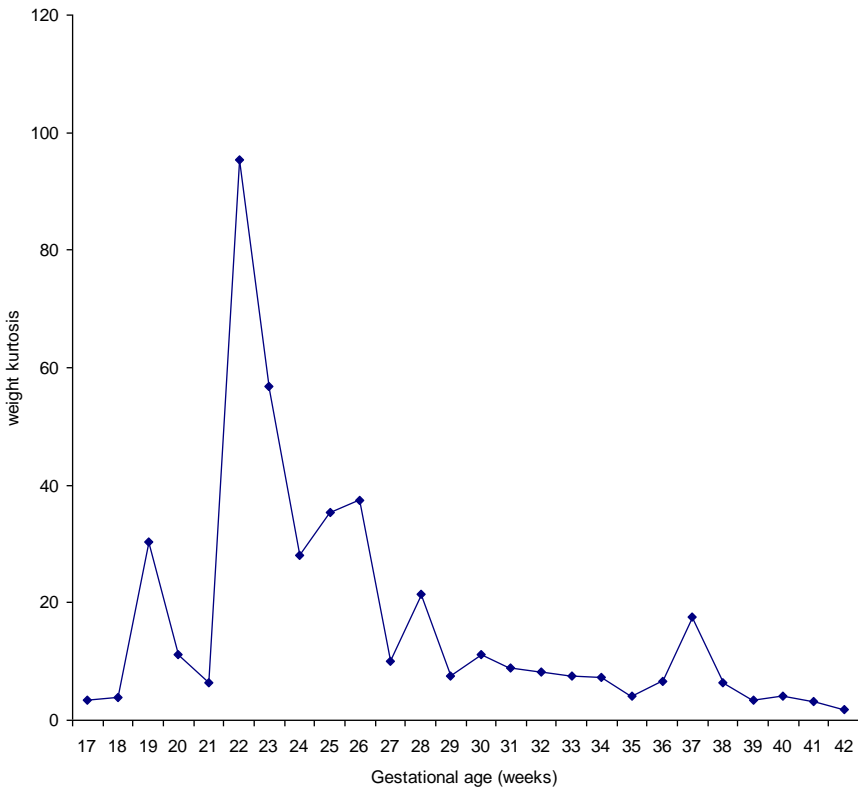


**Fig. 6.74** Weight data of 12,080 fetuses subjected to kurtosis analysis at different gestational age ranging from 12 – 42 weeks.

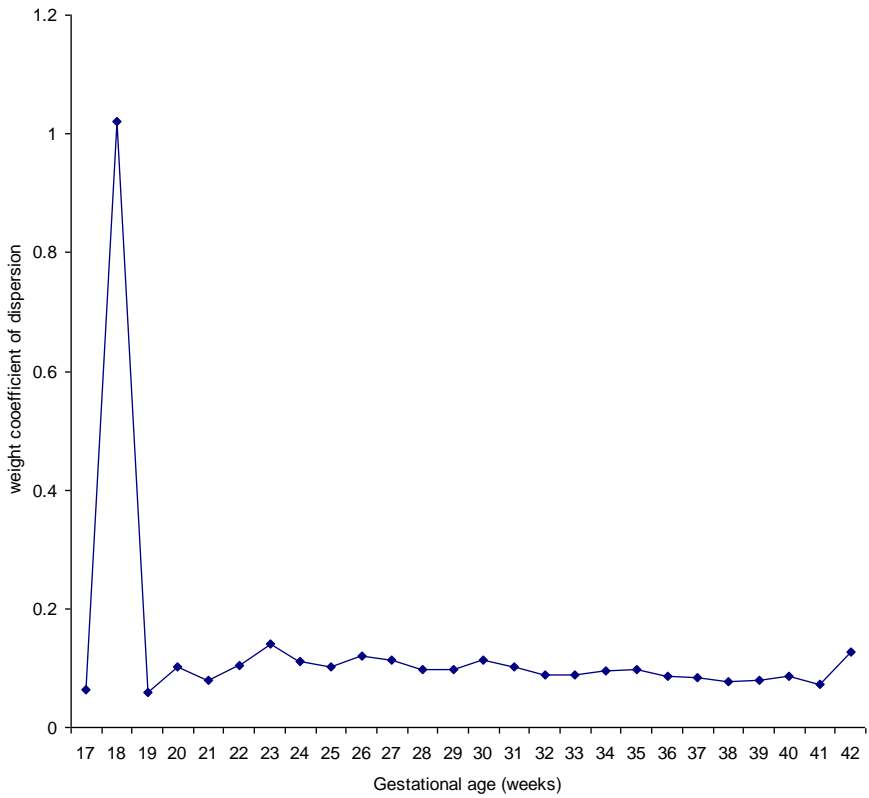


**Fig. 6.75** *Weight coefficient of dispersion in 12,080 fetuses of gestational ages between 12 to 42 weeks.*

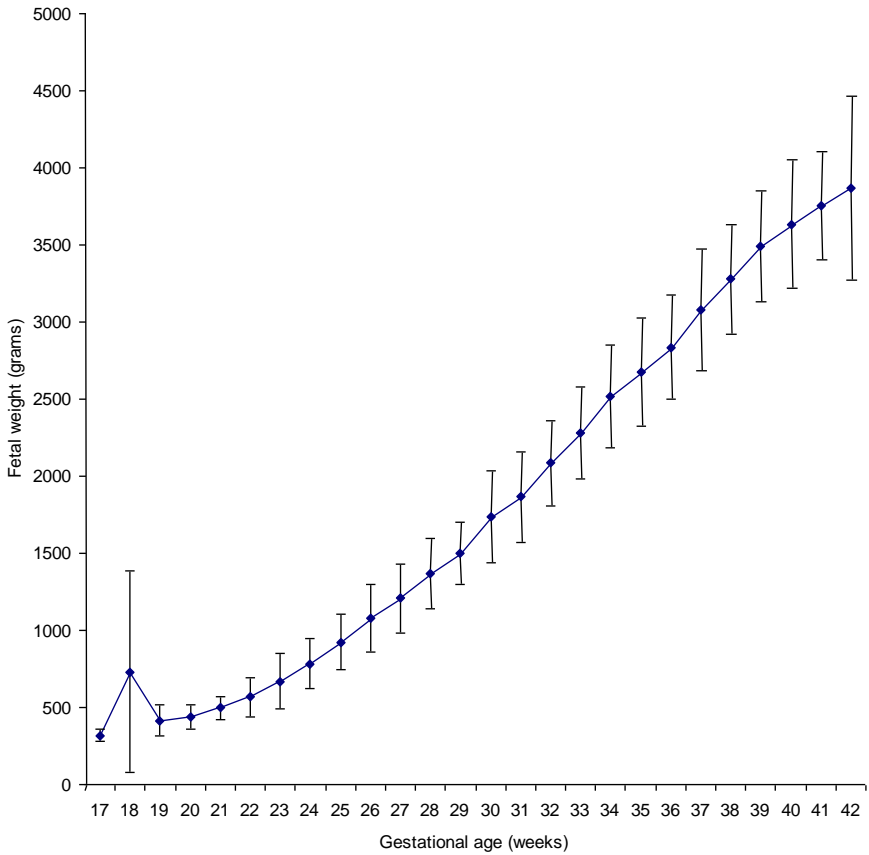


**Fig. 6.76** Mean fetal weight values in 12,080 fetuses of women at different gestational ages between 12 – 42 weeks. The vertical bars show the values of  $\pm SD$ .

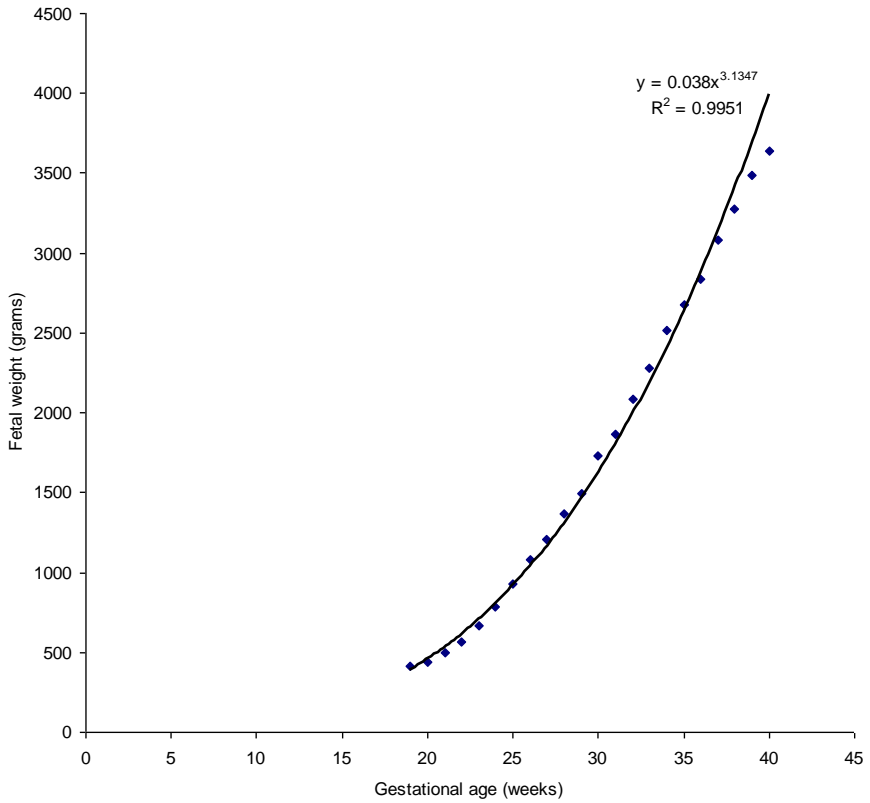


**Fig. 6.77** Correlation and regression equation of mean fetal weight values in 12,080 Nigerian fetuses in Jos plotted against gestational age.

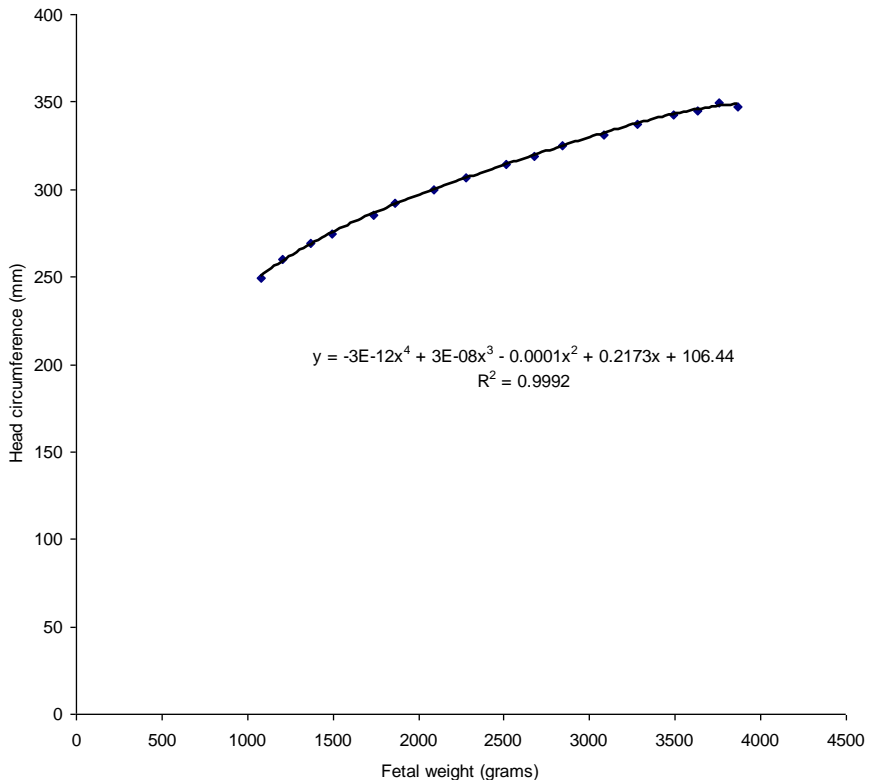


**Fig. 6.78** Correlation and regression equation of mean head circumference values in 12,080 Nigerian fetuses in Jos plotted against fetal weight in grams.

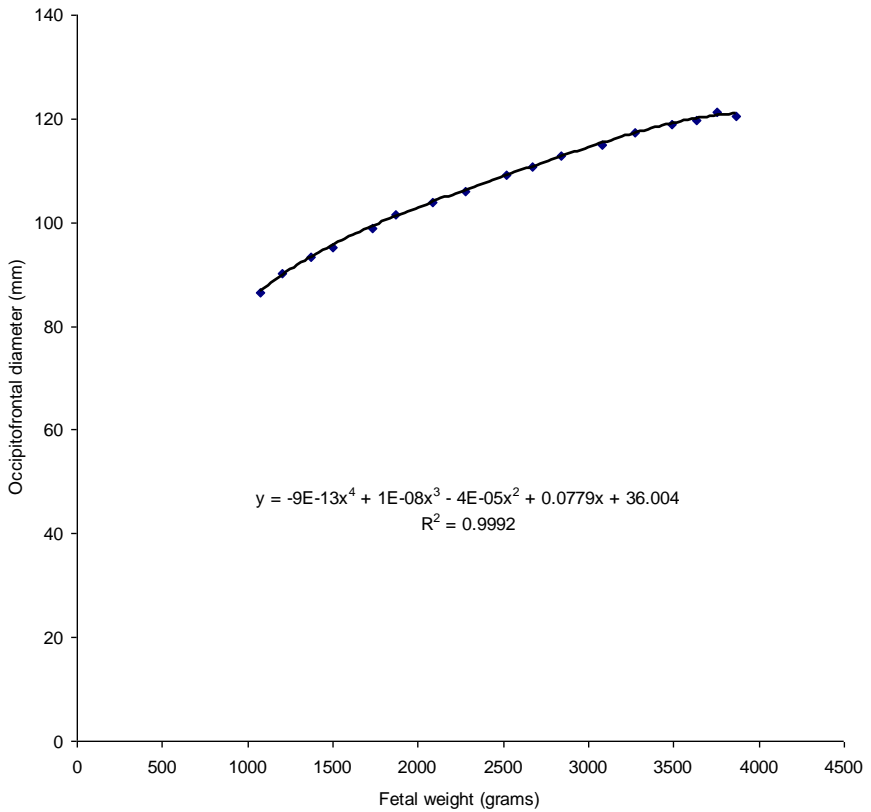


**Fig. 6.79** Correlation and regression equation of mean occipitofrontal diameter values in 12,080 Nigerian fetuses in Jos plotted against fetal weight in grams.

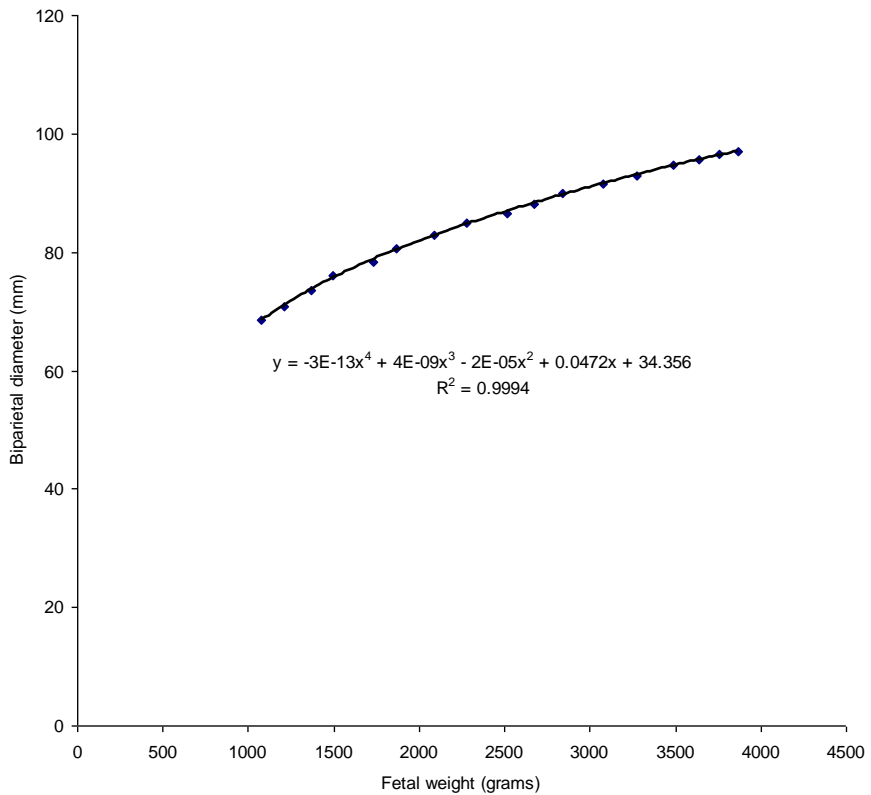


**Fig. 6.80** Correlation and regression equation of mean biparietal diameter values in 12,080 Nigerian fetuses in Jos plotted against fetal weight in grams.

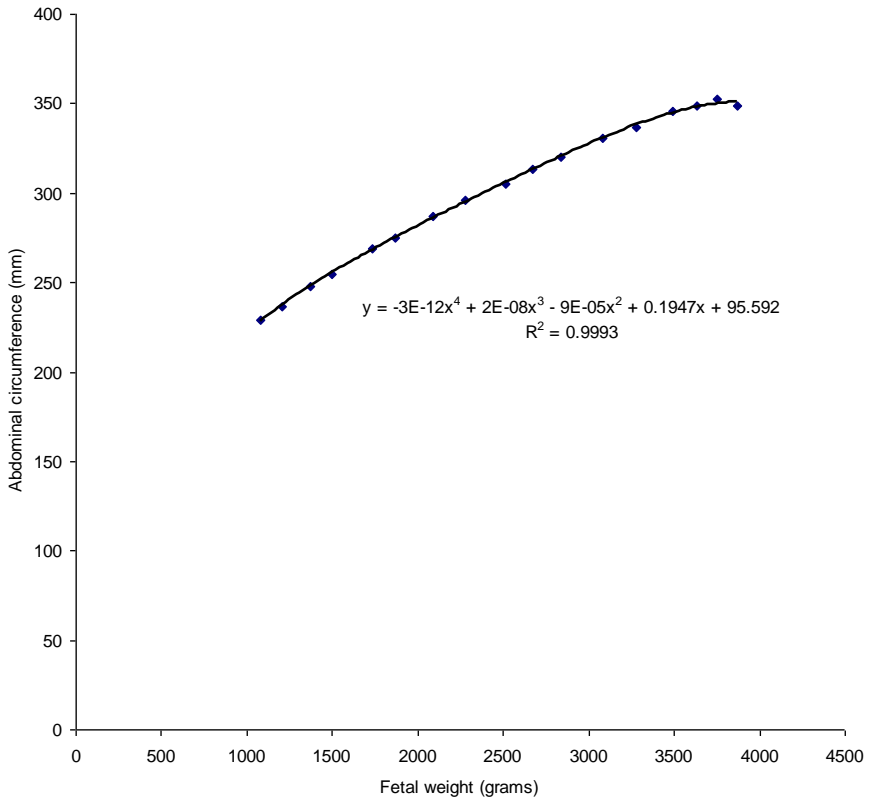


**Fig. 6.81** Correlation and regression equation of mean abdominal circumference values in 12,080 Nigerian fetuses in Jos plotted against fetal weight in grams.



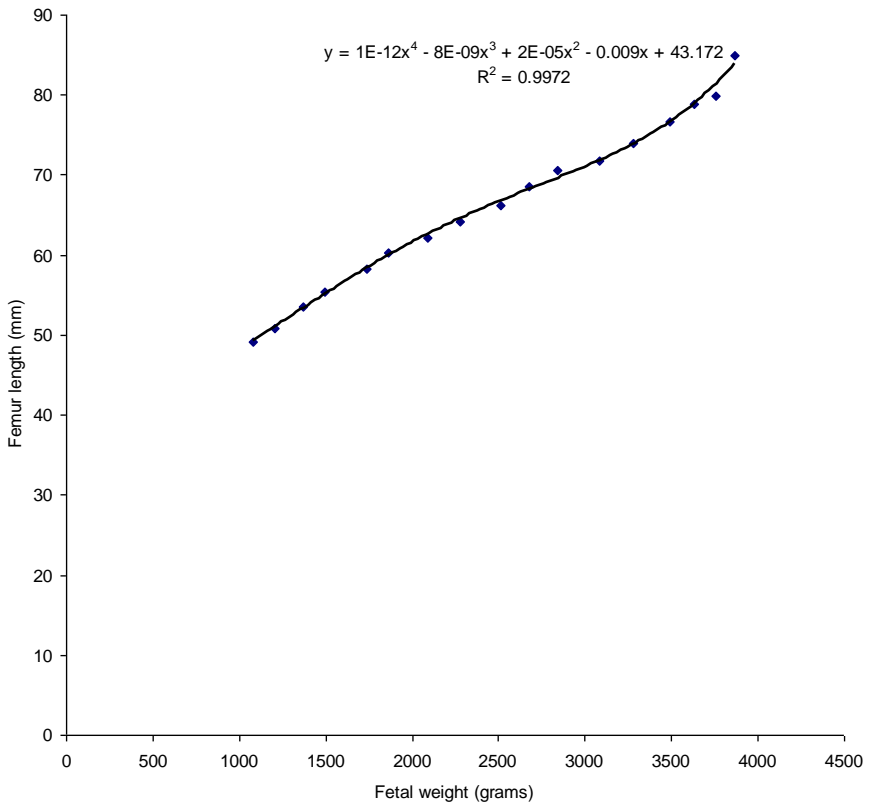


**Fig. 6.82** Correlation and regression equation of mean femur length values in 12,080 Nigerian fetuses in Jos plotted against fetal weight in grams.

Fig. 6.83 is a graph showing fetal weight gain from 17 – 42 weeks. From this graph, it can be seen that the human fetus gains the highest weight at 18 weeks but loses it by 19 weeks before it starts gaining weight again as from 20 weeks; and the weight gain keeps rising and becomes relatively constant towards the end of the third trimester. Fig. 6.84 shows histogram of fetal weight during the 5<sup>th</sup> month of intrauterine life while Fig. 6.85 shows histogram of fetal weight gain during 5<sup>th</sup> month of life. From this histogram it can be seen that the human fetus loses weight considerably at 19 weeks. Taking a look at the growth velocity of fetal biparietal diameter, occipitofrontal diameter, head circumference,

abdominal circumference and fetal femur length from 13 – 42 weeks, it can be seen that there is a drop in the growth velocity of these parameters at 19 weeks. At the same time the fetus losses about 318g during this period which seems not to happen by chance. Most likely, something takes place during this period which is yet to be unraveled – *the “19<sup>th</sup> week gestation problem”*.

When blood sample of pregnant women and non-pregnant women were analyzed, it was found out that there was significantly higher uric acid level in pregnant women as compared with the non-pregnant group. Among those that were pregnant, it also found out that women with multiple pregnancies as confirmed by ultrasound scan had significantly higher uric acid level than those with singleton pregnancy that fetuses are responsible for the production of the high uric acid seen in pregnancy. One other interesting finding that was discovered in the course of this study was that women diagnosed with molar pregnancy had significantly higher uric acid level than those with multiple gestations confirming that fetal tissue is likely to be the main source of uric acid as reported by Simmonds *et al* (1984) and Cohen *et al* (2002). Fig. 6.86 shows the variation of uric acid during normal singleton pregnancy from the 3<sup>rd</sup> month of life up to the 10<sup>th</sup> month.

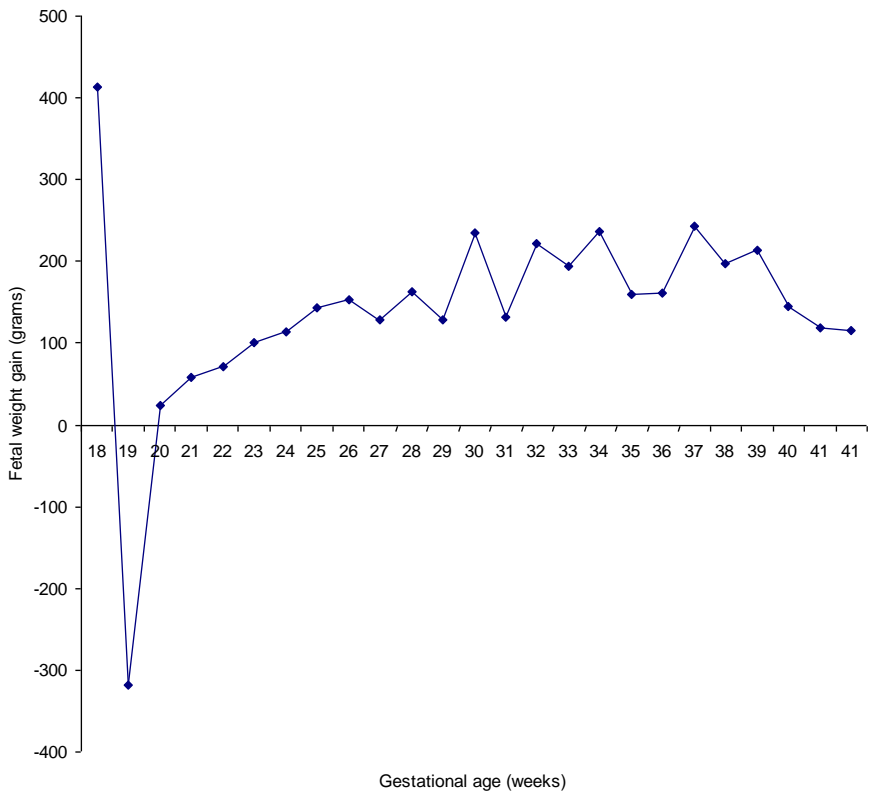


**Fig. 6.83** Mean fetal weight gain during normal pregnancy.

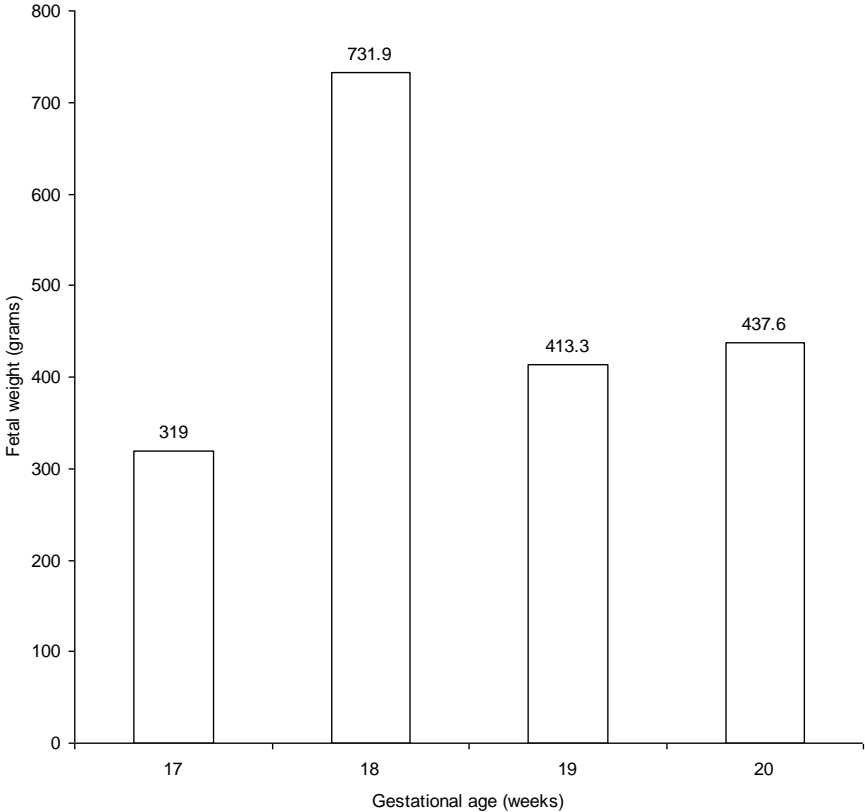


**Fig. 6.84** Mean fetal weight at 5 months.

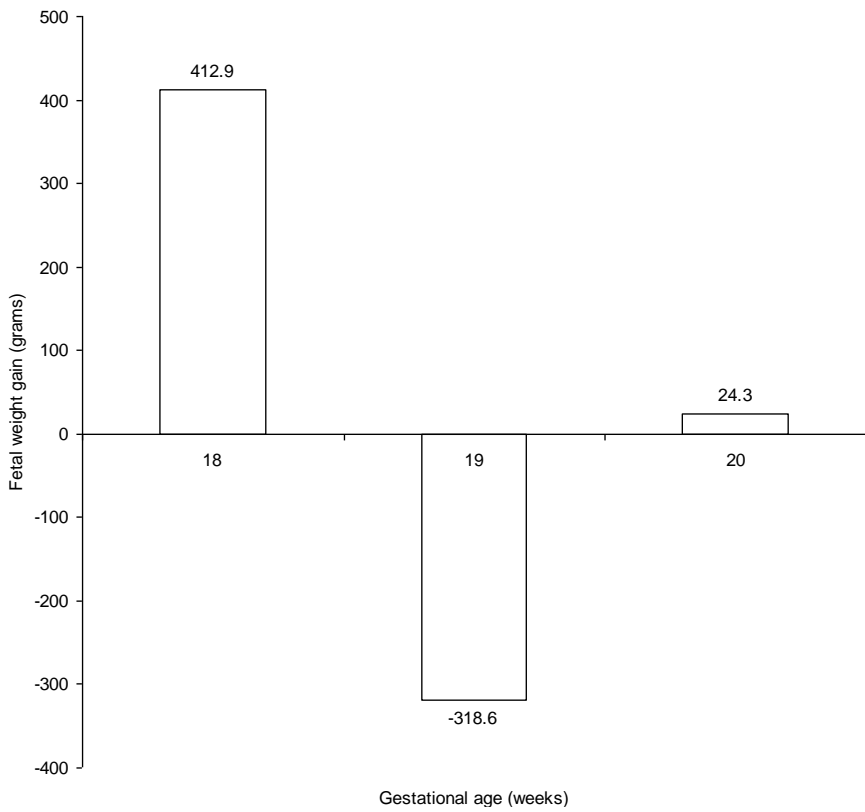


**Fig. 6.85** Mean fetal weight gain at 5 months.

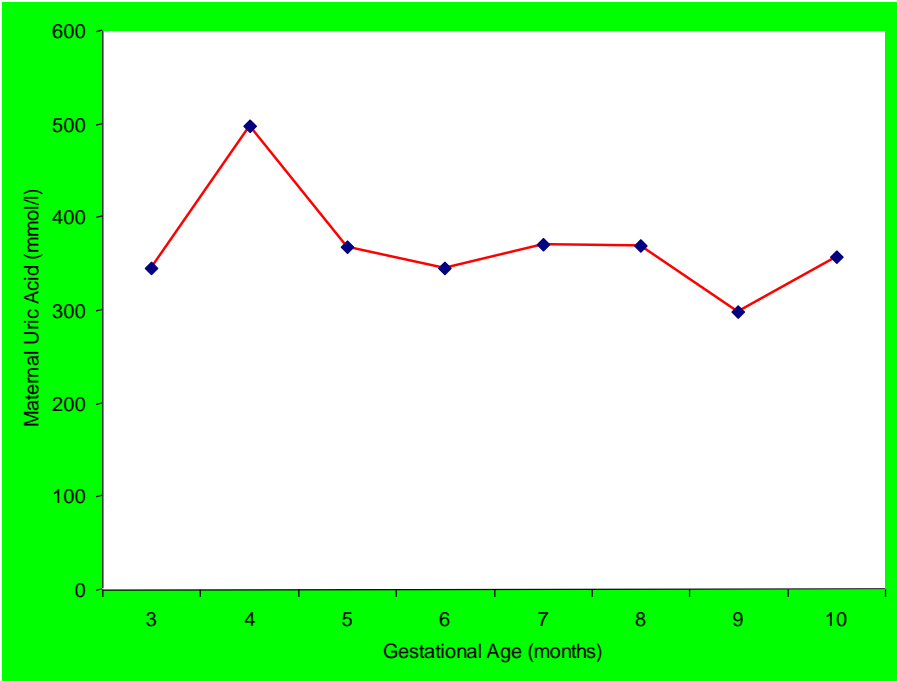


**Fig. 6.86** *Uric Acid level in Maternal Circulation during Normal Singleton Pregnancy.*

# 7

## **The Hypothesis**

**(Dr Mador, Dr Pam, & Dr Isichei)**





Science is clearly not a fixed, unchanging set of beliefs which, once learnt, one is expected to accept forever. Science has been and is a rapidly changing body of knowledge. It is an on-going attempt by scientists to understand and explain the living world that is why we should never look on science as a fixed set of beliefs laid down by some distant authority, which we are required to accept unquestioningly. On the contrary, one is expected and encouraged to be skeptical and critical of what one is told, or what one read. “What is the evidence of for this statement? What assumptions are implied in this explanation? Is this conclusion justified on the evidence, or would one be wiser to keep an open mind? It is on this premise that we wish to suggest a cause for preeclampsia-eclampsia. This cause has novel features which are of considerable biological interest.

The theory posited by Roberts and his colleagues in 1989 has continued to guide research related to preeclampsia-eclampsia aetiology (Roberts *et al.*, 1989). Drawing on past work that associated preeclampsia with shallow trophoblast invasion and subsequent reduction in placental perfusion, they hypothesized that the ischaemic placenta released a damaging factor(s) into the maternal circulation. Although the identity of this factor was hitherto unknown, the circulating factor was hypothesized to have caused endothelial dysfunction and would lead to activation of coagulation cascade, blood pressure abnormalities and loss of fluid from intravascular space. In our opinion, this placental factor is unsatisfactory for two reasons. Firstly, we believe that the factor which causes endothelial dysfunction is a genetic material of embryonic origin and not a gene product released by the placenta. Without the genetic material, it is not clear why the disease condition will be seen in primigravidas or during first pregnancy in multiparous women who have changed partner. Secondly, the placental factor does not cause endothelial dysfunction in subsequent pregnancies if it did not cause damage in the first pregnancy except when there is multiple gestation or

molar pregnancy.

The 1980 discovery of nitric oxide as an endothelial cell-derived relaxing factor resulted in an unprecedented biomedical research of nitric oxide and established it as one of the most important cardiovascular system molecule. A reduction in endothelial cell nitric oxide levels leading to “endothelial dysfunction” has been identified by several investigators as a key pathogenic event preceding the development of hypertension. The reduction in endothelial nitric oxide in cardiovascular disease has been attributed to the action of antioxidants that either directly react with nitric oxide or uncouple its substrate enzyme. Gersch and his co-worker demonstrated in 2008 that uric acid reacts directly with nitric oxide in a rapid irreversible reaction resulting in the formation of 6-aminouracil and depletion of nitric oxide (Gersch *et al.*, 2008; Khosla *et al.*, 2005).

As a follow-up to this research finding, we designed a study to assess the level of uric acid in maternal circulation during normal pregnancy and we found out that uric acid level was significantly higher in pregnant women than none pregnant women with levels in the 4<sup>th</sup>, 7<sup>th</sup> and 8<sup>th</sup> months being higher when compared to the other months of gestations. Based on this, we propose that the damaging factor released into the maternal circulation by the ischaemic placenta is uric acid produced from the cells of embryonic origin. This might explain why women with molar and multiple pregnancies develop preeclampsia-eclampsia.

Uric acid is generated in mammalian systems as an end-product of purine metabolism. Hyperuricemia may result when there is increased synthesis of purine, increased purine intake, increased turnover of nucleic acids, increased tissue breakdown or increased tissue damage. It possesses free-radical-scavenging properties (Kuzkaya *et al.*, 2005; Robinson *et al.*, 2004) and is the most abundant antioxidant in human plasma (Ames *et al.*, 1981; Hediger, 2002). In addition, uric acid inhibits system A amino acid uptake (Bainbridge *et al.*, 2009) and has

endogenous danger signaling properties (Behrens *et al.*, 2012) that ultimately lead to suppression of growth rate. We wish to put forward a radically different evidence for uric acid as a cause of preeclampsia-eclampsia. This evidence is anthropometric in nature (Fig 1, 2). From figure 1, it can be seen that during intrauterine life, fetal growth rate is high from week 13 – week 18 but as the fetus enters week 19, the growth rate drops as low as 1mm/day (Mador *et al.*, 2012). We assumed that during this period, the level of uric acid in maternal circulation is high reflecting its level in fetal circulation. This high uric acid level in fetal circulation most likely inhibits system A amino acid uptake and triggers endogenous signaling properties of uric acid in fetal tissue leading to suppression of growth rate in the fetus as seen during week 19. In addition to suppressing growth rate, it reduces endothelial cell nitric oxide levels leading to “endothelial dysfunction” which has been described as the key pathogenic event preceding the development of hypertension. Furthermore, suppression of growth rate around the 19<sup>th</sup> week makes the fetus to rapidly loose approximately 318 grams. We assumed that as uric acid level rises in the 4<sup>th</sup> month of life, it reacts directly with endothelial nitric oxide thereby depleting it leading to endothelial dysfunction hence the manifestation of preeclampsia-eclampsia as from 20 weeks of gestation. As fetal growth and development continues uric acid level in maternal circulation drops from higher levels at the 4<sup>th</sup> month only to peak again around the 7<sup>th</sup> and 8<sup>th</sup> months of life. Since the fetal purine which is unique is determined by the fusion of maternal and paternal gametes at fertilization, it elicits immunological response that will protect the endothelial cells of maternal vasculature in subsequent pregnancies. However, when such a woman changes partner, her first pregnancy with the new husband will form different sets of purine at fertilization which will be new when released in the maternal circulation thereby eliciting a fresh response in the mother causing endothelial dysfunction. In subsequent pregnancies, the maternal immune system would have developed defense against the uric acid produced. In multiparous women with twin pregnancy, the level of uric acid produced doubles the level of singleton pregnancies thereby

readjusting the nitric oxide depletion threshold leading to endothelial dysfunction. Similarly, in molar pregnancy the level of uric acid produced is much higher than the level in singleton and multiple pregnancies thereby giving an insight as to why preeclampsia-eclampsia occur earlier in molar pregnancy before 20 weeks. Going by Hill's criteria for causation, uric acid fulfills almost all the criteria outlined.

The novel feature of uric acid as the cause of preeclampsia-eclampsia is the manner in which its synthesis can be regulated using xanthine oxidase inhibitors during first pregnancies in order to prevent the occurrence of the disease and its ability to activate immune effectors of both the innate and adaptive immune systems thereby preventing the disease in subsequent pregnancies. Towards this end, we are planning to carry out a randomized clinical trial in order to determine the usefulness of xanthine oxidase inhibitors in the prevention of preeclampsia-eclampsia as well as its use in the treatment of pre-term labour. It has not escaped our notice that depletion of nitric oxide from the uterine myometrium at term might be responsible for causing the onset of labour.

## References

- [1] Ames BN, Cathcart R, Schwiers E, Hochstein P: Uric acid provides an antioxidant defense in humans against oxidant-and radical – caused aging and cancer: a hypothesis. *Proc Natl Acad Sci USA* 1981; 78: 6853–6862.
- [2] Aruoma OI, Halliwell B. Inactivation of alpha-antiproteinase by hydroxyl radicals. The effect of uric acid. *FEBS Lett.* 1989; 244:76–80.
- [3] Bagnati M, Perugini C, Cau C, Bordone R, Albano E, Bellomo G. When and why a water-soluble antioxidant becomes pro-oxidant during copper-induced low-density lipoprotein oxidation: A study using uric acid. *Biochem J.* 1999; 340:143–152.
- [4] Behrens MD, Wagner WM, Krco CJ, Erskine CL, Kalli KR, Krempsi J, Gad EA, Disis ML, Knutson KL: The endogenous danger signal, crystalline uric acid, signals for enhanced antibody immunity. *Immunobiology* 2012; 111(3):1472–1479.
- [5] Brosens IA, Robertson WB, Dixon HG. The role of the spiral arteries in the pathogenesis of preeclampsia. *Obstet Gynecol Annu.* 1972; 1:177–191. [PubMed].
- [6] Brosens I, Robertson WB, Dixon HG. The physiological response of the vessels of the placental bed to normal pregnancy. *Journal Path Bacteriol.* 1967; 93(2):569–579.
- [7] Caraway WT. Uric Acid. In: Seligson, D, ed. *Standard methods of Clinical Chemistry.* New York: Academic Press, 1965:239.
- [8] Caniggia I, Taylor CV, Ritchie JW, Lye SJ, Letarte M. Endoglin regulates trophoblast differentiation along the invasive pathway in human placental villous explants. *Endocrinology.* 1997; 138(11):4977–4988.
- [9] Chesley LC. *Hypertensive disorders in pregnancy.* New York, NY: Appleton-Century- Crofts; 1978.
- [10] Christen P, Peacock WC, Christen AE, Wacker WE. Urate oxidase in primate phylogenesis. *Eur J Biochem* 1970; 12:3–5.
- [11] Cohen SB, Kreiser D, Erez et al. Effect of Fetal number on maternal serum uric acid concentration. *Am J Perinatol.* 2002; 19:291 – 296.

## References

- [12] Denman T. Introduction to the practice of midwifery. NY: E. Bliss & E White; 1821.
- [13] Doehner W, Schoene N, Rauchhaus M et al. Effects of xanthine oxidase inhibition with allopurinol on endothelial function and peripheral blood flow in hyperuricemic patients with chronic heart failure: results from 2 placebo-controlled studies. *Circulation*.200; 105:2619–2624.
- [14] Doherty M. New insights into the epidemiology of gout. *Rheumatology* 2009; 48:ii2–8.
- [15] Eastman NJ, Hellman LM. Williams's obstetrics. 13. New York, NY: Meredith Publishing Company; 1966.
- [16] Elosha E, Chike N, Marquetta F. Preeclampsia. *Journal of Pregnancy*. 2012: 1–7.
- [17] Farquharsan CA, Butler R, Hill A et al. Allopurinol improves endothelial dysfunction in chronic heart failure. *Circulation*. 2002; 106:221–226.
- [18] Feig DI, Johnson RJ. Uric acid and cardiovascular risk. *N Engl J Med* 2009; 360:540–1.
- [19] Feichtmeier TV, Wrenn HT. Direct determination of Uric Acid using Uricase. *Am J Clin. Pathol*. 1995; 25:833.
- [20] Forstermann U. Janus-faced role of endothelial NO synthase in vascular disease: Uncoupling of oxygen reduction from NO synthesis and its pharmacological reversal. *Biol Chem*. 2006; 387:1521–1533.
- [21] Friedlander WJ. The history of modern epilepsy: The beginning, 1865–1914. Westport, CT: Greenwood Press; 2001.
- [22] Gersch C, Palii SP, Kim KM, Angerhofer A, Johnson RJ, Henderson GN: Inactivation of Nitric Oxide by Uric Acid. *Nucleosides Nucleotides Nucleic Acids* 2008; 27(8): 967–978.
- [23] Goldstone AB, Liochev SI, Fridovich I. Inactivation of copper, zinc superoxide dismutase by H<sub>2</sub>O<sub>2</sub>: Mechanism of protection. *Free Radic Biol Med*. 2006; 41:1860–1863.
- [24] Gulmezoglu AM, Hofmeyr GJ, Oosthuisen MM. Antioxidants in the treatment of severe preeclampsia: an explanatory randomized controlled trial. *Br J Obstet Gynaecol*. 1997 104:689–696.

- [25] Gerretsen G, Huisjes HJ, Elema JD. Morphological changes of the spiral arteries in the placental bed in relation to pre-eclampsia and fetal growth retardation. *British Journal of Obstetrics and Gynaecology*. 1981; 88(9):876–81.
- [26] Hayashi S, Fujiwara S, Noguchi T. Evolution of urate-degrading enzymes in animal peroxisomes. *Cell Biochem Biophys* 2000; 32:123–9.
- [27] Hediger MA: Kidney function: gateway to a long life? *Nature* 2002; 417: 393–395
- [28] Bainbridge SA, Versen-Hoyneck FV, Roberts JM: Uric acid inhibits Placental System A Amino Acid Uptake. *Placenta* 2009; 30(2): 195–200.
- [29] Hediger MA. Kidney function: Gateway to a long life? *Nature*. 2002; 417:393–395.
- [30] Hill AB. The environment and disease: association or causation? *Proc R Soc Med*. 1965; 58:295–300.
- [31] Hladunewich M, Karumanchi SA, Lafayette R. Pathophysiology of the clinical manifestations of preeclampsia. *CJASN*. 2007; 2:543–549.
- [32] Irgens HU, Reisaeter L, Irgens LM et al. Long term mortality of mothers and fathers after preeclampsia: Population based cohort study. *BMJ*.2001; 323:1213–1217.
- [33] Iseki K, Oshiro S, Tozawa M, Iseki C, Ikemiya Y, Takishita S. Significance of hyperuricemia on the early detection of renal failure in a cohort of screened subjects. *Hypertension Res*. 2001; 24:691–697.
- [34] Jerkic M, Rivas-Elena JV, Prieto M, Carron R, Sanz-Rodriguez F, Perez-Barriocanal F, López-Nova JM. Endoglin regulates nitric oxide-dependent vasodilatation. *FASEB Journal*. 2004; 18(3):609–611.
- [35] Johns R. Observations of puerperal convulsions. *Dublin Journal of Medical Science*. 1843; 24(1):101–115.
- [36] Johnson RJ, Kang DH, Feig D et al. Is there a pathogenetic role for uric acid in hypertension and cardiovascular and renal disease? *Hypertension* 2003; 41:1183–90.
- [37] Johnson RJ, Feig DI, Kang DH, Herrera-Acosta J. Resurrection of uric acid as a causal risk factor in essential hypertension. *Hypertension*. 2005; 45:18–20.
- [38] Jhonson RJ, Tittle S, Cade JR, Rideout BA, Oliver WJ. Uric acid, evolution and primitive cultures. *Semin Nephrol* 2005; 25:3–8.

## References

- [39] Kanabrocki EL, Third JL, Ryan MD et al (2000): Circadian relationship of serum uric acid and nitric oxide. *JAMA*. 2000; 283:2240–2241.
- [40] Kand'ar P, Zakova P, Muzakova V. Monitoring of antioxidant properties of uric acid in humans for a consideration of measuring levels of allantoin in plasma by liquid chromatography. *Clin Chim Acta*. 2006; 365:249–256.
- [41] Khosla UM, Zharikov S, Finch JL, Nakagawa T, Roncal C, Mu W, Krotova K, Block ER, Prabhakar S, Johnson RJ: Hyperuricaemia induces endothelial dysfunction. *Kidney Int* 2005; 67: 1739–1742.
- [42] Kittridge KJ, Willson RL. Uric acid substantially enhances the free radical-induced inactivation of alcohol dehydrogenase. *FEBS Lett*. 1984; 170:162–164.
- [43] Kong TY, De Wolf F, Robertson WB, Brosens I. Inadequate maternal vascular response to placentation in pregnancies complicated by pre-eclampsia and by small-for-gestational age infants. *British Journal of Obstetrics and Gynaecology*. 1986; 93(10):1049–1059.
- [44] Kuzkaya N, Weissmann N, Harrison DF, Dikalov S: Interactions of peroxynitrite with uric acid in the presence of ascorbate and thiols: implications for uncoupling endothelial nitric oxide synthase. *Biochem Pharmacol* 2005; 70: 345–354.
- [45] Kutzing MK, Firestein BL. Altered uric acid levels and disease states. *J Pharmacol Exp Ther* 2008; 324:1–7.
- [46] Leeman L, Fontaine P. Hypertensive disorders of pregnancy. *American Family Physician*. 2008; 78(1):93–100.
- [47] Lee FI, Loeffler FE (1962): Gout and Pregnancy. *J Obstt Gynaecol Br Emp* 69: 299–304.
- [48] Lueck J, Brewer JI, Aladjem S, Novotny M. Observation of an organism found in patients with trophoblastic disease and in patients with toxemia of pregnancy. *American Journal of Obstetrics and Gynecology*. 1983; 145(1):15–26.
- [49] Mador ES, Mutihir JY, Ogunranti JO (2012). Fetal Head Circumference as an Anthropometric Index. In: Preedy VR (editor). *Handbook of Anthropometry: Physical Measures of Human Form in Health and Disease*. UK, Springer; 2012: 477–516.
- [50] Mador, E. S. In: *Ultrasonic Fetal Biometry: Anthropometric Reference Values &*



- Predictive Formulae of Fetal Parameters. LAP LAMBERT Academic publishing GmbH & Co. KG, Heinrich-Bocking-str.6-8, 66121 Sacrbuken, Germany: 2012.
- [51] Mador ES, Pam IC, Isichei CO. Uric Acid: A hypothetical cause of preeclampsia – eclampsia. *Nig Med J*. 2013; 54(5): 362–364.
- [52] Masuo K, Kawaguchi H, Mikani H, Ogihara T, Tuck ML. Serum uric acid and plasma norepinephrine concentrations predict subsequent weight gain and blood pressure elevation. *Hypertension*. 2003; 42:474–480.
- [53] Mauriceau F. In: *The diseases of women with child, and in childbed: As also, the best means of helping them in natural and unnatural labours.... To which is prefix'd an exact description of the parts of generation in women...The fourth edition corrected, and augmented with several new figures*. Chamberlen H, translator. London: 1710. (Original work published 1668).
- [54] McMillen S. Eclampsia. In: Kiple KF, editor. *The Cambridge historical dictionary of disease*. New York, NY: Cambridge University Press; 2003. pp. 110–112.
- [55] Nakagawa T, Hu H, Zharikov S, Tuttle KR, Ahort RA, Glushakova O, Ouyang X, Feig DI, Block ER, Herrera-Acosta J, Patel JM, Johnson RJ. Uric acid a causal factor for fructose-induced metabolic syndrome. *Am J Physiol Renal Physiol*. 2006; 290:F625–F631.
- [56] Nawal MN. An Introduction to Maternal Mortality. *Rev Obstet Gynecol*.2008; 1(2):77–81.
- [57] Oda M, Satta Y, Takenaka O, Takahata N. Loss of urate oxidase activity in hominoids and its evolutionary implications. *Mol Biol Evol* 2002; 19:640–53.
- [58] Papoutsis DV, Irwin RL, Curry JJ, Zuspan FP. Parasitic etiology for preeclampsia: Fact or artifact? *American Journal of Obstetrics and Gynecology*. 1983; 147(8):977–979.
- [59] Pennington KA, Schlitt JM, Jackson DL, Schulz LC, Schust DJ. Preeclampsia: multiple approaches for a multifactorial disease. *Dis Model Mech*. 2012; 5(1):9–18.
- [60] Rao A K, Daniels K, El-Sayed Y. Y, Moshesh M. K, and Caughey A. B (2006): “Perinatal outcomes among Asian American and Pacific Islander women,” *American Journal of Obstetrics and Gynecology*. 2006; 195: 834–838.
- [61] Richette P, Bardin T. Gout. *Lancet*. 2010; 375:318–28.

## References

- [62] Riches PL, Wright AF, Ralston SH. Recent insights into the pathogenesis of hyperuricemia and gout. *Hum Mol Genet.* 2009; 18:R177–84.
- [63] Roberts JM, Taylor RN, Musci TJ, Rodgers GM, Hubel CA, McLaughlin MK: Preeclampsia: An endothelial cell disorder. *American Journal of Obstetrics & Gynecology.* 1989; 161(5):1200–1204.
- [64] Robinson KM, Morre JT, Beckman JS, Triuret: A novel product of peroxynitrite-mediated oxidation of urate. *Arch Biochem Biophys.* 2004; 423: 213–217.
- [65] Roberts JM, Hubel CA. The two stage model of preeclampsia: Variations on the theme. *Placenta.* 2009; 23:S32–S37.
- [66] Roberts JM, Gammill HS. Preeclampsia: Recent insights. *Hypertension.* 2005; 46:1243–1249.
- [67] Saugstod OD. Hypoxanthine as measurement of hypoxia. *Paediatr Res.* 1975; 9:158–161.
- [68] Sanguinetti SM, Batthyany C, Trostchansky A, Botti H, Lopez GI, Wikinski RLW, Rubbo H, Schreier LE. Nitric oxide inhibits prooxidant actions of uric acid during copper-mediated LDL oxidation. *Arch Biochem Biophys.* 2004; 423:302–308.
- [69] Shepard, M., and Filly, R. A. A standard plane for biparietal diameter measurement. *Journal of Ultrasound in medicine.* 1982; 1:145–150.
- [70] Sibai BM, Spinnato JA. Hydatocystic mole: Artifact produced by sulfation. *American Journal of Obstetrics and Gynecology.* 1983; 147(7):854.
- [71] Simmonds HA, Stutchbury JH, Webster DR et al. Pregnancy and Xanthinuria: Demonstration of Fetal Uric Acid Production? *J Inher Metab Dis.* 1984 7: 77–79.
- [72] Sinclair EB, Johnston G. *Practical midwifery: Comprising an account of 13,748 deliveries which occurred in the Dublin Lying-in Hospital, during a period of seven years, commencing November, 1847.* Dublin, Ireland: The University Press; 1858.
- [73] Smith WT. *Parturition and the principles and practice of obstetrics.* Philadelphia, PA: Lea & Blanchard; 1849.
- [74] Speert H. *Obstetric and gynecologic milestones: Essays in eponymy.* NY: The Macmillan Company; 1958.

- [75] Temkin O. *The falling sickness: A history of epilepsy from the Greeks to the beginnings of modern neurology*. Baltimore, MD: The Johns Hopkins Press; 1971. (Rev. ed.)
- [76] Tietz N. *Clinical guide to Laboratory tests*. Philadelphia: WB Saunders, 1995.
- [77] Thomas H. *Classical contributions to obstetrics and gynecology*. Baltimore, MD: Charles C Thomas; 1935.
- [78] Tomita M, Mizuno S, Yamanaka H, Hosoda Y, Sakuma K, Matuoka Y, Odaka M, Yamaguchi M, Yosida H, Morisawa H, Murayama T. Does hyperuricemia affect mortality? A prospective cohort study of Japanese male workers. *J Epidemiol*. 2000; 10:403–409.
- [79] Toporsian M, Gros R, Kabir MG, Vera S, Govindaraju K, Eidelman DH, et al. A role for endoglin in coupling eNOS activity and regulating vascular tone revealed in hereditary hemorrhagic telangiectasia. *Circ Res*. 2005; 96(6):684–692.
- [80] Watanabe S, Kang DH, Feng L et al. Uric acid, hominoid evolution and the pathogenesis of salt-sensitivity. *Hypertension* 2002; 40:355–60.
- [81] World Health Organization (WHO). *The World Health Report 2005: Make Every Mother and Child Count*. Geneva, Switzerland: WHO; 2005.
- [82] Wu X, Muzny DM, Lee CC, Caskey CT. Two independent mutational events in the loss of urate oxidase during hominoid evolution. *J Mol Evol*. 1992; 34:78–84.
- [83] Wu X, Wakamiya M, Vaishnav S et al. Hyperuricemia and urate nephropathy in urate oxidase-deficient mice. *Proc Natl Acad Sci USA* 1994; 91:742–6.
- [84] Wu X, Muzny DM, Lee CC, Caskey CT. Two independent mutational events in the loss of urate oxidase during hominoid evolution. *J Mol Evol*. 1992; 34:78–84.





It is proposed that the damaging factor released into maternal circulation by the ischaemic placenta is uric acid produced from genetic material of cells of embryonic/fetal origin.

Fetus  
Uric acid  
Theory  
Preeclampsia  
Aetiology

To order additional copies of this book, please contact:  
Science Publishing Group  
[book@sciencepublishinggroup.com](mailto:book@sciencepublishinggroup.com)  
[www.sciencepublishinggroup.com](http://www.sciencepublishinggroup.com)

ISBN 978-1-940366-39-5



Price: US \$80